

Design of Tiltrotor VTOL and Development of Simulink Environment for Flight Simulations

A thesis submitted
in partial fulfillment for the award of the degree of

Master of Technology

in

Aerospace Engineering

by

Pavan N



**Department of Aerospace Engineering
Indian Institute of Space Science and Technology
Thiruvananthapuram, India**

August 2020

Certificate

This is to certify that the thesis titled ***Design of Tiltrotor VTOL and Development of Simulink Environment for Flight Simulations*** submitted by **Pavan N**, to the Indian Institute of Space Science and Technology, Thiruvananthapuram, in partial fulfillment for the award of the degree of **Master of Technology** in **Aerospace Engineering** is a bona fide record of the original work carried out by him/her under my supervision. The contents of this thesis, in full or in parts, have not been submitted to any other Institute or University for the award of any degree or diploma.

Dr. Dhayalan R
Thesis advisor
Assistant professor
Dept of Aerospace Engineering

Dr. Manoj T. Nair
Head of the Department
Dept of Aerospace Engineering

Place: Thiruvananthapuram
Date: August 2020

Declaration

I declare that this thesis titled ***Design of Tiltrotor VTOL and Development of Simulink Environment for Flight Simulations*** submitted in partial fulfillment for the award of the degree of **Master of Technology** in **Aerospace Engineering** is a record of the original work carried out by me under the supervision of **Dr. Dhayalan R**, and has not formed the basis for the award of any degree, diploma, associateship, fellowship, or other titles in this or any other Institution or University of higher learning. In keeping with the ethical practice in reporting scientific information, due acknowledgments have been made wherever the findings of others have been cited.

Place: Thiruvananthapuram

Pavan N

Date: August 2020

(SC18M034)

Acknowledgements

I sincerely thank my guide Dr.Dhayalan R., IIST for giving me an opportunity to work under his guidance and supervision. His continuous support and insights led me to the completion of the project. I would like to thank Mr. Rahul Raj, Flight mechanics lab, IIST for his help with practical aspects of design and support....

Pavan N

Abstract

This thesis deals with the study of Tilt rotor Unmanned Aerial Vehicles capable of Vertical Take Off and Landing. The combination of superior performance of fixed-wing aircraft and operational advantages of multirotor aircraft has made this technology very popular. A tiltrotor UAV capable of VTOL is designed. A mathematical model of the aircraft is developed and a simulation environment is created in MATLAB Simulink. Ardupilot flight stack is tested for the designed aircraft through flight simulations.

A UAV is designed with a total weight of 6 kg and an endurance of 30min. The aircraft is of balsa wood construction with carbon fiber reinforcements. A quad motor layout is used for propulsion with front two motors tilting forward. The thesis presents the conceptual design, preliminary sizing and detailed design of the aircraft. Procedures for performance evaluation, static and dynamic stability using Xflr5 software is explained. A CAD design of individual elements and components has been prepared, ready to be used for UAV manufacture.

Various aspects of UAV like aerodynamics, propulsion and flight dynamics are mathematically modelled. Simulation environment created in Simulink is integrated with the developed mathematical model. It has provisions for future improvements such as Navigation and Guidance, Sensors, Wind and disturbances. Control systems used in commercial flight controllers are tested with the simulation environment.

Contents

List of Figures	xi
List of Tables	xv
Abbreviations	xvii
Nomenclature	xix
1 Introduction	1
1.1 Vertical Take-Off and Landing for Fixed-wings	2
1.2 Challenges	6
1.3 Thesis objectives	6
1.4 Organisation of Thesis	7
2 Conceptual design	8
2.1 Design requirements	8
2.2 Subsystems and Components	11
2.3 Design methodology	12
2.4 Fixed-wing configuration	16
2.5 Motor Layout	18
2.6 Preliminary Design	20
3 Detailed design	22
3.1 Airfoil selection	22
3.2 Wing design	26
3.3 Tail design	29
3.4 Fuselage design	33
3.5 Control surface design	35

3.6 Aircraft structure	36
4 Performance and Stability	40
4.1 Xflr5 Analysis	40
4.2 Performance	41
4.3 Centre of Gravity	44
4.4 Static stability	47
4.5 Dynamic stability	47
5 Mathematical model of the aircraft	50
5.1 Aircraft flight mechanics	50
5.2 Propulsion	52
5.3 Aerodynamics	59
5.4 Simulink implementation	64
6 Flight control and Simulations	67
6.1 Fixed-wing flight mode	67
6.2 Hover flight mode	76
6.3 Flight mode Transition	84
7 Conclusions and Future Work	91
7.1 Conclusions	91
7.2 Future Work	91
Bibliography	92

List of Figures

1.1	Harrier Jump Jet (left) and Yakovlev Yak-38 (right)	2
1.2	V-22 Osprey (left) and V-280 Valor	3
1.3	Lockheed Martin F-35B	3
1.4	VTOL thrust control scheme in F-35B	4
1.5	Bell Eagle Eye and IAI Panther	5
1.6	Quantum Tron and Nimbus VTOL	6
2.1	Design Overview	13
2.2	Conceptual design	13
2.3	Detailed design	15
2.4	Aircraft configuration	17
2.5	Motor layouts considered Bicopter, Y3, X4, Y6, X8 [1]	19
2.6	Vayu - Search and Rescue drone	20
3.1	Lift curves	24
3.2	Efficiency curves	24
3.3	Drag polar	25
3.4	Spanwise Lift Distribution	28
3.5	Spanwise Reynolds number and Induced angle of attack	28
3.6	Tail size and placement with respect to wing	32
3.7	Components inside Fuselage	34
3.8	Fuselage sizing	35
3.9	Aileron size in mm	36
3.10	Elevator and Rudder size in mm	36
3.11	Wing structure	37
3.12	Tail structure	38
3.13	Fuselage structure	38

3.14	Tilt mechanism	39
3.15	Aircraft assembly	39
4.1	Aircraft geometry modelled in Xflr5	41
4.2	Flow visualisation using Xflr5	42
4.3	Pressure distribution on the aircraft surfaces	42
4.4	Thrust available vs Flight speed	43
4.5	Drag vs available thrust	44
4.6	Coordinates for CG Calculations	45
4.7	Pitching moment curve	48
5.1	APC 12x3.8SF - Thrust characteristics	53
5.2	APC 12x3.8SF - Power characteristics	54
5.3	APC 12x3.8SF - Efficiency curves	54
5.4	APC 12x3.8SF - 6000rpm	55
5.5	APC 12x3.8SF - Curve fit for C_T	55
5.6	APC 12x3.8SF - Curve fit for C_Q	56
5.7	Thrust alignment	57
5.8	Curvefit for drag profile	60
5.9	Simulation Environment	64
5.10	Aircraft dynamics block	66
6.1	Actuators for control in forward flight	68
6.2	Roll attitude controller	69
6.3	Pitch attitude controller	70
6.4	Yaw attitude controller	70
6.5	Simulation of pitch control	72
6.6	Simulation of roll control	73
6.7	Flight path of UAV for roll input	74
6.8	Effect of yaw damper	75
6.9	Motor placement for hover flight	77
6.10	Thrust vectoring for hover flight	78
6.11	Position controller	81
6.12	Attitude controller	81
6.13	Altitude control	82
6.14	x-axis control	83

6.15	y-axis control	83
6.16	General flight path 1	84
6.17	General flight path 2	84
6.18	Hover to Forward flight transition	86
6.19	Transition with different tilt angle limits	87
6.20	Transition with different tilt rates	88
6.21	Transition characteristics of the UAV	89
6.22	Forward flight to hover transition	90

List of Tables

2.1	Flight Controller components	12
2.2	Thrust and take-off weights for each configuration	18
2.3	Weight distribution in Vayu	21
2.4	Preliminary sizing of UAV	21
3.1	Airfoil comparison	23
4.1	Center of Gravity calculations	46
4.2	Center of Gravity of the UAV	46

Abbreviations

UAV	Unmanned Aerial Vehicle
VTOL	Vertical Take Off and Landing
STOL	Short Take Off and Landing
TOW	Take-Off Weight
BLDC	Brush-Less Direct Current
ESC	Electronic Speed Controller
CG	Center of Gravity
MAC	Mean Aerodynamic Chord
DoF	Degrees of Freedom
LLT	Lifting Line Theory
VLM	Vortex Lattice Method
PID	Proportional Integral Differential

Nomenclature

m	Mass, kg
g	Acceleration due to gravity, m/s^2
W	Weight, N
I_{xx}, I_{yy}, I_{zz}	Moments of Inertia, $kg\ m^2$
I_{xy}, I_{yz}, I_{zx}	Products of Inertia, $kg\ m^2$
s	Plan-form area, m^2
c	Chord, m
b	Span, m
\bar{c}	Mean Aerodynamic Chord (MAC), m
AR	Aspect Ratio
e	Span efficiency factor
i_w, i_h	Wing and tail incidence angle, deg
V_t	Magnitude of relative wind velocity, m/s
α	Angle of Attack, rad or deg
β	Angle of Sideslip, rad or deg
ρ	Density of air, kg/m^3
Q	Dynamic pressure, N/m^2
C_L	Co-efficient of lift
C_D	Co-efficient of Drag
C_X, C_Y, C_Z	Body frame force Co-efficient
C_l, C_m, C_n	Body frame moment Co-efficient
L, D	Lift and drag forces, N
X, Y, Z	Body frame forces, N
L, M, N	Body frame moments, $N\ m$

u, v, w	Body frame components of velocities, m/s
p, q, r	Body frame angular velocities, rad/s
ϕ, θ, ψ	Euler angles, rad or deg
X_E, Y_E, Z_E	Position in NED frame, m
δ_a	Aileron deflection, rad or deg
δ_e	Elevator deflection, rad or deg
δ_r	Rudder deflection, rad or deg
ω	Motor speed, rpm or rps

Chapter 1

Introduction

The past decade has seen a rapid growth in the use of Unmanned Aerial Vehicles driven by low cost and easily accessible electronic systems. Technology that was once limited to military applications is now easily available for civilian use. Today, an RC modelling enthusiast can easily acquire parts and make a UAV that can capture images, provide live video feed and deliver payloads. Small size, portability and lower costs have made UAVs find applications like surveillance, mapping, search and rescue, wild life monitoring and package deliveries in remote areas.

Development of smaller, cheaper and more reliable electronic systems have brought advanced controls and automation to hobbyist's remotely piloted model aircrafts. Advancements in battery technology, power electronics and motors have drastically increased the performance and reliability of UAVs. Fibre composite manufacturing, rapid prototyping and other manufacturing processes are now cheaper and more accessible, leading to better airframes. Most importantly, technology for developing state of the art UAVs is now being open sourced and shared among hobbyists, research community and industry.

A wide range of aircraft configurations are in use for different applications. Most popular among these small UAVs are multirotors due to their ability operate in closed spaces. A large variant of fixed wing UAVs are also in use due to their performance and reliability. The configuration of aircraft used depends on the requirements and constraints of the operation. This aspect is the motivation for the thesis, a fixed wing aircraft capable of taking off and landing like a rotorcraft. A Vertical Take-Off and Landing (VTOL) aircraft that integrates hovering capabilities with the long-range performance of fixed wing aircraft. Such configurations enable them to operate off of any unprepared flat surface like rotorcraft while still retaining the performance of fixed wing aircraft.

Although rotorcraft (helicopters, multirotors, etc.) also perform Vertical Take-Off and Landings, the term VTOL aircraft is popularly used for Fixed-wings with VTOL capability. These aircraft are also called as Hybrid aircrafts. In the thesis, VTOL aircraft will refer to such aircrafts unless specified. Flight regime of such aircraft can be divided into three modes or phases – Hovering flight, Transition and Forward flight.

1.1 Vertical Take-Off and Landing for Fixed-wings

The contrast between fixed wing aircraft and rotorcraft is how they achieve lift. In a fixed wing aircraft, lift is generated due to airflow over wings and engines provide forward thrust to maintain forward speed. Rotorcraft use spinning rotors (a rotary wing) to produce thrust that directly oppose their weight. While the engines on a rotor craft must produce thrust greater than or equal to aircraft's weight, fixed wings need thrust that is only a fraction of its weight. This key difference is what makes a fixed wing highly more efficient than a rotorcraft.

The operational advantages that VTOL capabilities give has been of keen interest for military applications since World War II. VTOL aircraft can operate in remote areas, damaged or smaller airports and naval carriers. As of today many VTOL aircraft are in military service around the world in transport and combat roles. The British Harrier Jump Jet (1967) [2] and Soviet Yakovlev Yak-38 (1970) [3] use vectored thrust nozzles on its turbojet engines to take off and land on aircraft carriers (figure 1.1). They use engine bypass air for pitch and roll control by means of vectored nozzles.



Figure 1.1: Harrier Jump Jet (left) and Yakovlev Yak-38 (right)

The American Bell Boeing V-22 Osprey (1989) [4] being the world's first production tilt rotor aircraft, uses two rotors that can tilt 90deg for Vertical Take-Off and Landing. Each rotor comprises of a three-bladed propeller powered by a turboprop engine mounted on each wingtips. It is also capable of partially tilting the rotors for Short Take-off and Landing (STOL) for increased payload capacity. A successor to the V-22 Osprey, the Bell V-280 Valor (2017) [5] is under development with higher cruise speeds and better manoeuvring capabilities. With layout similar to the Osprey, it uses fixed turboprop engines with only the rotors tilting.



Figure 1.2: V-22 Osprey (left) and V-280 Valor

The Lockheed Martin F-35 Lightning II [6] series has a variant F-35B (figure 1.3) that is STOL and VTOL capable. The main engine nozzle at the back tilts down deflecting the engine thrust. Unlike previous concepts that use more vectored nozzles, the F-35B uses a lift fan near the cockpit powered by the main engine via a shaft.



Figure 1.3: Lockheed Martin F-35B

The lift fan provides counter balancing thrust during hovering and disengages in forward flight. Two wing-mounted thrust nozzles provide roll control at low speeds using bypass air from the engine. Figure 1.4 shows the nozzle, lift fan and roll control nozzles during hover phase of flight.

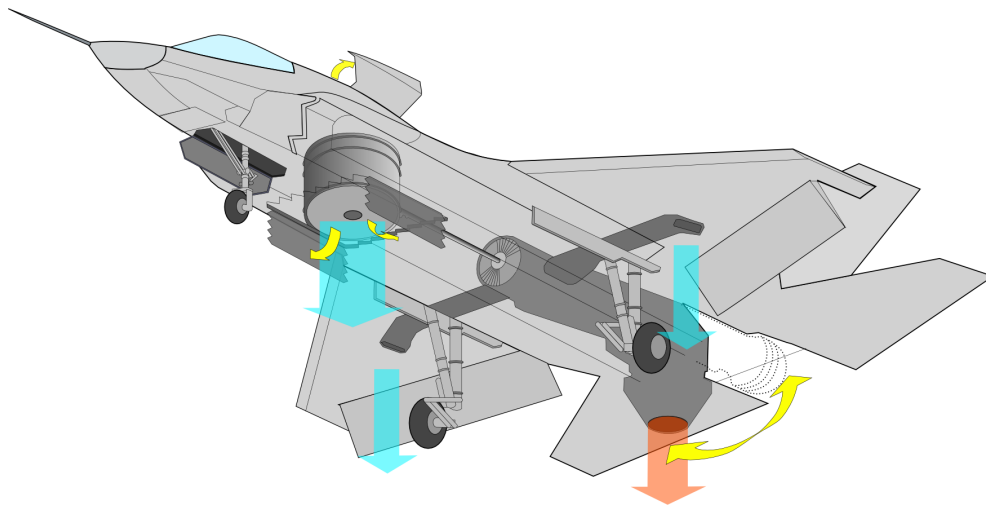


Figure 1.4: VTOL thrust control scheme in F-35B

All the above aircraft are or were in active service and have been proven in concept. It is worth noting that the addition of VOTL capability comes with an addition of weight that is unnecessary for forward flight. The VTOL capability is traded for reduced range, endurance or payload capacity. While this offers operational advantage, it cannot compete with the cost advantages of conventional aircrafts. Hence many of these aircraft perform STOL when fuel and payload weight is heavier. STOL refers to Short Take-Off and Landing where the engine thrust partly is augments aerodynamic lift to take-off and landing in shorter runways.

For small class UAVs, need for runways can be eliminated by using catapults or hand-launches for take-off; and parachute recovery or catching nets can be used to land the aircraft. It may appear that additional weight, cost and complexity due to VTOL capability is not required for small scale UAVs, but there are applications where UAV is required to take-off and land in closed spaces. A VTOL UAV can perform precision landings that a parachute or belly landing will not allow. It can also perform multiple take-off and landings if the mission requires. It is in such cases that a VTOL aircraft is very useful and the operational advantage outweighs the increased weight, cost and complexities.

Apart from the operational advantage that a VTOL UAV can give, eliminating the landing gear reduces the weight of the airframe. When the UAV is not required to be launched using a catapult or withstand impacts during landings, the airframe need not be as structurally strong as in a conventional UAV. Hence would also reduce the weight of the airframe.

For small scale UAVs, multiple techniques can be used to achieve VTOL capability. A classification of types of Hybrid UAVs is described in [7] based on how the UAV transforms between a hover craft and a fixed wing. ArduPilot documentation [1] also gives a classification based on the type of control algorithm used for transition. They can be classified into Dual propulsion, Tilt rotor, Tilt wing and Tailsitter configurations.

Military UAVs like the Bell Eagle Eye and IAI Panther use tiltrotor concept to achieve VTOL. The Bell Eagle Eye is a medium sized UAV that is a scaled down unmanned version of V-22 Osprey [8]. It uses two tiltrotors with variable pitch propellers. The IAI panther uses a tricopter layout for hover capability and tilts front two rotors for forward flight. It uses fixed pitch propeller due to size limitations of the motors [9].



Figure 1.5: Bell Eagle Eye and IAI Panther

Due to advancements in electronics the principles of fixed wings with VTOL has been widely research in the past decade. Tiltrotor UAV have already become popular in the civilian sector. The Quantum Tron from Quantum systems and Nimbus VTOL from Foxtech FPV are some of the latest drones available for mapping and surveillance.



Figure 1.6: Quantum Tron and Nimbus VTOL

1.2 Challenges

Although addition of VTOL capability to fixed wing UAV seem simple and straight forward, the design of a UAV that can integrate it while optimising its performance is hard. The addition of Hovering flight and VTOL capabilities brings challenges in the Flight dynamics and control of the UAV. The complex dynamics of such flight regimes requires better control systems compared to either fixed-wing or rotary aircraft. These applications call for advanced control algorithms for robust and efficient operations. The design of control systems is also harder due the unique flight regimes involved and experiments with flight tests are expensive. A good mathematical model and a simulation environment is required to better understand the dynamics of such aircraft and design flight control algorithms.

1.3 Thesis objectives

The thesis a part of ongoing work at the Flight Mechanics Laboratory in the Indian Institute of Space Science and Technology, Trivandrum to research and develop Vertical Take-Off and Landing Aircraft for various civilian applications. The research work intends to develop a mathematical model of the aircraft dynamics, aerodynamics, propulsion and their interactions for simulations. The model can be utilised to design and test control algorithms for flight transition and other phases of flight.

The work described is the first step in this research and the following are the objectives of the thesis.

- To design a fixed wing UAV capable of Vertical Take-Off and Landing.
- To develop mathematical model of different subsystems involved in the design UAV.

- To create a simulation environment to study UAV dynamics in different phases of flight.

1.4 Organisation of Thesis

The thesis is organised into five chapters as follows.

Chapter 2 - Conceptual design - describes the initial phase of the design where the requirements for the UAV, subsystems involved and design methodology are evaluated. The conceptual design and preliminary design are also discussed in this chapter.

Chapter 3 - Detailed design - describes detailed design of the UAV where individual components are designed. It consists of selection of airfoil, wing and tail sizing, fuselage design and control surface design. The structure of the airframe and tilt mechanism are modelled for fabrication.

Chapter 4 - Performance and Stability - discusses the xflr5 analysis done for performance and stability evaluation. Center of Gravity calculations, static and dynamic stability are studied. The performance evaluation with consideration of the propulsion is done.

Chapter 5 - Mathematical model of the aircraft - explains the derivation of mathematical model of the aircraft dynamics, propulsion, aerodynamics. Simulink implementation of the model and a simulation environment is also explained.

Chapter 6 - Flight control and Simulations - presents the controller used for forward flight, hover flight and transition with flight simulations of the derived mathematical model of the UAV in MATLAB Simulink.

Chapter 2

Conceptual design

This chapter presents the conceptual design of the UAV. Aircraft design starts with conceptual design and commences with preparation of requirements set for the UAV to be designed. Then the components in each subsystems involved in the UAV are listed and their effect on design is studied. This list of requirements and subsystems is used to prepare a comprehensive statement of the problem and develop a methodology to approach the problem of designing the aircraft.

The result of conceptual design is the overall aircraft configuration. At this stage, results obtained are without precise calculations and primary tool used is selection. Well defined design process are not defined for this stage of design and past design experiences are crucial for this stage of design.

After the configuration of the aircraft is decided, a preliminary design or a preliminary sizing of the aircraft is done with some basic calculations. The main purpose of this stage is to obtain a starting solution to the design problem which is refined further down the design process. The parameters like weight and size of the aircraft, engine thrust and endurance of the aircraft are estimated.

2.1 Design requirements

The primary purpose of the UAV being design is to study and research the concept of VTOL or Hybrid UAVs. Hence the UAV must be a Fixed-wing aircraft capable of Vertical Take-Off and Landing using Tiltrotor concept. The aircraft will be manufactured and used to prove the concept of Tiltrotor VTOL.

Mission profile

The mission profile of the VTOL UAV will involve three flight mode – Hover flight, Forward flight and Flight transition. The VTOL UAV should take-off and land in hover flight mode which is the primary reason of adding VTOL capability to a fixed-wing. The UAV should also hover like a Rotorcraft at a place if the mission requires it. The UAV will primarily fly as a fixed-wing to reach required destination or loiter around a spot. Transition between these two types of flight is the third flight mode.

Since the design is for an experimental UAV and will involve conventional take-off and landings during initial phase of flight tests. This requires the UAV to have optional landing gear.

Aircraft type and Manoeuvrability

The VTOL UAV will be a hybrid of a Fixed-wing and a Multirotor aircraft configuration. The aircraft is not required to be highly manoeuvrable hence a conventional aircraft type is used for the fixed wing part of the design and General Aviation type of flying quality should suffice the requirements.

Propulsion

Considering multirotor concept involved in the VTOL configuration, electric propulsion is considered to be the best option for propulsion of the aircraft. Brushless DC motors with Lithium Polymer (LiPo) batteries are the most popular and viable choice for small scale UAVs. They offer very good performance at this scale and are very convenient during operation when compared to IC engines.

A constraint while selecting the propulsion for the UAV is to utilise motors available at hand in the lab. Emax MT3515 650kv motors are selected for propulsion for the aircraft due to their availability. Since these motors are designed to be used for multirotors, they do not operate well at high advance ratios which should be considered for the flight speeds.

Flight controller

The inherent aerodynamic stability like in case of Fixed-wings cannot not be incorporated to hover phase and transition phase of flight. Hence an active flight controlled system is required for the operation of the VTOL UAV. For this purpose, Pixhawk Cube is used as flight controller. It also has capabilities for autonomous flights and flight logging. In future, it can be used to test and implement various controls for flight [1].

Payload

Although any defined payload is not a requirement for the experimental UAV being designed, future uses may require the use of a small camera such as a GoPro. Hence, a GoPro Hero 6 camera and a gimbal is taken as payload. When required camera and gimbal can be substituted for additional avionics or batteries for increased endurance.

Flight speeds

In forward flight, cruise speed of the aircraft is directly linked with weight and size of the aircraft as lift is linked to the relative velocity of aircraft with air. For experimental purposes, operational convenience of the aircraft is more important than performance. The range of flight speeds that is comfortable for a test pilot to fly is between $10m/s$ and $20m/s$ [10]. A cruise speed of $15m/s$ is set as the requirement for the aircraft. Although higher speeds are prepared for missions, slower stall and cruise speeds make tests safer in case of crashes and lower speeds are more efficient for the motors being used.

Multiorotors used for utility purposes operate at flight speeds less than $5m/s$ [1]. Since the VTOL UAV designed has large lifting surfaces, it will offer more drag and hence maximum speed in hover mode is set at $3m/s$. Climb rates of $1m/s$ are set for take-off and landings. The limits of this parameters are interest of further studies.

Operating conditions

The UAV will be operating below altitudes of $200m$ AGL at the IIST, Trivandrum. The city has an elevation of approximately $10m$ above sea level with temperatures between $30^{\circ}C$ and $35^{\circ}C$. For the purpose of design and simulations, altitude of $100m$ and temperature of $35^{\circ}C$ are used. Corresponding to this condition, density of air is $1.140kg/m^3$.

Endurance

Since the mission profile of the UAV is a hybrid of Hover flight and Forward flight, endurance cannot be defined as simply as for a conventional UAV. Also since the purpose of the UAV is of experimental nature, endurance is not of concern. A minimum endurance of $15min$ in hover flight or $30min$ in forward flight is taken as minimum for the design.

Landing gear

Although a conventional landing gear is not required for a VTOL capable UAV, a provision for adding a landing would help during initial experiments. It will help test the forward

flight characteristics of the UAV without performing flight mode transitions. It also gives an option of conventional landings in case of any failure.

2.2 Subsystems and Components

The UAV can be described as a combination of different subsystems. Breaking down the UAV into such subsystems simplifies the design by approaching the design of each of each subsystems individually.

Airframe

The airframe is the most important part of the UAV and is the main aspect of the UAV design. It consists of the Wings, Tail, Fuselage and all other components used to hold them together. Among other subsystems, airframe and its properties are the least defined during this stage of design. This subsystem design also comprises of most of the UAV design in this thesis.

The airframe is fitted with all other subsystems and their components. The airframe is also responsible for Lift generation, and structurally holding itself and other parts of the UAV. Its design also influences the stability and control of the aircraft.

Propulsion

The electric propulsion used in the UAV consists of the propellers, the BLDC motors that drive them, ESC (Electronic Speed Controller) that control the speed of the motors and the power cables. Propulsion in the case of VTOL UAV will have motors that contribute thrust for both hover and forward flight.

Tilt Mechanism

In the case of a Tiltrotor VTOL, the motors or a subset of motors are used for both upward thrust in hover flight and for forward thrust in forward flight. Hence a tilt mechanism is required to tilt the motors between upward and forward positions.

Flight Controller

The flight controller and associated components enable the user to control the UAV either by manual flying or autonomous flight. Due to the flight modes used, a flight controller is necessary to stabilise the UAV.

Table 2.1: Flight Controller components

Component	Mass (g)
Pixhawk Cube	74
GPS module	47
Power module	13
Airspeed sensor	20
Wiring	20
Telemetry radio	18
Receiver	20
Total weight	212

The weight of Flight controller components is listed in table 2.1. The total weight of 212g is constant and takes as payload throughout the design process.

Payload

The UAV must be able to include an optional payload of a GoPro Hero 6 camera weighing at 116g and a gimbal weighing 150g. This payload can be swapped with other avionics or additional batteries.

2.3 Design methodology

The Tiltrotor VTOL is a hybrid of Fixed-wing aircraft and a Multirotor. The UAV operates in two distinct flight regimes and the design of aircraft for each flight type is very distinct. Forward flight is heavily influenced by aerodynamics where stability and control is achieved by the lifting surfaces. Hover flight is achieved using the thrust produced by the motors. The stability and control of the UAV in this flight mode is done by varying the speeds of the motors using a flight controller.

The design approach for the Tiltrotor VTOL will be to design the UAV to satisfy the necessary conditions for both flight regimes.

- To design the UAV to suit the forward flight regime, the weight of all the components – Airframe, Propulsion, Tilt mechanism, Flight controller and Payload are taken as the overall weight of the aircraft. The motors that tilt forward are considered for thrust. Hence the airframe is now designed as a pure fixed wing aircraft.

- To design the UAV to satisfy requirements for the hover flight, the whole UAV is considered as a multirotor body. The complex aerodynamics associated with the fixed wing aircraft is not considered.

Fixed-wing design

The design methodology for the fixed wing part of the UAV is adapted from design procedures explained by Raymer [11] and Sadraey [12]. The design methods explained in the books are focused on manned fixed-wing aircrafts but still form the framework for fixed-wing aircrafts for any type and size.

The design is broadly classified as conceptual design, preliminary design and detailed design shown in figure 2.1. Conceptual design and Preliminary design of the UAV are explained in chapter ???. Detailed design of the UAV is explained in chapter ??, 4 and ??.



Figure 2.1: Design Overview

Conceptual Design

The first step in the design process of the UAV is the conceptual design. As described by Sadraey [12], this phase of the design involves very less calculations and involves a Systems engineering approach. The conceptual design of the aircraft is done by selection and recommendations. The design process for this step varies with requirements of the aircraft, type of application, available resources, etc. and is mainly dependent on the experience of the designer.

The design flow for conceptual design is shown in figure 2.2. The main purpose of conceptual design is to reduce the analytical work required in selection of aircraft configuration from a very broad design options.

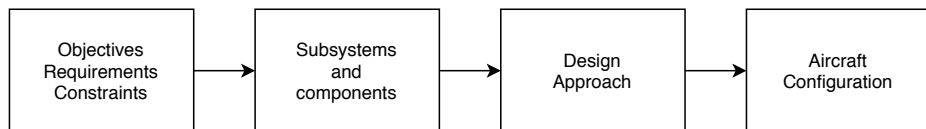


Figure 2.2: Conceptual design

- Conceptual design starts with description of objectives, requirements, constraints and other aspects set in front of the designer.
- Various subsystems involved in the aircraft are listed. The components in each subsystem, their influence on the overall design and extent of work required are studied.
- With the Requirements and Subsystems described, a design methodology is prepared to approach the design problem.
- The resultant conceptual design of an aircraft is the overall configuration of the aircraft. This is done via a selection of various type of configurations available after comparison of their advantages, disadvantages and their influence on other subsystems.

Preliminary design

The aircraft configuration obtained from conceptual design has to be turned into a design with precise calculations. The process involves design of individual subsystems and iterations to verify their performance with the overall design. These iterations require a starting solution that can be improved upon. This starting solution is obtained from preliminary sizing of the aircraft.

Preliminary design uses previously existing norms, statistics and aircraft data to obtain a design with very basic calculations. Some important parameters like weight of the aircraft, thrust rating, endurance are estimated. These values keep changing with every iteration of the design till performance is satisfactory.

Detailed Design

Here the design obtained from preliminary design is subjected to detailed study. Detailed designs of various subsystems and the characteristics of the UAV with these subsystems are studied in iterations. Each iteration will have a design change in individual subsystem to improve the performance of overall design until a satisfactory design is obtained that meets the requirements.

Detailed design has a main process flow to design each subsystem as shown in the figure 2.3 that has been adapted from [12] (pg. 40). There are multiple evaluations in each iteration to assess the UAV as an overall design.

- The main design process involves airfoil selection, wing and tail sizing, fuselage design and control surface sizing.

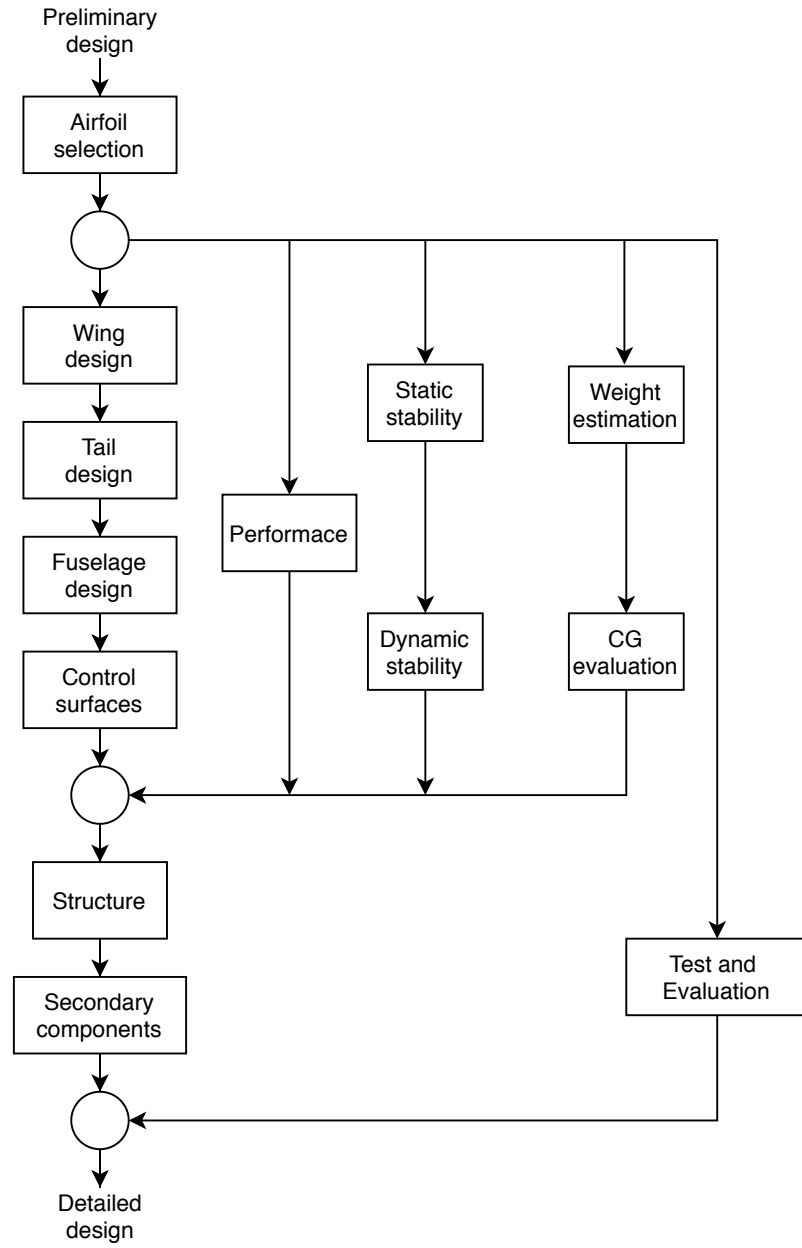


Figure 2.3: Detailed design

- Aircraft mass, Center of Gravity and mass distribution is calculated at various stages of the design.
- Assessment on aircraft performance is done on the UAV's propulsion to calculate endurance.
- Static and Dynamic stability of the UAV is checked to satisfy stability criteria. Con-

trol surfaces are studied for controllability.

- The airframe is evaluated to ensure structural integrity along with secondary components involved.

2.4 Fixed-wing configuration

For the forward flight part of the UAV, a conventional fixed wing configuration is chosen for its simplicity and stability. The flight dynamics of such an aircraft is well described in literature and will reduce complexities in the design.

Wing

The common choices for wing geometry are rectangle, elliptical and tapered wings. While the rectangular profile is simplest in design and construction, the lift distribution is less desirable compared to that of elliptical. An elliptical profile is most efficient in terms of lift generation but curved leading and trailing edges makes construction of the wing complex. A tapered offers similar aerodynamic efficiency as that of an elliptical profile while simplifying the construction. Tapered wing also increases the stiffness of the wing, reduces the weight of the construction and bending moments are lower than in case of a rectangular wing.

High wing configuration increases lateral stability of the UAV and increases ground clearance during take-offs and landings. High wing places the wing spars at the top of the fuselage hence clearing up space for internal components. Hence a high wing with taper is chosen.

Tail

An aft tail is chosen for the aircraft which offers very good stability compared to no tail or canard configurations. Among conventional tail, T –tail, H-tail, V-tail and other types, T-tail is chosen mainly to move the Horizontal tail away from the propeller wash which may cause flutter. This also reduces the effects of downwash from wing on the tail. Downside to choosing a T-tail is the need to structurally reinforce the tail. Hence T-tail is selected.

Fuselage

In case of current design, the components to be housed inside the fuselage is less compared to usual transport aircraft. A full length fuselage avoided to save weight and is limited to

house components and arms for the motors. The tail is extended to required length by using a tail boom.

Landing gear

As described in the requirements, landing gear need for conventional landings during initial flight tests. The estimated weight of the UAV does not allow it to be hand launched and allow for belly landings. Two common types of landing gears used in small sized UAV are Tricyle and Tail dragger configurations. Among these, the tricycle landing gear has better controllability at high ground speeds. A tail dragger will also increase loades on the tail boom. Hence Tricyle landing gear is selected.

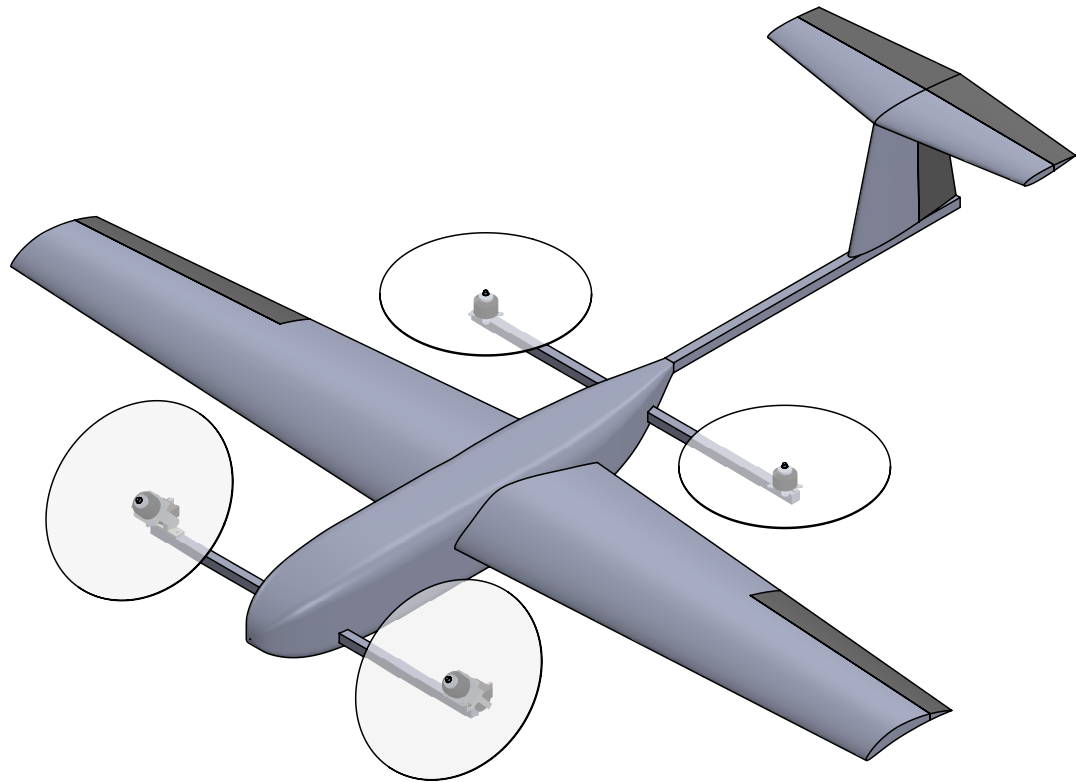


Figure 2.4: Aircraft configuration

Motor Layout

The multirotor aspect of the UAV also influences the fixed wing design. The motors need to have sufficient clearance between the frame and the propellers. The arms for fixing the

motors also have to be accommodated within the airframe. The motor layout is decided based on the weight of the aircraft.

From further analysis, Quad motor layout is selected with two motors in front of the wing and the other two behind the wing in front of tail. This placement is shown in the figure 2.4.

2.5 Motor Layout

Motor Layout used for hover capability in the case of current design is decided based on number of motors required to balance the weight of the aircraft. A constraint in the design process is to use Emax MT3515 650kv motors. Since these motors are designed to be used for Multirotors which operate close to static conditions, the propellers usable for these motors operate near low advance ratios. To keep advance ratio low for forward flight condition, it is favourable to use smaller propellers at high rpm.

The combination of Emax MT3515 650kv motors with APC 12x3.8 SF propellers are used with 6 cell LiPo batteries with nominal voltage of 22.2V. As per data provided by the manufacturer, this combination produces a maximum static thrust of 2.5kg.

Preliminary study for five configurations is conducted to check for feasibility of the design shown in figure 2.5. In case of configurations with co-axial motors, maximum thrust is taken as 1.6 times that of single motor [13]. Ardupilot documentation [1] suggest weight to maximum thrust ratios between 0.5 and 0.7 to ensure proper operation of a multirotor.

The total thrust available in each configuration, maximum and minimum allowable take-off weights (TOW) are calculated and listed in table 2.2.

Table 2.2: Thrust and take-off weights for each configuration

Configuration	Bicopter	Y3	X4	Y6	X8
No. of Motors	2	3	4	6	8
Mass of Motors & ESC (kg)	0.52	0.78	1.04	1.56	2.08
Max total thrust (kg)	5	7.5	10	12	16
Max TOW (kg)	3.5	5.25	7	8.4	11.2
Min TOW (kg)	2.5	3.75	5	6	8

The calculations from motor layouts and preliminary design is studied to select a suit-

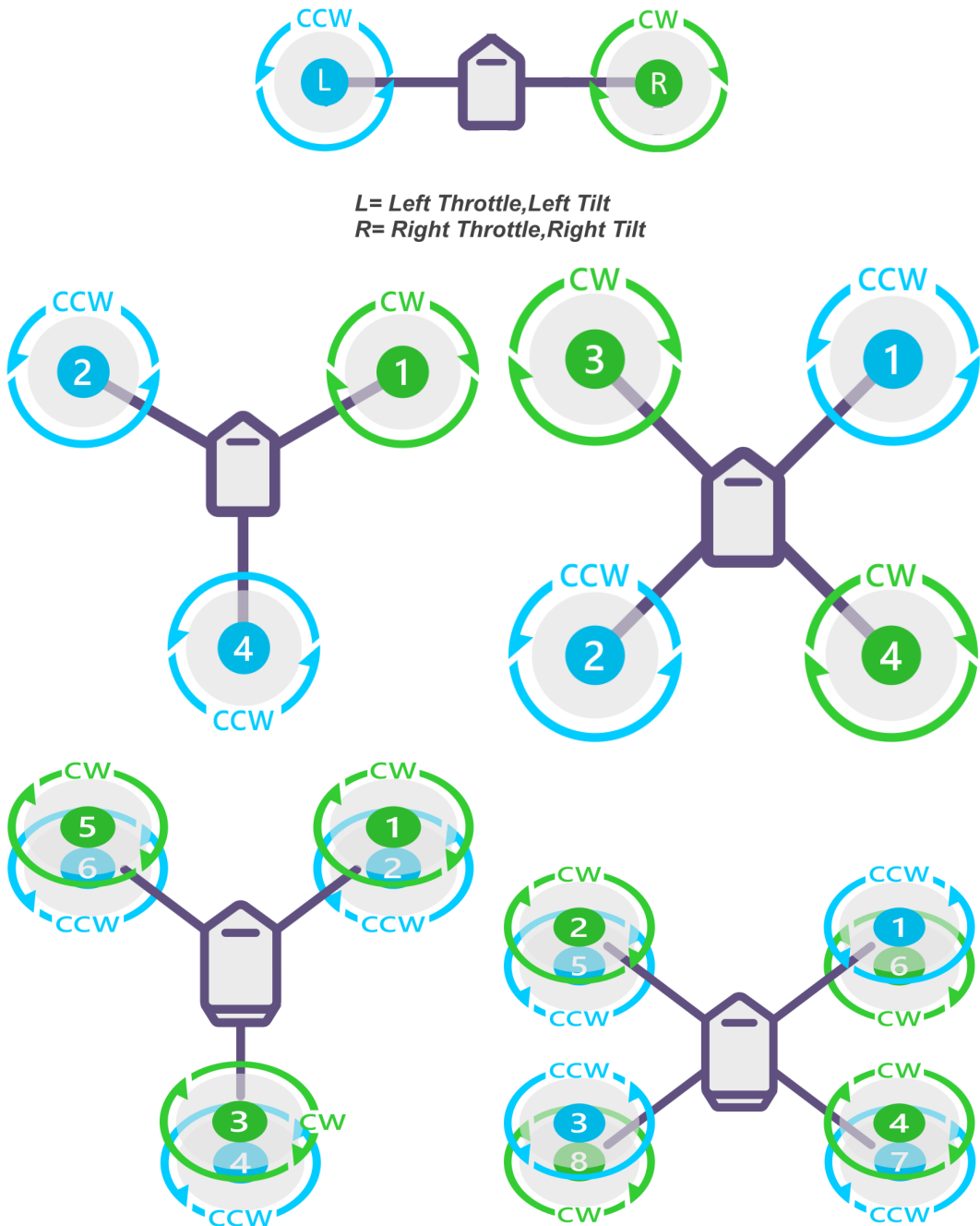


Figure 2.5: Motor layouts considered
Bicopter, Y3, X4, Y6, X8 [1]

able Motor Layout. The X4 motor layout which allows for a take-off weight of 6kg is selected.

2.6 Preliminary Design

Preliminary design establishes an approximate sizing of the aircraft based on previously existing norms, statistics and aircraft data. In the current case, the requirements and size of the aircraft match the UAV designed and manufacture by the author for Bachelor of Engineering final year project at R V College of Engineering in 2017 [14]. Hence preliminary sizing of the aircraft is done based on this UAV.

The UAV, Vayu was designed as a search and rescue drone which included Pixhawk for autopilot, Video transmission equipment and a droppable payload. The current design also includes similar payload except for the droppable payload. But this matches the excess weight of motors and arms required for VTOL capability.



Figure 2.6: Vayu - Search and Rescue drone

Vayu, shown in figure 2.6, had a TOW of 6.5 kg with an endurance of 45min. The airframe construction was of Balsa wood spaceframe with carbon fiber reinforcements. The weight distribution of various components of the plane are listed in table 2.3.

Initial Weight estimation

From the ratios of weight of each subsystem to the total weight of the UAV, an initial sizing of the UAV can be obtained. The weight of components like Flight controller and the Camera payload have already been determined. This can be used to determine the size of the UAV as listed in table 2.4.

Table 2.3: Weight distribution in Vayu

Subsystem	Weight (g)	Percentage
Flight controller	185	2.86
Video transmission	560	8.66
Droppable payload	720	11.14
Propulsion	550	8.51
Batteries	1800	27.84
Landing gear	350	5.41
Wings	900	13.92
Fuselage	950	14.69
Tail	450	6.96
Total	6465	

Table 2.4: Preliminary sizing of UAV

Subsystem	Weight (g)
Flight controller	212
Camera system	270
Propulsion	1040
Tilt Mechanism	350
Batteries	1800
Landing gear	400
Wings	800
Fuselage	800
Tail	300
Total	5972

For the purpose of Detailed design process, the total weight of the UAV is taken as 6kg. During initial design process, weight estimation of the components of airframe is done by using ratio mass of the component to the planar area or surface area.

Chapter 3

Detailed design

The process of detailed design is through iterations. The starting solution obtained from preliminary design is taken and individual components of the airframe are designed. This result is evaluated after each iteration to check if the design as an overall system is satisfactory.

This chapter describes the design of various components of the airframe. It starts with selection of suitable airfoil from literature. The wing and tail are designed from statistics to obtain the geometry of the aircraft. A fuselage suitable for fixing the wing, tail and housing other components is designed. Finally control surfaces are designed. This design is evaluated using procedures described in chapter 4 till a satisfactory design is obtained.

3.1 Airfoil selection

As described in requirements for the UAV, it is not required to be highly manoeuvrable and is not at risk of high angle of attack stalls. Hence high lift airfoils suitable for low Reynolds number flows are considered for the wing.

A selection of airfoils were made from “Summary of Low-Speed Airfoil Data” Volume 1 [15] and Volume 2 [16]. Airfoils are studied low Reynolds number flows between 60,000 and 300,000 which are typical conditions for model aircraft and small UAV. These airfoils are classified for type of application and aircraft for which they are suitable. CH 10-48-13, FX 63-137, FX 74-C15-140, S1210, S1223 from Volume 1 and E423, S1223 RTL from Volume 2 were selected for further study. In addition NACA9412 was also considered due to its similarities with CH 10-48-13 and E423.

The following were the criteria for the selection for airfoil - Aerodynamic performance, Structural integrity and Manufacturability. The airfoils were compared using data from computations using Xfoil code. Xfoil code incorporated into Xflr5 was used in the study for its simplicity and user friendly GUI.

As described in [15] and [16], from previous design experiences [14] and further design process, it found that the wing operates between Reynolds numbers of 150,000 and 350,000. Hence airfoils are compared at an average Reynolds number of 250,000. The analysis is done at Transition criteria, $N_{crit} = 9$ which simulates a wind tunnel with low turbulence [16] (pg. 17). Since turbulence during flight will be higher, performance of airfoils should be better.

For an aircraft with high lift and low manoeuvrability requirements, $C_{l,max}$, α_{stall} , $(C_l/C_d)_{max}$ and C_l at $(C_l/C_d)_{max}$ are taken as selection criteria. The results of Xfoil analysis of these parameters are listed in table 3.1.

Table 3.1: Airfoil comparison

Airfoil	$C_{l,max}$	α_{stall}	$(C_l/C_d)_{max}$	α_{optm}	$C_{l,optm}$
CH 10-48-13	2.0094	11.4	79.6421	3.8	1.5578
E423	1.9880	12.6	78.9943	6.0	1.6731
FX 63-137	1.6745	13.2	95.6405	4.0	1.3141
FX 74-C15-140	2.1158	11.6	84.2656	2.8	1.4974
NACA 9412	1.9713	12.4	87.2296	4.6	1.4702
S1210	1.9128	13.2	94.8870	5.8	1.6795
S1223	2.2540	13.6	79.2878	4.0	1.6365
S1223 RTL	2.1784	12.0	64.2868	5.2	1.6766

To reduce the stall speed of the aircraft, $C_{l,max}$ of the aircraft has to be high. This will also reduce conventional take-off and landing distance during initial flight tests. The stall angle, α_{stall} is also an important parameter to consider as it allows for higher climb rates and turns rates which require high lift.

The aerodynamic efficiency of the airfoil C_l/C_d and the angle of attack where it occurs is critical as it decides the cruise performance of the aircraft. High lift co-efficient, C_l at $(C_l/C_d)_{max}$ reduces the area and weight of the wing.

Although the aerodynamic performance of the S1210 and S1223 airfoils are superior

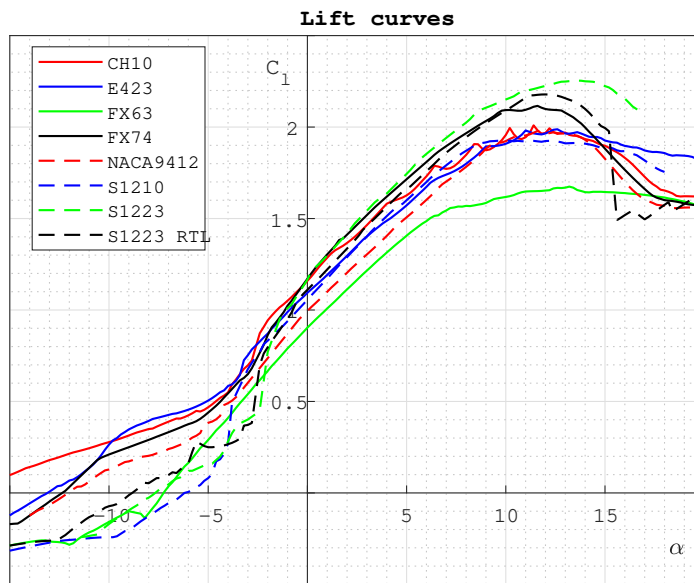


Figure 3.1: Lift curves

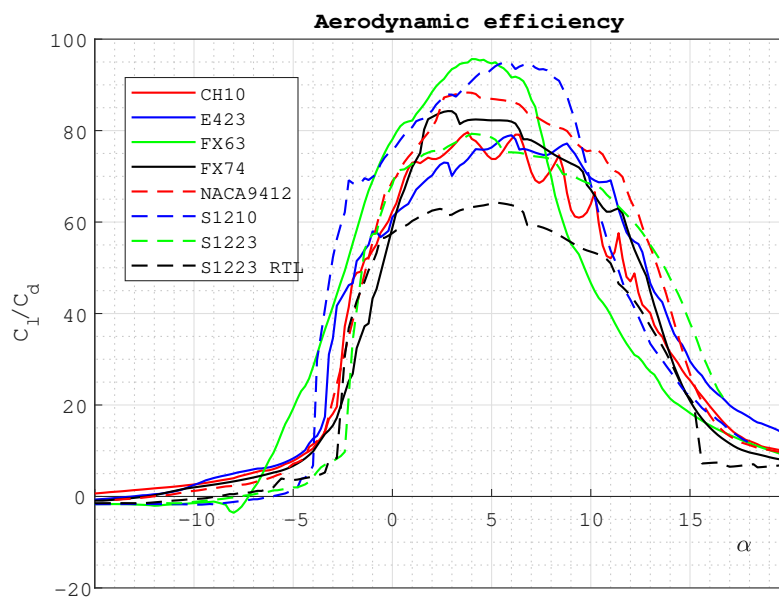


Figure 3.2: Efficiency curves

to others, from structural point of view these airfoils are not preferable. Because balsa wood construction is selected for the airframe, the thickness of the airfoil along the chord

should be sufficiently high to maintain strength and accommodate spars and carbon fibre tubes. The trailing edge of these airfoils are also too thin to be acceptable for this type of construction. CH 10-48-13, E423 and NACA 9412 were chosen for further deliberation considering the above said criteria.

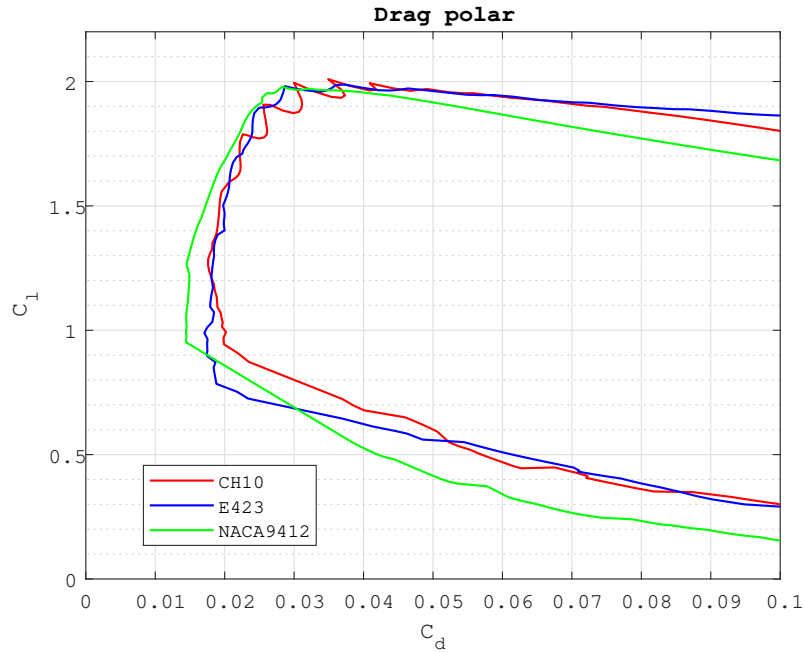


Figure 3.3: Drag polar

Among the Drag curves of the three airfoils, CH 10-48-13 and E423 curves show irregularities. This is an indication of formation of laminar bubbles on the airfoils. All three airfoils offer very similar performance on terms of Lift coefficient and Efficiencies. But NACA 9412 is chosen for the wing due higher aerodynamic efficiency and smoother Drag curve profile at chosen Reynolds number.

For the horizontal stabilizer, symmetric and low cambered NACA series airfoils of 12% thickness were selected. For the vertical stabilizer, a symmetric airfoil is selected. NACA 0012 is selected for both horizontal and vertical stabilizers. Generally horizontal stabilizer is set at a negative angle of attack that is calculated from longitudinal stability requirements. If the setting angle is very high on the negative side, an inverted airfoil of slight camber can be used.

3.2 Wing design

The wing being the most important part for forward flight is the main contributor of lift and drag. The design of the wing influences and is influenced by the design of empennage, fuselage size and structure of the airframe. Hence wing design is an iterative process. A good preliminary sizing of the wing is very essential for this iterative process.

Wing vertical location

The wing placement is has no requirement from operation point of view. But because the wing box will involve two carbon fibre tubes running through fuselage, a mid-wing placement will interfere with components inside the fuselage. High wing configuration chosen for its dihedral effect and better clearance while take-off and landing.

Wing area (s)

The size of the wing is a requirement of amount of lift developed and in turn the weight of the aircraft. Hence initial weight estimates are taken and iterated to obtain the size of the wing. Along with the effect of finite wing, the presence of a fuselage and negative setting angle of the horizontal stabilizer reduce the overall lift coefficient of the aircraft. Although these effects can only be determined after complete sizing of the aircraft, the overall lift coefficient can be predicted from past designs of similar aircraft.

The overall lift coefficient, C_L of the aircraft is calculated from Lift force, L of the aircraft and Wing planform area, s as reference. It is given by

$$L = \frac{1}{2} \rho V^2 s C_L$$

From the aircraft designed in [14], the overall lift coefficient of the aircraft is taken as $C_L = 0.8$ for initial sizing of the wing. The sizing is refined if required in iterations after fuselage and tail sizing is done.

Other parameters are arrived at in the previous sections: $V = 15\text{m/s}$ from operation requirements and constraints. $\rho = 1.140\text{ kg/m}^3$ from environment conditions ($T = 35^\circ\text{C}$ and $h = 100\text{ m}$). From preliminary weight estimates and further iterations, total weight of the aircraft is arrived at 6 kg .

Taking cruise condition as criteria for wing size estimation, Lift can be equated to

weight. This gives projected wing area for 0.57368 m^2 . This result is analysed and modified further down the design process to 0.55 m^2 .

Aspect ratio (AR)

By increasing the aspect ratio of wing, Lift curve slope of the wing increases and induced drag reduces. But with increase in AR, roll damping increases with reduces the manoeuvrability of the aircraft. High aspect ratio also increases bending moment at the root of the wing, which requires higher structural strength and hence increasing weight.

Aspect ratio is selected from historic data given in [11] and [12]. Reymer lists subsonic aircraft types with AR ranging from 5 to 8 [11] (pg. 47). Sadreay suggests AR for General aviation aircraft between 5 and 9, and for Low-subsonic transport aircraft between 6 and 9 [12] (pg. 198).

Another constraint for the aspect ratio of the wing is its span. Because the chosen method of construction for the wing is balsa wood ribs with carbon fibre tubes, wings span has to check. The wingspan is should also have modularity and facilitate transport. Considering the wing size and above mentioned constraints, wingspan is fixed at 2m.

This results in a wing with span, $b = 2\text{ m}$; $AR = 7.2727$; and mean geometric chord, $c_{geo} = 0.275\text{ m}$. This conforms to the suggested AR in literature.

Taper ratio (λ)

Tapering the wing changes the lift distribution along its span and hence modifies the Oswald span efficiency factor (e). A tapered wing has lower induced angle of attack at the tips, increasing the tendency to tip stall when combined with a backward swept wing.

Taper also has structural advantages as it thickens the airfoil section close to the root. It also moves the lift force closer to the root, reducing bending moments. But for the size of the wing developed, the tip airfoil section should be large enough to accommodate carbon fibre tubes and spars for the structure.

Considering the size limitation at wingtips, tip chord (c_t) of 0.2 m and root chord (c_r) of 0.35 m is set. This results in taper ratio, $\lambda = 0.571$ and $e = 0.986$. In comparison, a taper ratio of 0.45 has highest efficiency factor of about 0.997. Lift distribution and efficiency

factor of the wing are arrived at using Lifting line theory (LLT) at flow velocity of 15 m/s.

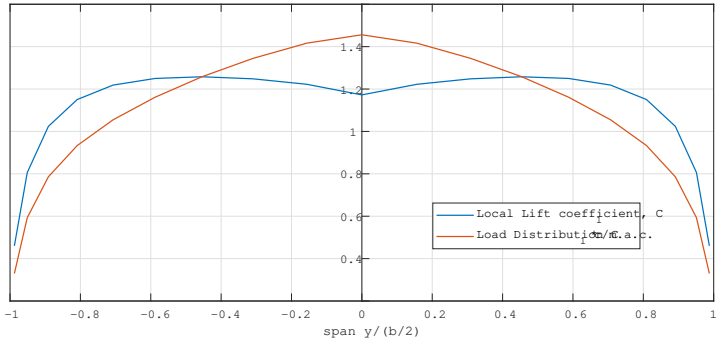


Figure 3.4: Spanwise Lift Distribution

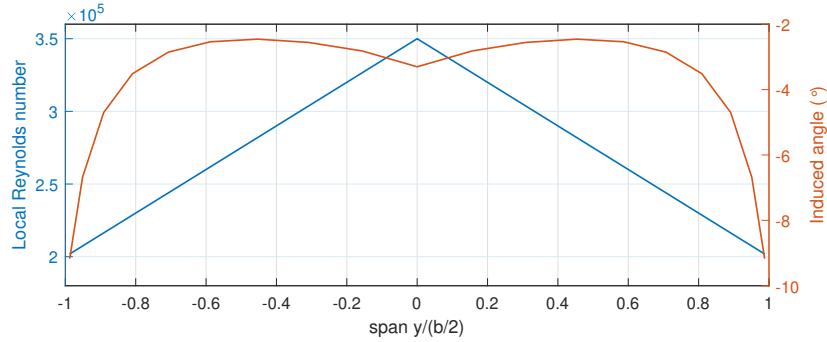


Figure 3.5: Spanwise Reynolds number and Induced angle of attack

Although lift distribution on the wing changes when fuselage is included and further changes have to be made to improve efficiency factor, current taper was found satisfactory and close to statistics presented in [11] (pg. 57).

Twist

Any further optimisation in Oswald span efficiency factor would require either geometric or aerodynamic twist. Although this would improve the performance of the wing, structure design of the wing and airfoil placement will be complicated for manufacturing.

Sweep (Λ)

For the low-subsonic flow conditions of the aircraft, wave drag reduction is not needed. Sweep can be introduced to alter lateral stability of the aircraft or to move the neutral point away front the root of the wing but these two requirements were not found to be necessary.

A highly swept wing will also complicate the structure. Hence, sweep along quarter chord $\Lambda_{c/4}$ is set at zero to allow for easy placement of carbon fibre tubes and balsa spars.

Dihedral (Γ)

Dihedral in the wing will help stabilise the aircraft in roll axis and in spiral mode. But will reduce stability in Dutch roll mode, which in turn would require larger vertical stabiliser. Dihedral will also require bent spars to reinforce the wing and carbon fibre tubes cannot be used to strengthen the wing.

For UAVs that are flown in line of sight or using an autopilot, spiral mode instability is not an issue. More over a high configuration already provides some amount of dihedral stability. Autopilot on the aircraft will also improve self-levelling in roll axis. Hence no dihedral angle is given to the wing.

Wing incidence (i_w)

Wing incidence or wing setting angle is essential for cruise performance of the aircraft. Cruise performance is considered to maximise either Range or Endurance. Because the aircraft's primary purpose is to study and develop VTOL capability and no mission profile is set up, the performance requirement is set to be partway between both.

Wing incidence has to be decided based on performance of whole aircraft and is decided after iterations done with fuselage and tail. This is simplified by setting fuselage at zero incidence or angle of attack and Horizontal stabiliser set at angle solely based on stability criteria.

Performance analysis was done to maximise C_L/C_D using Xflr5. The results and procedures are discussed in chapter 4. It was decided to set wing incidence at 5° .

3.3 Tail design

An important aspect in design of fixed wing aircrafts is that the aircraft itself is stable without a flight controller as compared to a multirotor. Although a controller can make an unstable aircraft stable to an extent, inherent aerodynamic stability definitely helps. A stable fixed wing aircraft is easier to tune and control.

A conventional aircraft derives its stability mainly from the tail. The horizontal stabiliser makes the aircraft stable in longitudinal or pitch axis and the vertical stabiliser in the directional or yaw axis. The tails also provide trim and control in these respective axes.

Design Methodology

The parameters for the tail design is taken from “Empennage statistics and sizing methods for dorsal fins” [17] where suggestions from a number of authors have been listed and analysed. The design is also influenced by parameters listed by Reymer [11] and Sadraey [12].

Tail sizing is done using Tail volume coefficients. These non-dimensional parameters represent the stability offered by horizontal and vertical tails with relation to the wing geometry.

$$V_H = \frac{s_H l_H}{s_w c_w}$$

$$V_V = \frac{s_V l_V}{s_w b_w}$$

The results from these coefficients are further analysed for stability and necessary corrections are made. Tail setting angle is set for trim angle of attack from static stability analysis using Xflr5.

Configuration

As discussed in conceptual design, T-tail configurations is used to increase tail efficiency and put the horizontal stabiliser away from prop-wash. Because the vertical stabiliser holds the horizontal stabiliser up, it experiences higher loads than in a conventional tail. Also the tail has to be mounted on a boom which makes mount the tail harder from structural stand point. The vertical tail is fixed permanently to the boom and horizontal tail is made detachable.

Tail arm (l_H and l_V)

Tail arm is the distance between Aerodynamic centre of the wing and each tail. Tail arm must be set to optimise the configuration to minimise drag, improve structural strength, stability and controllability. Such study would require multidisciplinary optimisation and is not necessary for this project. Determining tail arm for the aircraft here is done based on historic data.

Raymer [11] (pg. 112) and Sadraey [12] (pg. 276) list typical tail arm to fuselage length ratios for aircrafts with different engine placements. This list considers engine location and tail arm for the purpose of Centre of Gravity balance. The aircraft being designed does not conform to any classification in the list.

Sadraey (pg. 298) also suggests a method where an optimal tail arm found to minimise wetted area of Horizontal tail and Fuselage, and hence reducing parasitic drag. But this method cannot be used for in current design as the fuselage length is fixed and tail is fixed with a boom. Also this method does not consider wetted area on the vertical tail and structural implications. The aircraft operates at very low Reynolds number considerations were laminar effects of flow are very dominant. Hence a consideration while setting tail arm is to make sure Reynolds number at the tail is sufficiently high when considering very long tail arms.

Due to lack of methods to find optimal tail arm for small UAVs and model aircraft, tail arm is chosen from statistics of model aircraft designs. Usually tail arm is 2 to 4 times the wing MAC for general purpose model aircraft [10] (pg. 33). For the purpose of initial sizing, tail arm of 1m (approximately 3.5 times MAC of wing) is selected and varied during successive iterations.

Tail volume coefficients (V_H and V_V)

Raymer (pg. 112) and Sadraey (pg. 303) list typical volume co-efficient for different types of aircrafts. The designed aircraft will require similar stability and controllability as Sailplanes (gliders), Homebuilt and General Aviation aircrafts. In forward flight, aircraft will be powered by two motors located at the front.

Horizontal volume co-efficient between 0.5 and 0.7 for the above aircrafts and 0.8 for twin prop general aviation aircrafts is suggested. Hence tail volume co-efficient of 0.65 is considered for initial sizing of the aircraft.

Vertical volume co-efficient between 0.2 and 0.4 for the above aircrafts and 0.7 for twin prop general aviation aircrafts is suggested. Very high tail volume for vertical tail suggested to provide sufficient stability and control in case of engine failure on one side. In the current design with very low dihedral stability, spiral stability will be affected if large vertical tails are used. And in case of motor failure, the aircraft will have to glide and land.

Hence a volume co-efficient of 0.045 is considered.

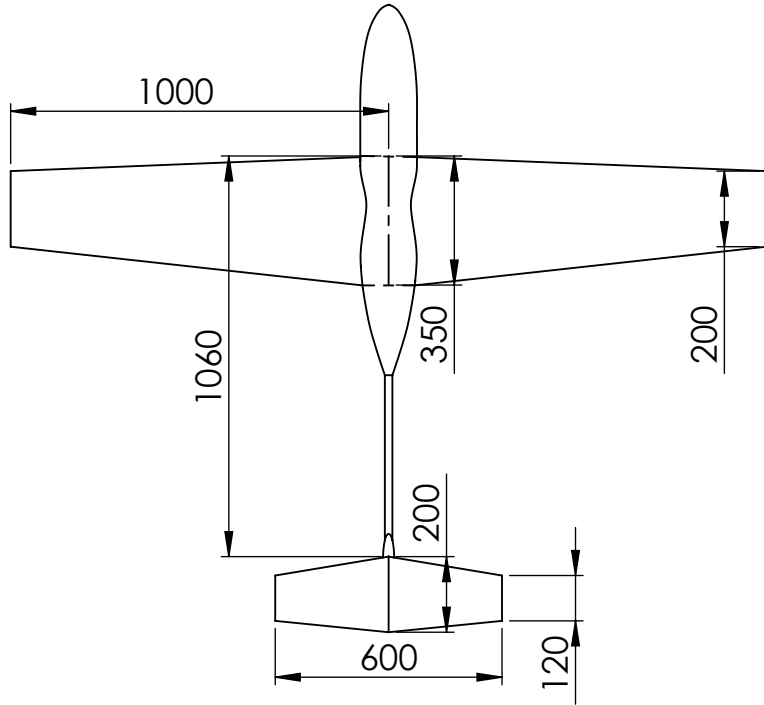


Figure 3.6: Tail size and placement with respect to wing

Aspect ratio (AR) and Taper ratio (λ) For low aspect ratio wings, slope of the lift curve decreases but stall angle increases. Since tails do not operate at max lift condition at cruise and are mainly for control, low aspect ratios are preferred for tails. Generally, horizontal tail AR between 12 and 23 times the aspect ratio of wing and vertical tail AR of half of horizontal tail AR is used for model aircraft [10] (pg. 33). Reymer suggests AR_H of 3 - 5 and AR_V of 0.7 – 1.2 for T-tails (pg. 76).

Tapering the tail promotes tip stalling. Hence taper ratio on tails must be higher compared to the wing. Reymer suggests λ_H of 0.3 – 0.6 and λ_V of 0.6 - 1.0 for T-tails (pg. 76). Lower aspect ratio and higher taper ratio for T-tail increases the structural strength. End-plate caused by horizontal tail increases its effective span and compensates for lower aspect ratio.

Sweep (Λ) and Dihedral (Γ)

Sweep on the tail is not a required for the aircraft. A sweep is set such that hinge line for

control surfaces are straight and perpendicular to fuselage axis. From structure requirements, no dihedral is given to the tail sections. This allows for use of carbon fibre tubes along the span.

Tail incidence (i_H and i_V)

Tail incidence comes from trim requirements in longitudinal and directional axes. Since the aircraft is symmetric in the x-z plane, forces are symmetric. No incidence is given for the vertical tail.

It is possible to calculate Incidence angle for horizontal stabiliser using longitudinal trim equation, but will require further CFD analysis. Hence incidence angle is found through iterations using VLM analysis in Xflr5. Incidence for the horizontal stabilizer is set at $i_H = -1^\circ$ for $\alpha_{trim} = 0.277^\circ$.

3.4 Fuselage design

Fuselage design is the third major step in detailed design process after wing and tail design. The design criteria for fuselage is to house necessary components and allow for attaching wing, tail and arms for propulsion. While doing so, weight of the fuselage and drag caused by it must be reduced. Another factor affecting fuselage design is to balance the centre of gravity (CG) of the entire aircraft at desired location. This primarily affects the length and placement of fuselage with respect to wing and tail. A special requirement in present case is also to accommodate arms where the motors are mounted.

Design Methodology

Fuselage in broad can be considered to have the following three parameters to define its design.

- The cross section of the fuselage is designed based on the components to be housed and the size of the ribs used in the construction.
- The length of the fuselage should be sufficient to house both components and the arms of motors, but be as minimal as possible to reduce weight and drag.
- The placement of fuselage with respect to wing and tail decided from the CG requirements. The resultant CG of the entire aircraft should match the stability requirements.

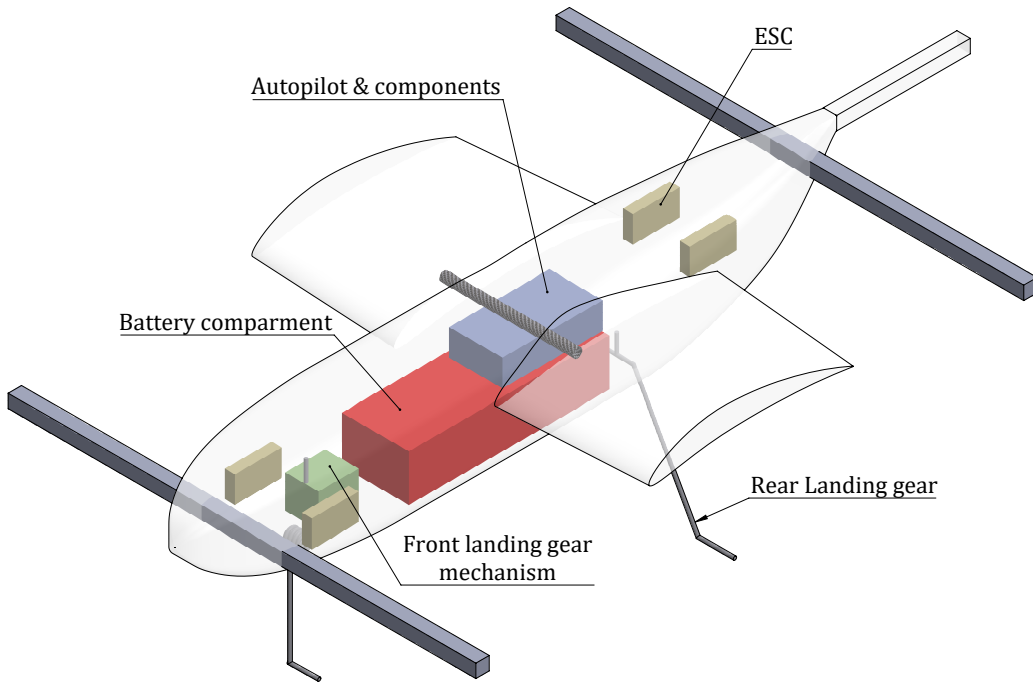


Figure 3.7: Components inside Fuselage

The placement of components inside the fuselage is shown in the figure 3.7.

Fuselage sizing

The constraining factor for determining the cross section of the fuselage is the height required to accommodate Flight controller and Batteries under the wing box inside it. For best performance, the flight controller has to be placed as close to CG as possible. This is avoid accelerometers from picking up disturbances from angular movements. Due to its unique configuration and motor placement, it requires batteries to be placed under the wing for CG balance. The structure also requires wing box consisting of two carbon fibre tubes to pass through the fuselage.

To accommodate the wing box, flight controller and batteries fuselage outer cross-section is set at 150mm x 150mm. The size of ribs at each section is 15mm and is changed if required during structure design. The fuselage length should be sufficient to accommodate the required components and to fix the arms for the motors. The arms are located at a distance of 750 mm from each other. To fix them on the fuselage, a length of 950 mm

is needed. The fuselage at its rear side is tapered upward to shift the arm and tail boom upwards for the T-tail.

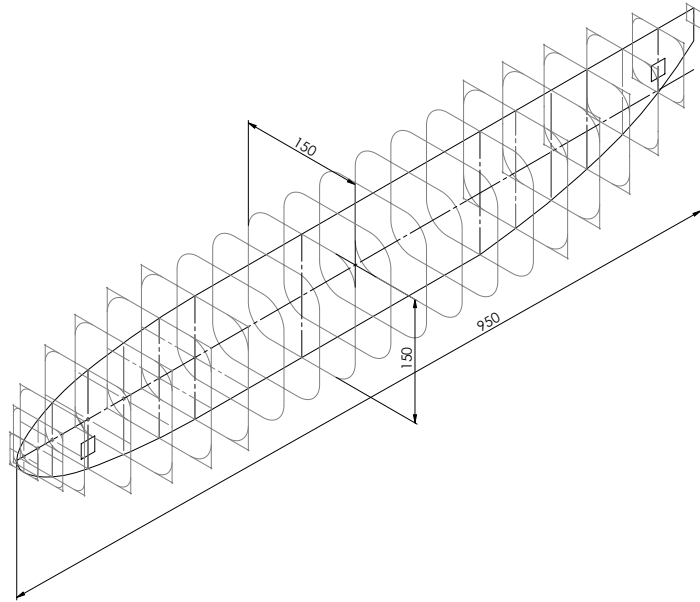


Figure 3.8: Fuselage sizing

The design of the fuselage is also influenced by the location of Center of Gravity of the UAV. The fuselage must accommodate all the components such that the CG requirements from Static and Dynamic stability are satisfied. This process is explained in section 4.3.

3.5 Control surface design

Control surface design is based on statistics given in [11], [12], [10] and [17]. The size of the control surfaces depends on the type of aircraft being designed and the handling qualities required. In case of small UAV, norms and regulations for handling qualities are not well described. Hence a pure statistical approach is used for Control surface design.

Aileron Design

Aileron size and placement influences the roll control of the UAV. The parameters for sizing the aileron are taken from statistics of model aircraft given in [10].

Aileron span is set at 0.45m on each wing towards the tip of the wings and a uniformly varying chord of $0.25 c_w$ is selected as shown in the figure.

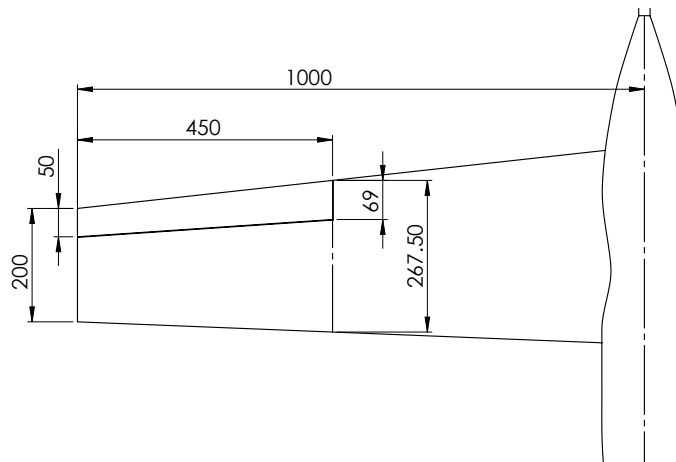


Figure 3.9: Aileron size in mm

Elevator and Rudder Design

Elevator and Rudder size determine the pitch and yaw control of the aircraft. The parameters for elevator and rudder sizing are taken from [17] which gives statistics of tail design on various aircraft.

Both elevator and rudder are design to be full spanned with uniformly varing chord of $0.4 c$ as shown in the figure.

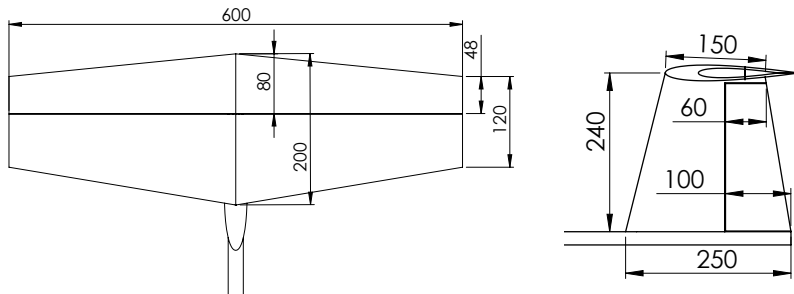


Figure 3.10: Elevator and Rudder size in mm

3.6 Aircraft structure

Detailed design concludes with designing of the individual parts that will be used for the fabrication of the UAV. Two common types of structures are a monocoque design and a spaceframe design. A monocoque frame uses the outer skin of the frame to handle the loads and a space frame uses a cage like structure to handle the loads. By comparison a

spaceframe structure is lighter and easier to fabricate. If damaged, it is easier to fix compared to a monocoque frame.

This phase of the design involves drafting and modelling individual parts in Solidworks. Modelling of the parts is done through a process of checking the dimensions of the parts like secondary components, size of the motors, servos and batteries. The parts for fabrication of the frame are modelled and assembled using Solidworks.

Structure design

The airframe structure must be light as possible while being able to handle loads during all phases of flight. An optimal design of such structure would require Finite Element Analysis and is a study on its own, hence the structure designed based on experience from previous designs like Vayu [14].

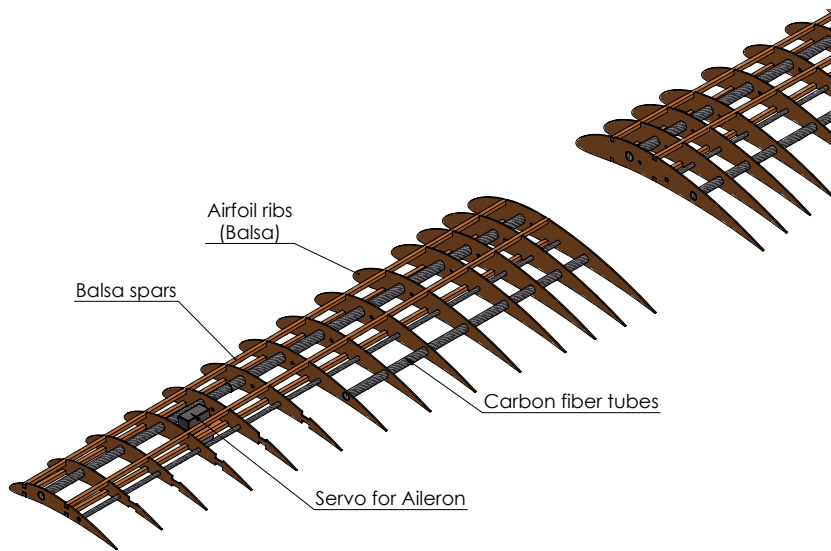


Figure 3.11: Wing structure

Tilt Mechanism

In the case of a Tiltrotor VTOL, the motors or a subset of motors are used for both upward thrust in hover flight and for forward thrust in forward flight. Hence a tilt mechanism is required to tilt the motors between upward and forward positions.

The tilt mechanism is designed out of Aluminium and will be manufacture using CNC

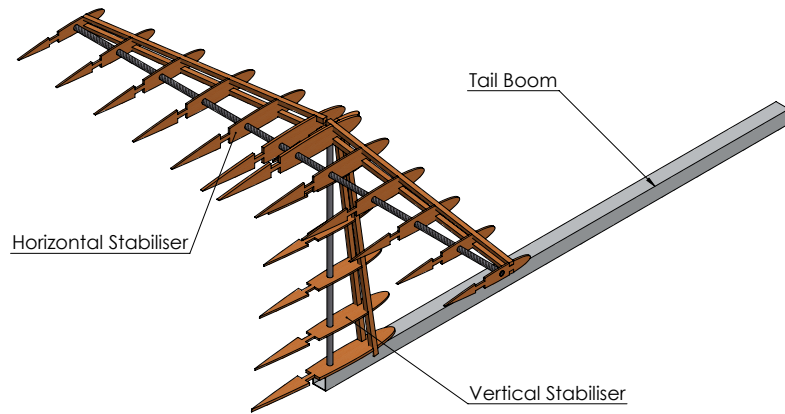


Figure 3.12: Tail structure

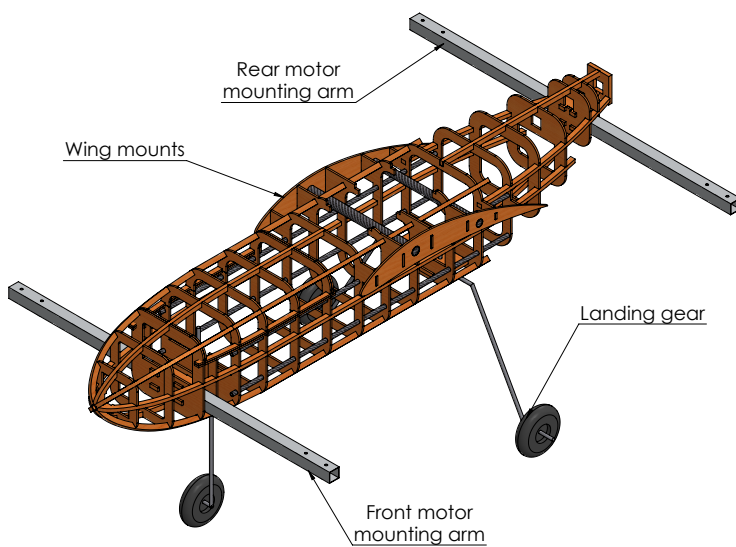


Figure 3.13: Fuselage structure

milling. A servo is used to tilt the motor between upward and forward positions.

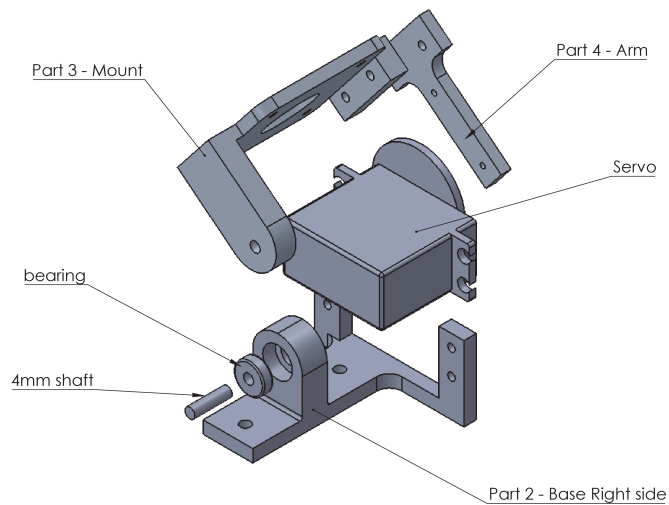


Figure 3.14: Tilt mechanism

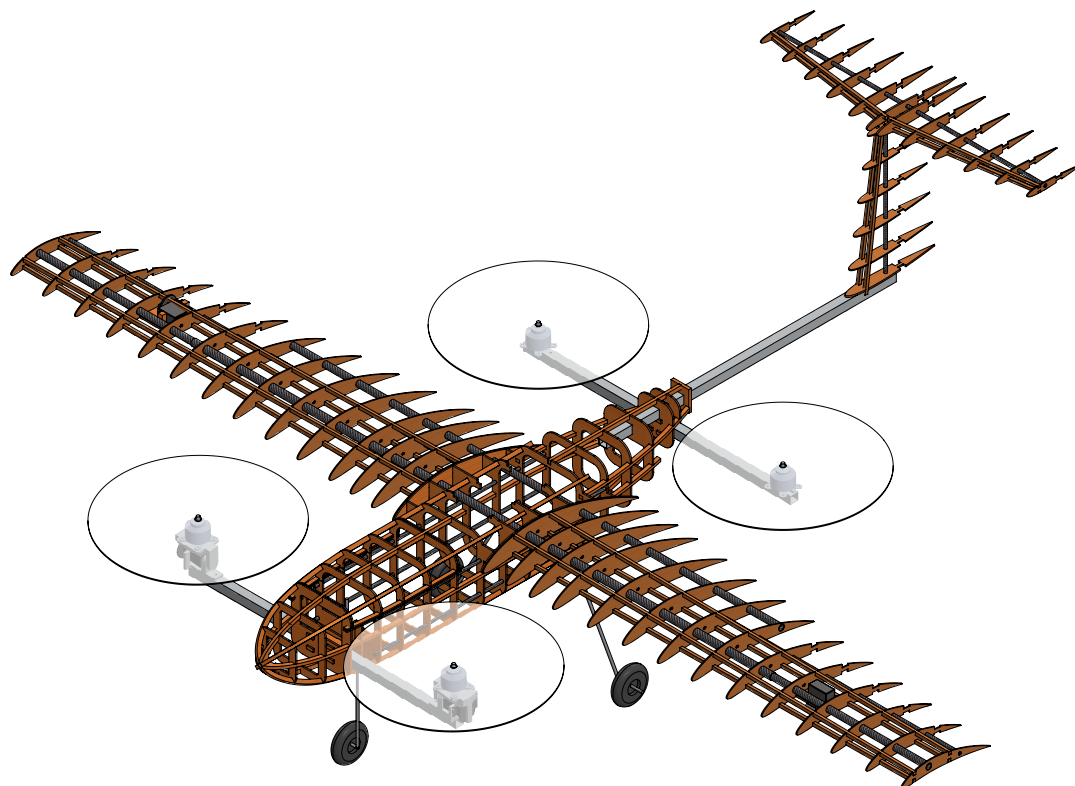


Figure 3.15: Aircraft assembly

Chapter 4

Performance and Stability

The design obtained after Wing and Tail sizing has to be analysed for Performance and Stability. This chapter presents the process of evaluation using Xflr5 to determine stability and performance of the aircraft. For stability analysis, location of CG is also found using analytical calculations.

4.1 Xflr5 Analysis

The aerodynamic study of the aircraft can be done in one of these ways - CFD analysis, wind tunnel tests and flight tests. But during initial stages of design, it is more practical to used CFD analysis. CFD methods like Finite Volume Methods used in most commercial packages are computation intensive and requires complex meshing for the given UAV design. Hence Vortex Lattice Methods are used for preliminary studies using Xflr5.

Xflr5 is an open source software that can be used to study airfoils, wings and planes operating at low Reynolds numbers. It uses Xfoil code for Airfoil analysis with viscous boundary layers and can predict stall characteristics. It also can be used for study of flow around lifting surfaces using Lifting Line theory. The aspect of interest for this study is its ability to study Plane configurations using Vortex Lattice Method (VLM). The software can also be used to study stability characteristics of an aircraft. Although VLM methods used have shortcoming when predicting viscous properties of the flow, the results obtained are good enough for initial aircraft designs and modelling.

The aircraft obtained from detailed design is modelled in Xflr5. The contribution of landing gear, motors and arms are neglected in the analysis. They have to be accounted for extra drag by providing a safety margin in engine thrust. The software is not capable of

analysing the effects of propeller wash.

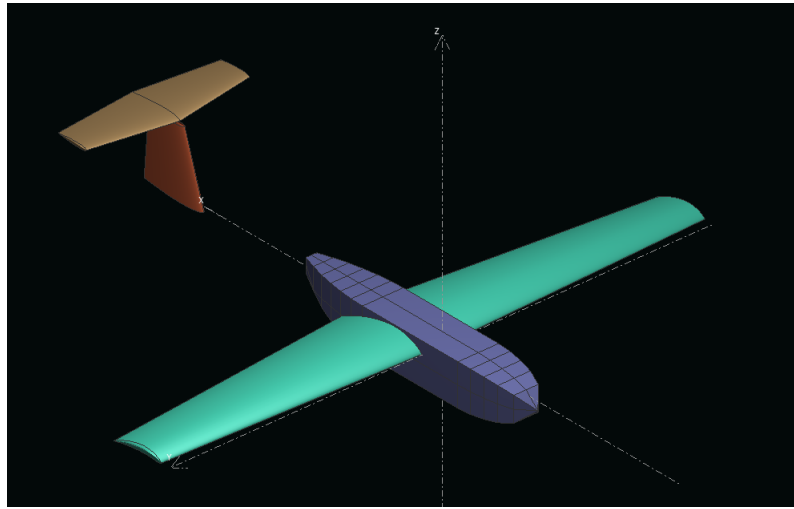


Figure 4.1: Aircraft geometry modelled in Xflr5

Prior to aircraft analysis, the airfoils used for wing and tail are analysed using Xfoil code built into Xflr5 at various Reynolds numbers. The CG location, mass of the aircraft and operating conditions are specified. A viscous analysis using VLM is done using the UI provided. Figure 4.2 shows the visualisation of streamlines and figure 4.3 shows the pressure distribution in the aircraft.

The interface also gives graphs of lift curves, pitching moment co-efficient and drag profiles that can be used to study performance and static stability of the aircraft. Xflr5 also has an option to study the dynamic stability which gives the root locus plots for flight modes and can determine stability derivatives.

4.2 Performance

Performance of the aircraft deals with translational motion of the aircraft where aerodynamic forces and propulsion are evaluated. In the current case, the design is evaluated only for steady level flight due to complexities in the type of propulsion used. The electric motors with fixed pitch propellers used do not provide propulsive power. Hence the performance evaluation is only done to check if the powerplant used is satisfactory.

Propulsion

The combination of Emax MT3515 650kv motors with APC 12x3.8 SF propellers are used

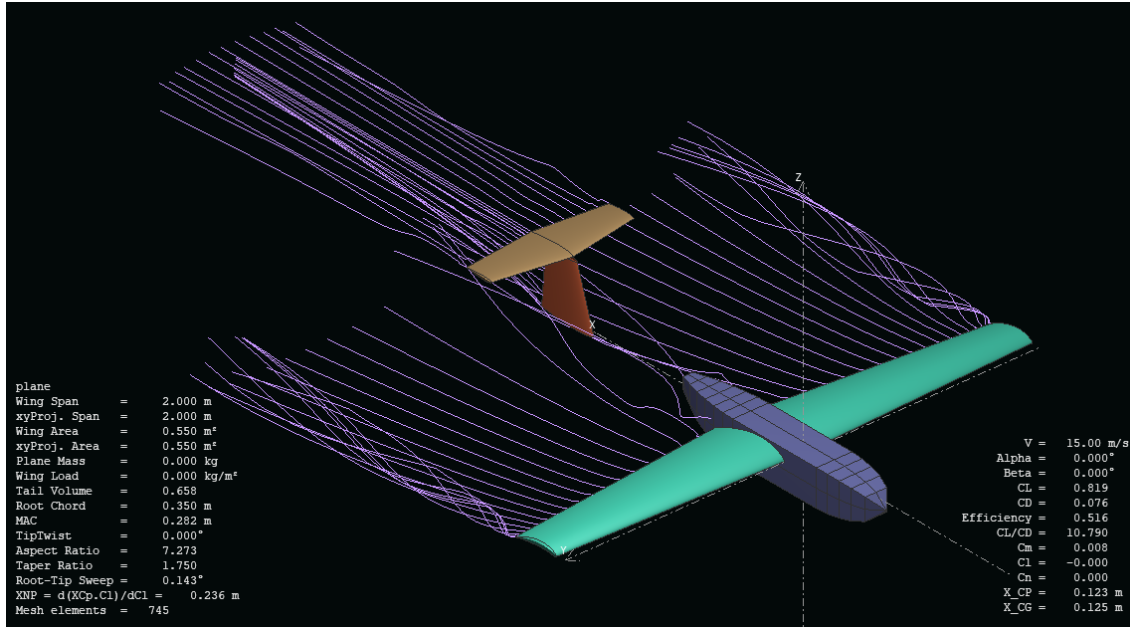


Figure 4.2: Flow visualisation using Xflr5

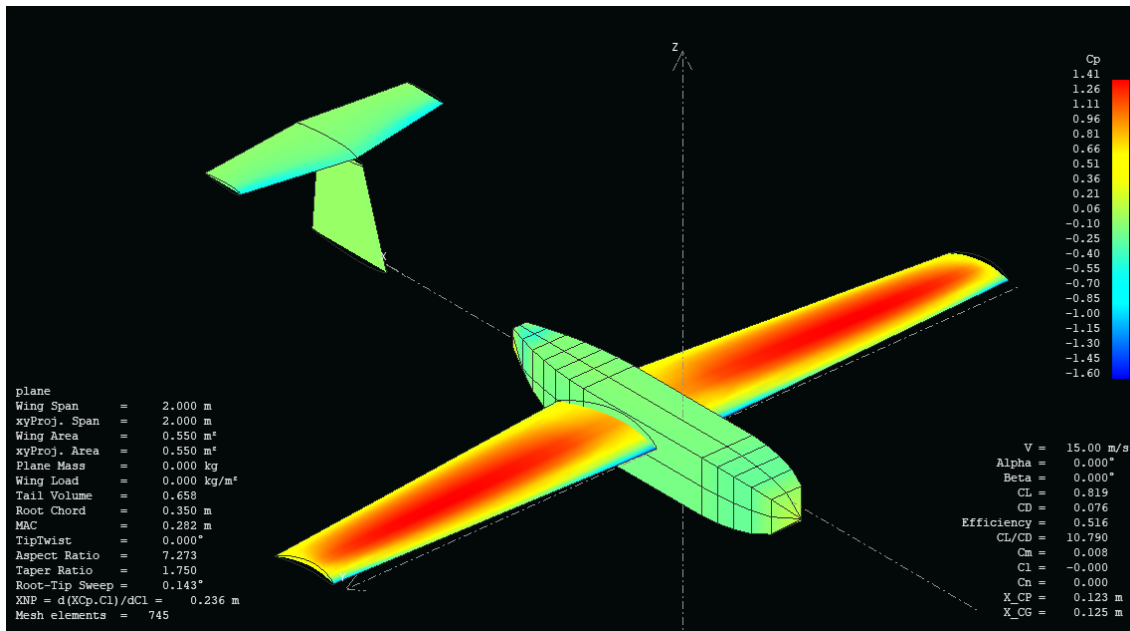


Figure 4.3: Pressure distribution on the aircraft surfaces

with 6 cell LiPo batteries with nominal voltage of 22.2V. As per data provided by the manufacturer, this combination produces a maximum static thrust of 2.5kg. But as the flight speed increases, the maximum thrust available reduces till the effect of wind milling occurs. Wind milling occurs when the velocity of external flow is so high, propeller will be

operating at zero angle of attack.

Propeller data for APC 12x3.8 SF propellers is taken from the manufacturer's website [18]. The motor operates at a maximum speed of 10000 rpm at static conditions which increases with flow velocity. As a factor of safety, 9000 rpm is taken as maximum speed for the propeller across all flow speeds and maximum thrust available is obtained 5.1.

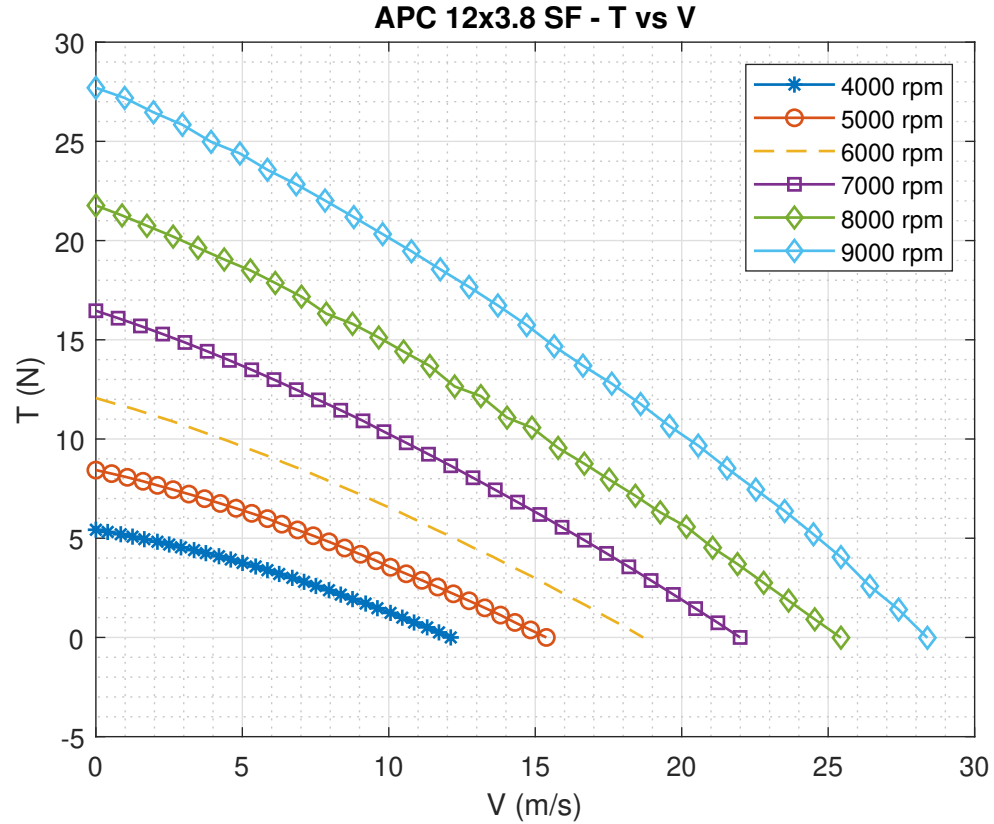


Figure 4.4: Thrust available vs Flight speed

Drag and available thrust

From Xflr5 analysis, drag force on the aircraft at different speeds is calculated for steady level flight. At designed condition with cruise speed of 15 m/s, drag force of 5.45 N acts on the UAV. In case of forward flight, front two motors together provide thrust.

Matching the drag and thrust profile shows that at steady level flight, the motors operate at 6000 rpm each. Because the propulsion used for the VTOL requirement, the aircraft will have much higher thrust than required as evident from figure 4.5.

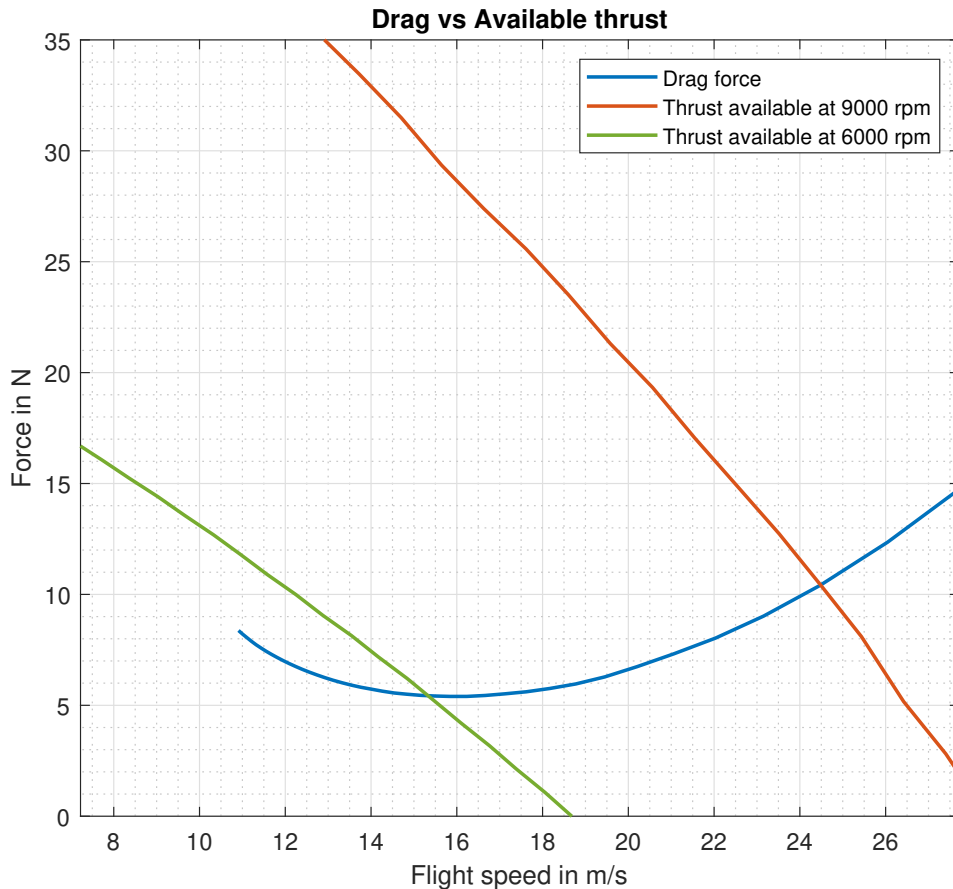


Figure 4.5: Drag vs available thrust

4.3 Centre of Gravity

Once the aircraft geometry has been designed, the stability and control characteristics of the aircraft depends on the position of Centre of Gravity of the aircraft. With design of fuselage and distribution of components inside it, location of CG must match the required position determined from stability studies.

During initial stages of detailed design, CG calculations are done in an Excel sheet. Mass of each component and its location is listed. Total mass and total mass moment are calculated to find the CG of the configuration. The aircraft is symmetric about x-z plane

and components for the most part are placed in symmetric. Hence CG is assumed to be along the plane of symmetry.

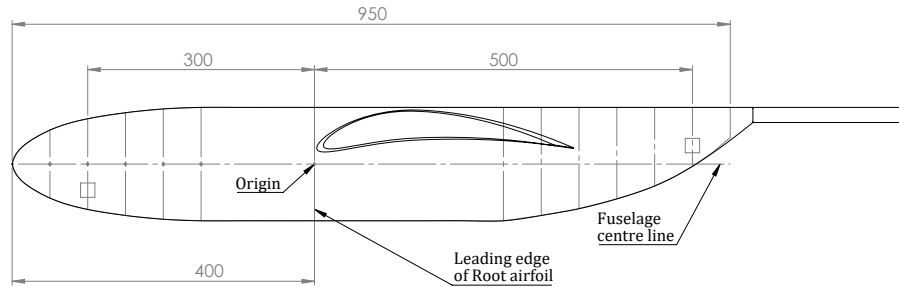


Figure 4.6: Coordinates for CG Calculations

The intersection of leading edge of the root airfoil and fuselage centre line is taken as origin. X-axis towards the nose of the aircraft, Y-axis towards right wing of aircraft and Z-axis towards bottom of the aircraft is taken for CG calculations. The co-ordination convention is shown in figure 4.6.

Table 4.1 shows the excel sheet used to calculate the position of the Center of Gravity of the UAV. The battery position has a wide space which can be used to adjust the CG of the whole UAV. Hence the CG of the whole UAV is calculated in table 4.2.

Table 4.1: Center of Gravity calculations

Subsystem	Component	Mass (g)	x (cm)	z (cm)	m-x (g-cm)	m-z (g-cm)
Propulsion	Motor 1	185	25	0	4625	0
	Motor 2	185	25	0	4625	0
	Motor 3	185	-50	0	-9250	0
	Motor 4	185	-50	0	-9250	0
	ESC 1	75	25	0	1875	0
	ESC 2	75	25	0	1875	0
	ESC 3	75	-45	0	-3375	0
	ESC 4	75	-45	0	-3375	0
Tilt Mechanism	Arm 1	250	25	0	6250	0
	Arm 2	0	-50	0	0	0
	Servo 1	100	25	0	2500	0
	Servo 2	0	-50	0	0	0
Landing gear	Front	220	25	10	5500	2200
	Back	180	-25	10	-4500	1800
Flight controller	Pixhawk Cube	74	-12.5	0	-925	0
	GPS module	47	-12.5	10	-587.5	470
	Power module	13	-5	0	-65	0
	Airspeed sensor	20	30	0	600	0
	Wiring	20	-15	0	-300	0
	Telemetry radio	18	-20	0	-360	0
	Reciever	20	-20	0	-400	0
Camera	GoPro	119	-10	0	-1190	0
	Gimbal	150	-10	0	-1500	0
Control servos	Wing	80	-16	8	-1280	640
	Tail	80	-100	8	-8000	640
Airframe	Wing	800	-16	8	-12800	6400
	Fuselage	800	0	3	0	2400
	Tail	200	-100	8	-20000	1600
Power	Battery	1800	-15	0	-27000	0

Table 4.2: Center of Gravity of the UAV

Total Mass	6031
total m-x	-76307.5
x cg	-12.65
total m-z	16150
z cg	2.68

4.4 Static stability

Static stability is the tendency of an aircraft come back to its equilibrium or trim position when the disturbance disappears. Static stability in fixed wing aircraft generally studied only for longitudinal axis. In the directional axis, a vertical stabiliser placed behind CG is always statically stable.

Static Stability of the aircraft is evaluated using Xflr5. When the aircraft is analysed for given geometry, Neutral point of the aircraft is obtained. The required CG location is found by setting the Static Margin. Generally for model aircrafts, Static margin of 15% to 25% is preferred. In current case, a static margin of 35% is taken for added safety and uncertainty in locating Neutral point precisely.

A limitation of CFD analysis using VLM is the inaccuracy involved when analysis is done for plane with Body panels. VLM tends to underestimate the effect of body panels on pitching moment [19]. Due to this reason a high Static margin of 35% is used in the design. The true neutral point and CG adjustments have to be made using Wind tunnel tests or flight tests.

The aircraft is trimmed to zero angle of attack by varying the incidence angle of the horizontal stabiliser through iterations. . Incidence for the horizontal stabilizer is set at $i_H = -1^\circ$ for $\alpha_{trim} = 0.277^\circ$.

For the current aircraft design, MAC of wing is 28.3cm. NP is estimated at 22cm from leading edge of root airfoil section and CG is placed at 12.5 cm. This brings Static margin to 33.57%. The pitch moment co-efficient variation with angle of attack is shown in the figure 4.7. The graph shows negative slope indicating a statically stable system with zero moment at approximately zero angle of attack.

4.5 Dynamic stability

Dynamic stability of an aircraft refers to the nature of a disturbed system with respect to time. If the disturbed comes back to its equilibrium position after some amount of time, the system is said to be dynamically stable.

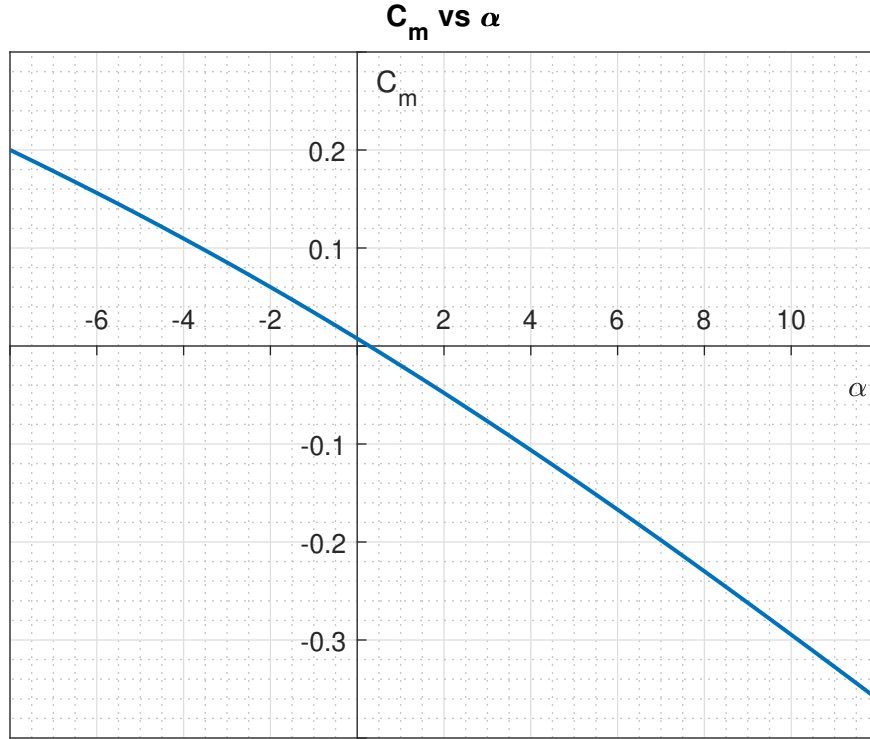


Figure 4.7: Pitching moment curve

Longitudinal modes

In longitudinal axis, both Short period mode and Phugoid mode are stable.

Short period mode

Eigenvalue = $-6.14217 \pm 8.69789i$

Undamped Natural Frequency = 1.695Hz

Damped Frequency = 1.384Hz

Damping Ratio = 0.706

Phugoid mode

Eigenvalue = $-0.03765 \pm 0.82050i$

Undamped Natural Frequency = 0.131Hz

Damped Natural Frequency = 0.131Hz

Damping Ratio = 0.046

Lateral – Directional modes

In the Lateral – Directional axes, Roll subsidence and Dutch roll mode are stable. But the aircraft is unstable in spiral mode.

Roll subsidence mode

Eigenvalue = $-9.02529 + 0.00000i$

Time to half amplitude = $0.077s$

Dutch roll mode

Eigenvalue = $-1.38299 \pm 4.30760i$

Undamped Natural Frequency = $0.720Hz$

Damped Natural Frequency = $0.686Hz$

Damping Ratio = 0.321

Spiral mode

Eigenvalue = $0.34713 + 0.00000i$

Time to double amplitude = $1.997s$

The spiral divergence can be attributed to zero dihedral given to the wing due to structural purposes. To increase the stability in spiral mode, dihedral angle of the wing must be increased but this does not allow for straight carbon fiber tube to be used as spars in the wing. For UAVs flown in line of sight or using an autopilot, spiral mode instability can be ignored. More over a high configuration already provides some amount of dihedral stability due to its fuselage which has not be accounted for in the xflr5 analysis. Hence aircraft design is not altered to achieve spiral stability.

Chapter 5

Mathematical model of the aircraft

This chapter describes the derivation of a mathematical model for the aircraft and its dynamics. Here non-linear rigid body equations of motion as used for the flight dynamics of the aircraft. The forces involved like gravity, propulsion and aerodynamics are modelled. This model integrated into a simulation environment in MATLAB Simulink.

5.1 Aircraft flight mechanics

The basis for the equations of motion is rigid body mechanics from Newton's laws of motion. The kinematic and dynamic equations for linear and angular motion of a rigid body are used to model the aircraft flight mechanics.

Coordinate system

To describe the motion of the aircraft, two reference frames are used – Inertial frame and Body frame of reference.

Inertial frame of reference is the stationary coordinate frame defined with respect to earth. Newton's laws of motion are applicable in this frame. This frame is required for Navigation and is defined as NED frame. In this frame x-axis points to North direction, y-axis points to East direction and z-axis points downward. The position and velocity in this frame are represented with suffix E.

Body frame of reference is the coordinate frame fixed with respect to the body and moves with it. In this frame, x-axis points to front of aircraft, y-axis points to right side and

z-axis points downward of the aircraft. The centre of the body frame aligns with the Centre of Gravity of the aircraft. Hence it is easier to model forces due to gravity, aerodynamics and propulsion in the Body frame of reference. The position and velocity in this frame are represented with suffix B.

Euler angles are used to describe body frame with respect to inertial frame. Direction Cosine Matrix formed using Euler angles is used to convert quantities between the two frames. The motion of the body is described with these twelve equations using the state vector $[u, v, w, p, q, r, \phi, \theta, \psi, x_E, y_E, z_E]$.

Equations of Motion

Equations of motion describing the motion of aircraft in scalar form are given as follows [20].

Force equations

$$F_x = m (\dot{u} + q w - r v)$$

$$F_y = m (\dot{v} + r u - p w)$$

$$F_z = m (\dot{w} + p v - q u)$$

Moment equations

$$L = \dot{p}I_x + qr(I_z - I_y) - (\dot{r} + pq)I_{xz}$$

$$M = \dot{q}I_y - pr(I_z - I_x) + (p^2 - r^2)I_{xz}$$

$$N = \dot{r}I_z + pq(I_y - I_x) - (\dot{p} - qr)I_{xz}$$

Euler angle rates

$$\dot{\phi} = p + \tan \theta (q \sin \phi + r \cos \phi)$$

$$\dot{\theta} = q \cos \phi - r \sin \phi$$

$$\dot{\psi} = \frac{q \sin \phi + r \cos \phi}{\cos \theta}$$

Navigation equations

$$\begin{aligned}\dot{x}_E &= u \cos \psi \cos \theta + v(\cos \psi \sin \theta \sin \phi - \sin \psi \cos \phi) + w(\cos \psi \sin \theta \cos \phi + \sin \psi \sin \phi) \\ \dot{y}_E &= u \sin \psi \cos \theta + v(\sin \psi \sin \theta \sin \phi + \cos \psi \cos \phi) + w(\sin \psi \sin \theta \cos \phi - \cos \psi \sin \phi) \\ \dot{z}_E &= -u \sin \theta + v \cos \theta \sin \phi + w \cos \theta \cos \phi\end{aligned}$$

Forces and Moments

For convenience, forces and moments acting on the aircraft is modelling in Body reference frame. The main forces and moments acting on the aircraft are due to Gravity (\mathbf{F}_g), Aerodynamics (\mathbf{F}_a and \mathbf{M}_a) and Propulsion (\mathbf{F}_p and \mathbf{M}_p). Hence, net force on aircraft is $\mathbf{F} = \mathbf{F}_g + \mathbf{F}_a + \mathbf{F}_p$ and net moment is $\mathbf{M} = \mathbf{M}_a + \mathbf{M}_p$ in body reference frame.

Gravitational force

Gravity acts at the centre of gravity of the aircraft, hence moment due to gravity on the aircraft in body frame is zero. Gravity is a constant force in the inertial frame given by

$$\mathbf{F}_g^E = [0 \ 0 \ mg]^T$$

Transforming gravity vector to body reference frame,

$$\mathbf{F}_g = \begin{bmatrix} -mg \sin \theta \\ mg \cos \theta \sin \phi \\ mg \cos \theta \cos \phi \end{bmatrix}$$

5.2 Propulsion

Propulsion system for the aircraft consists of 4 Emax MT3515 650kv motors with APC 12x3.8 SF propellers. For simplicity, it is assumed that aircraft geometry itself does not interfere with the operation of the propeller. While developing a model, propeller performance is assumed to be dependent only on the magnitude and direction of incoming airflow.

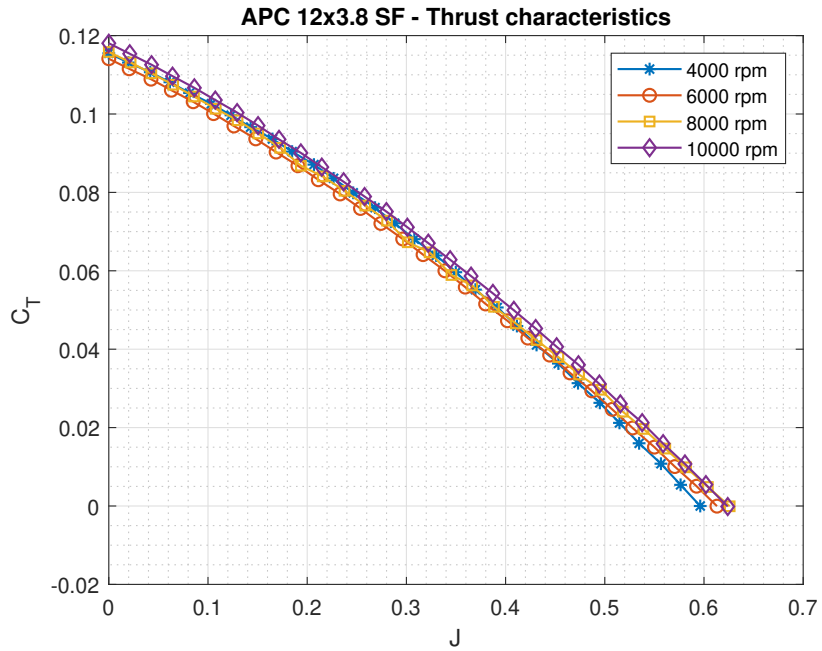


Figure 5.1: APC 12x3.8SF - Thrust characteristics

Propeller data

Propeller data for APC 12x3.8 SF propellers is taken from the manufacturer's website [18]. The raw data is used to find advance ratio (J), thrust coefficient (C_T), torque coefficient (C_Q) power coefficient (C_P) and efficiency (η). The definitions of the coefficients are given as

$$J = \frac{V}{n D}$$

$$C_T = \frac{T}{\rho n^2 D^4}$$

$$C_Q = \frac{Q}{\rho n^2 D^5}$$

$$C_P = \frac{P}{\rho n^3 D^5}$$

$$\eta = \frac{C_T J}{C_P}$$

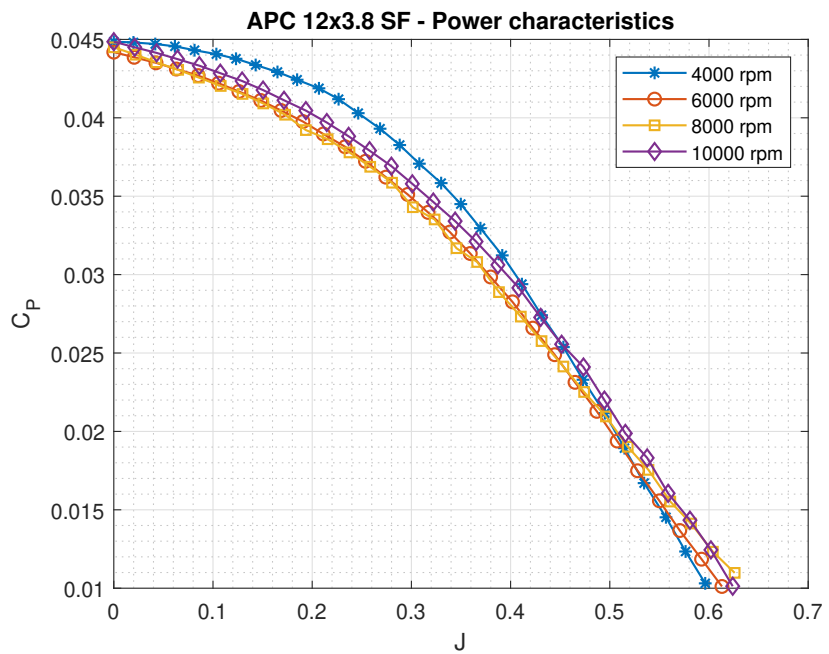


Figure 5.2: APC 12x3.8SF - Power characteristics

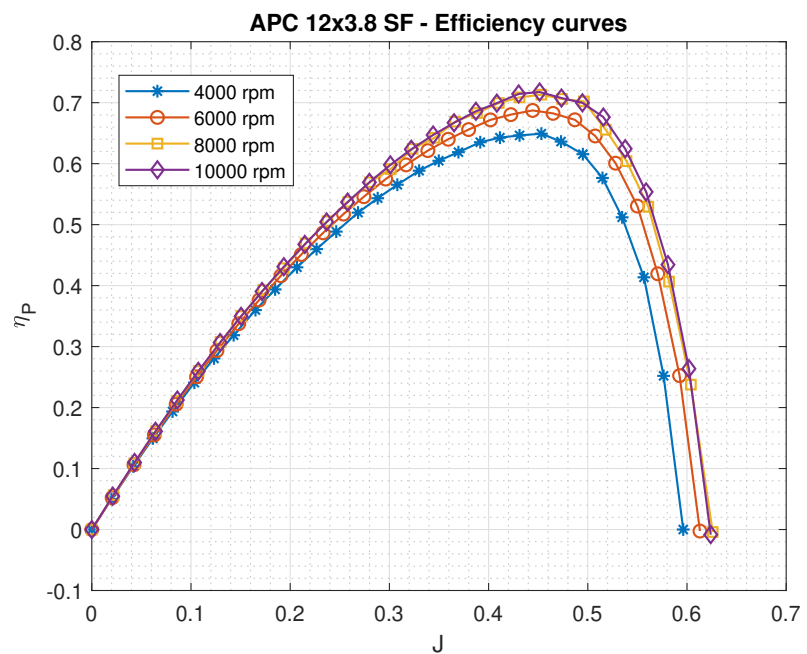


Figure 5.3: APC 12x3.8SF - Efficiency curves

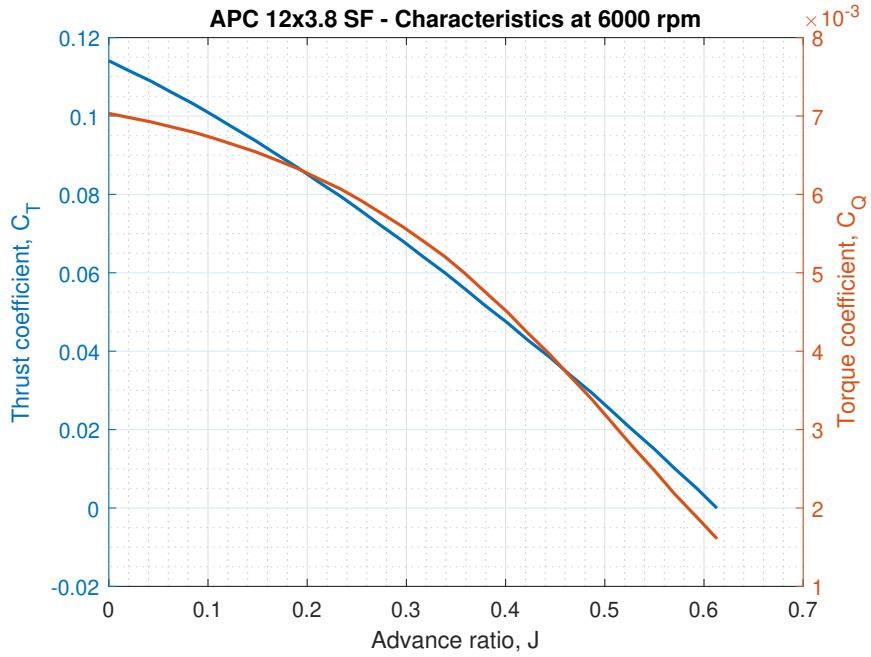


Figure 5.4: APC 12x3.8SF - 6000rpm

For simplicity, Thrust and Torque characteristics at 6000 rpm is taken for simulations. Curve fits for the data is generated for easy implementation.

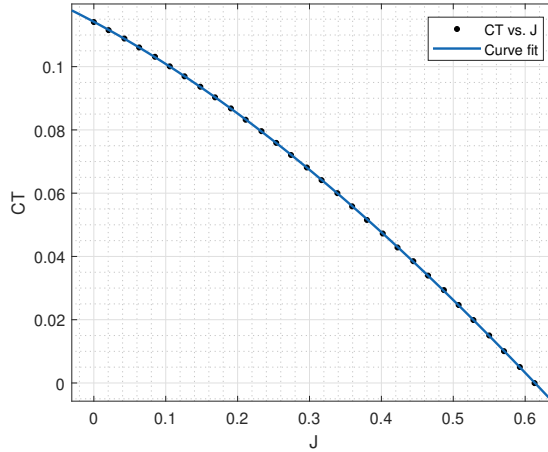


Figure 5.5: APC 12x3.8SF - Curve fit for C_T

Relations for Thrust coefficient and Torque coefficient are obtained from curve fits as follows.

$$C_T = 0.03338 J^3 - 0.1265 J^2 - 0.1210 J + 0.1142$$

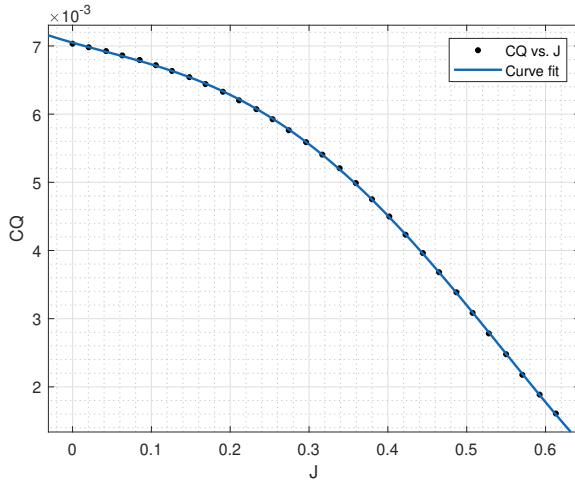


Figure 5.6: APC 12x3.8SF - Curve fit for C_Q

$$C_Q = 0.04280 J^4 - 0.05046 J^3 + 0.005711 J^2 - 0.003293 J + 0.007048$$

Motor dynamics

Another effect that has to be considered while developing a model for propulsion is the motor dynamics. There is a delay between the command input to the Motor and ESC, and the output speed of the propeller. The system is very complex to create a theoretical model but a system identification approach can be used to model the motor dynamics by experimental methods.

As described in [21], a sufficiently good model can be used by assuming the motors dynamics to be a first order system with a time constant. This can be determined by measuring speed of the motor, propeller and ESC combination with step input commands. Typical values of time constant for BLDC motors are between 50ms and 100ms. For the model developed for simulations, a time constant of 50ms is used.

The transfer function for such a first order system is

$$\frac{\omega}{u_m} = \frac{k}{\tau s + 1}$$

where ω is motor speed, u_m is motor command, k is motor gain and τ is the time constant of the system.

Propulsive Forces and Moments

The thrust and torque produced by the propellers can be evaluated using the curve fits obtained. But these forces are pointed along the motor axes. These have to be converted into forces and moments about the centre of gravity of the aircraft.

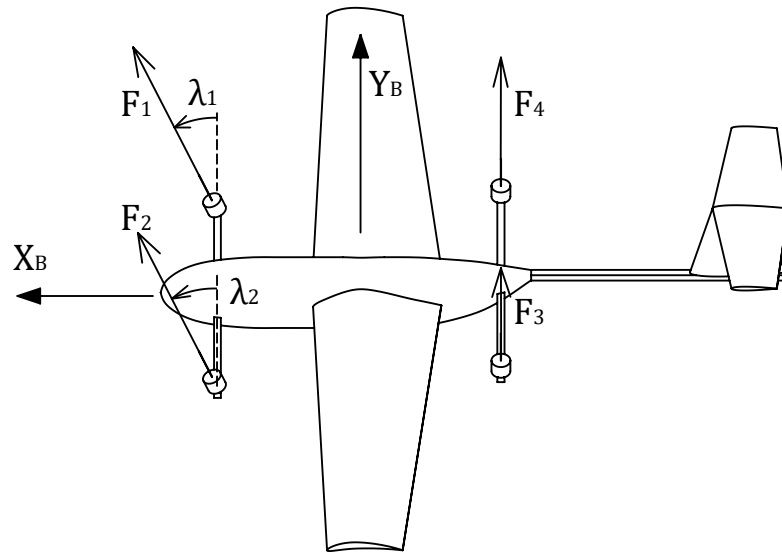


Figure 5.7: Thrust alignment

As shown in the figure 5.7, the motors are placed at the corners of a square with CG of aircraft at its center. The distance between the motors along x-axis and y-axis is 0.75m. The position of motors is given as

$$\mathbf{r}_1 = [\begin{array}{ccc} 0.375 & 0.375 & 0 \end{array}]^T$$

$$\mathbf{r}_2 = [\begin{array}{ccc} 0.375 & -0.375 & 0 \end{array}]^T$$

$$\mathbf{r}_3 = [\begin{array}{ccc} -0.375 & -0.375 & 0 \end{array}]^T$$

$$\mathbf{r}_4 = [\begin{array}{ccc} -0.375 & 0.375 & 0 \end{array}]^T$$

The thrust vectors are given as

$$\mathbf{F}_1 = F_1 \begin{bmatrix} \sin \lambda_1 & 0 & -\cos \lambda_1 \end{bmatrix}^T$$

$$\mathbf{F}_2 = F_2 \begin{bmatrix} \sin \lambda_2 & 0 & \cos \lambda_2 \end{bmatrix}^T$$

$$\mathbf{F}_3 = F_3 \begin{bmatrix} 0 & 0 & -1 \end{bmatrix}^T$$

$$\mathbf{F}_4 = F_4 \begin{bmatrix} 0 & 0 & -1 \end{bmatrix}^T$$

Hence net force due to propulsion is given as

$$\mathbf{F}_p = \mathbf{F}_1 + \mathbf{F}_2 + \mathbf{F}_3 + \mathbf{F}_4$$

The moments due to the propulsion is a combination of Torque due to propellers and the moment produced due to thrust forces acting at a distance from CG of aircraft.

The moment acting the aircraft due to each propeller is given as

$$\mathbf{Q}_1 = Q_1 \begin{bmatrix} \sin \lambda_1 & 0 & -\cos \lambda_1 \end{bmatrix}^T$$

$$\mathbf{Q}_2 = Q_2 \begin{bmatrix} \sin \lambda_2 & 0 & \cos \lambda_2 \end{bmatrix}^T$$

$$\mathbf{Q}_3 = Q_3 \begin{bmatrix} 0 & 0 & -1 \end{bmatrix}^T$$

$$\mathbf{Q}_4 = Q_4 \begin{bmatrix} 0 & 0 & -1 \end{bmatrix}^T$$

The moment acting the aircraft due to thrust of each propeller is given as

$$\mathbf{M}_1 = \mathbf{r}_1 \times \mathbf{F}_1$$

$$\mathbf{M}_2 = \mathbf{r}_2 \times \mathbf{F}_2$$

$$\mathbf{M}_3 = \mathbf{r}_3 \times \mathbf{F}_3$$

$$\mathbf{M}_4 = \mathbf{r}_4 \times \mathbf{F}_4$$

Hence the total moment acting on aircraft due to propulsion is

$$\mathbf{M}_p = \mathbf{Q}_1 + \mathbf{Q}_2 + \mathbf{Q}_3 + \mathbf{Q}_4 + \mathbf{M}_1 + \mathbf{M}_2 + \mathbf{M}_3 + \mathbf{M}_4$$

Both net force \mathbf{F}_p and net moment \mathbf{M}_p due to propulsion are in body frame of reference.

5.3 Aerodynamics

Due to the unique flight envelope of the aircraft, the aerodynamics is very complex. The flight involves three unique regimes of flight - Hover flight, Forward flight and flight transitions.

- In Hover flight regime, aerodynamic lift has very less influence. The forces are dominated by viscous drag. Generally for flight simulations involving multirotors, aerodynamics forces are neglected.
- In forward flight regime, aerodynamic lift and drag are very dominant. These forces allow the aircraft to fly and stabilise the aircraft. The aerodynamics in this case is well studied and easy to model.
- The transition flight involves a mixture of aerodynamics studied in forward flight and hover flight. The aerodynamics in this regime is varying due to large changes in flight speed and is very complex to model.

Fixed-wing Stability derivatives

The aerodynamics forces involved in the forward flight mode of flight is described using aerodynamic coefficients and stability derivatives. These coefficients are obtained by computational methods, wind tunnel tests or through flight tests. In the current case, stability derivatives are obtained from VLM analysis in Xflr5.

Longitudinal stability derivatives

The lift coefficient at zero angle of attack, its derivatives with respect to angle of attack α and pitch rate q are

$$C_{L_0} = 0.81857 \quad C_{L\alpha} = 4.09127 \quad C_{Lq} = 7.31097$$

Lift coefficient derivatives with respect to elevator deflection δ_e and aileron deflection δ_a are

$$C_{L\delta_e} = 0.50787 \quad C_{L\delta_a} = -0.85291$$

The change in lift coefficient is negative irrespective of the sign of aileron deflection.

Drag profile for aircraft with low cambered airfoils is given as

$$C_D = C_{D_0} + K C_L^2$$

Since the airfoil used in the UAV is high cambered, this drag profile will not fit for the designed UAV. For high cambered wings, drag can be described as

$$C_D = C_{D_{min}} + K (C_L - C_{L,C_{D_{min}}})^2$$

The data obtained from VLM analysis in Xflr5 is curve fitted into this drag polar as shown in the figure 5.8.

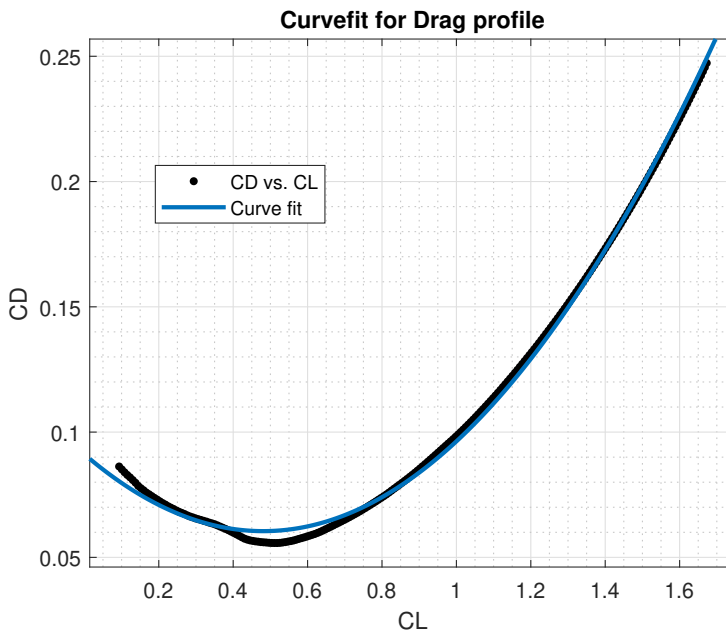


Figure 5.8: Curvefit for drag profile

$$C_{D_{min}} = 0.06047 \quad K = 0.1328 \quad C_{L,C_{D_{min}}} = 0.4806$$

Derivatives of Drag coefficient with respect to control surface deflections are

$$C_{D_{\delta_e}} = 0.016043 \quad C_{D_{\delta_a}} = 0.092132 \quad C_{D_{\delta_r}} = 0.0097403$$

The change in Drag coefficient is positive irrespective of the sign of control surface deflections.

The pitching moment coefficient at zero angle of attack, its derivatives with respect to angle

of attack α and pitch rate q are

$$C_{m_0} = 0.00763 \quad C_{m_\alpha} = -1.76966 \quad C_{m_q} = -19.22663$$

Pitching moment coefficient derivatives with respect to control surface deflections are

$$C_{m_{\delta_e}} = -1.83747 \quad C_{m_{\delta_r}} = 0.02991$$

The change in moment coefficient is positive irrespective of the sign of rudder deflection.

Lateral-Directional stability derivatives

Derivatives of side force coefficient with respect to sideslip angle β , roll rate p and yaw rate r are

$$C_{Y_\beta} = -0.001570 \quad C_{Y_p} = -0.001570 \quad C_{Y_r} = 0.18368$$

Derivative with respect to rudder deflection is $C_{Y_{\delta_r}} = 0.128915$.

The rolling moment coefficient derivatives with respect to sideslip angle β , roll rate p and yaw rate r are

$$C_{l_\beta} = -0.001610 \quad C_{l_p} = -0.47584 \quad C_{l_r} = 0.27153$$

Rolling moment coefficient derivatives with respect to control surface deflections are

$$C_{l_{\delta_a}} = 0.286593 \quad C_{l_{\delta_r}} = 0.013407$$

The yawing moment coefficient derivatives with respect to sideslip angle β , roll rate p and yaw rate r are

$$C_{n_\beta} = 0.09180 \quad C_{n_p} = -0.13267 \quad C_{n_r} = -0.08829$$

Yawing moment coefficient derivatives with respect to control surface deflections are

$$C_{n_{\delta_a}} = 0.0049274 \quad C_{n_{\delta_r}} = -0.067036$$

Aerodynamic Forces and Moments

The stability derivatives obtained are used to calculate the forces and moments due to airflow over the UAV. The equations used vary with the type of data available and approxima-

tions done. The equations are taken from [20] and [22].

The Lift and drag forces are calculated in wing axis frame and converted to body frame.

These coefficients are given as

$$\begin{aligned} C_L &= C_{L_0} + C_{L_\alpha} \alpha + C_{L_q} \frac{qc}{2V} + C_{L_{\delta_e}} \delta_e + C_{L_{\delta_a}} |\delta_a| \\ C_D &= C_{D_{min}} + K (C_L - C_{L,C_{D_{min}}})^2 + C_{D_{\delta_a}} |\delta_a| + C_{D_{\delta_e}} |\delta_e| + C_{D_{\delta_r}} |\delta_r| \\ C_Y &= C_{Y_0} + C_{Y_\beta} \beta + C_{Y_p} \frac{pb}{2V} + C_{Y_r} \frac{rb}{2V} + C_{Y_{\delta_a}} \delta_a + C_{Y_{\delta_r}} \delta_r \end{aligned}$$

The lift and drag coefficients are converted from wind axis to body axis.

$$\begin{aligned} C_X &= C_L \sin \alpha - C_D \cos \alpha \\ C_Z &= -C_L \cos \alpha - C_D \sin \alpha \end{aligned}$$

The moments coefficients due to aerodynamic interactions is given by

$$\begin{aligned} C_l &= C_{l_0} + C_{l_\beta} \beta + C_{l_p} \frac{pb}{2V} + C_{l_r} \frac{rb}{2V} + C_{l_{\delta_a}} \delta_a + C_{l_{\delta_r}} \delta_r \\ C_m &= C_{m_0} + C_{m_\alpha} \alpha + C_{m_q} \frac{qc}{2V} + C_{m_{\delta_e}} \delta_e + C_{m_{\delta_r}} |\delta_r| \\ C_n &= C_{n_0} + C_{n_\beta} \beta + C_{n_p} \frac{pb}{2V} + C_{n_r} \frac{rb}{2V} + C_{n_{\delta_a}} \delta_a + C_{n_{\delta_r}} \delta_r \end{aligned}$$

Hence the forces and moments are found using the dynamic pressure Q , wing area s , mean aerodynamic chord \bar{c} and wingspan b .

$$X = C_X Q s$$

$$Y = C_Y Q s$$

$$Z = C_Z Q s$$

$$L = C_l Q s b$$

$$M = C_m Q s \bar{c}$$

$$N = C_n Q s b$$

$$\mathbf{F}_a = [X \quad Y \quad Z]^T$$

$$\mathbf{M}_a = [L \quad M \quad N]^T$$

Aerodynamics for Hover and Transition flight

Due to the complexities in the aerodynamics involved in Hover flight mode and Flight transition, accurate models are not developed for these flight regimes.

Hover flight mode - A common approach to multirotor simulations is to neglect aerodynamics. Due to very low speeds involved and less surfaces exposed, this assumption gives good results. In the case of a VTOL UAV with large surfaces, this assumption does not hold. But due to complexities in developing an aerodynamic model, for simulations aerodynamics are neglected.

Flight transition - Although the motion in flight transition is very similar to forward flight, the low Reynolds number flows exist during the start of transition to forward flight and at end of transition flight to hover flight. These conditions do not agree with the conventional fixed-wing model. For simulations, fixed-wing aerodynamic model itself is used due to its simplicity. It is of opinion that at low flight speeds, the propulsive forces are dominant over aerodynamic forces.

5.4 Simulink implementation

This chapter explains the simulation environment created in MATLAB Simulink. The elements of the UAV are modelled as blocks using the results obtained in previous chapters. The simulation environment is created to accommodate extension for improved model in the future.

Overview

The simulation environment consists mainly of Controller, Actuator and Aircraft dynamics blocks. A user control reference and sensor feedback is connected to the controller block. A wind and disturbance block is connected to the aircraft dynamics block. A visualisation block takes information from all the blocks for the user.

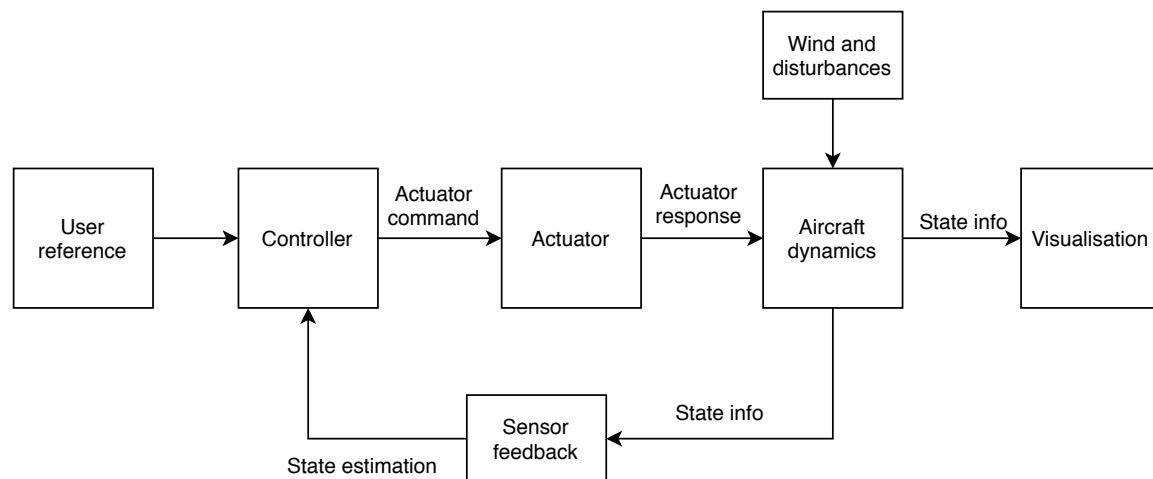


Figure 5.9: Simulation Environment

- The user reference is the block where user defined controls or an external guidance block can be added to provide the controller with a reference signal.
- The controller block receives the reference input and compares it with the estimated state of the system obtained from sensors. It takes appropriate action by controlling the actuators available.

- The actuator block calculates the response of the actuators like motors and servos with respect to the command received from the controller. It mimics the dynamics of the actuators used on the aircraft.
- Aircraft dynamics block is the mathematical model described in the previous chapters of the propulsion, aerodynamics and their effects on aircraft motion. This block takes propeller speed, control surface deflections, motor tilt angles etc to calculate the actual state of the aircraft with time.
- The visualisation block contains graphs to study the model, data storage and other aspects that a user is interested in.
- The sensor block is used to mimic how sensors take real world data and give a state estimation of the aircraft. External and internal noise, time delays etc and state estimation algorithms can be modelled here. This block has not been implemented in this thesis.
- Wind and disturbance block is used to introduce external winds, turbulence and other possible disturbances in the simulation.

Aircraft dynamics

Aircraft dynamics block is system of smaller blocks that are used to model the rigid body dynamics, gravity, aerodynamics and propulsion. It includes four blocks - 6DoF rigid body dynamics block, Gravity block, Aerodynamics block and Propulsion block shown in figure 5.10.

- The inputs to the Aircraft dynamics are Control surface deflections, Tilt angles, motor speeds, Wind condition.
- The gravity block takes the mass and gravity values to calculate the forces in body frame using Euler angles of the aircraft.
- The aerodynamics block takes the wind condition, Control surface deflections and current state vector as input. It calculates the aerodynamic forces and moments described in chapter 5.3 as output.
- The Propulsion block takes current state, motor tilt angles and motor speeds to calculate the forces and moments described in chapter 5.2.

- The forces and moments calculated by the three blocks are added and passed as input to the Rigid body dynamics block. This block uses current state and forces acting on it to integrate the rigid body equations 5.1. The result is state of the aircraft in next time step.

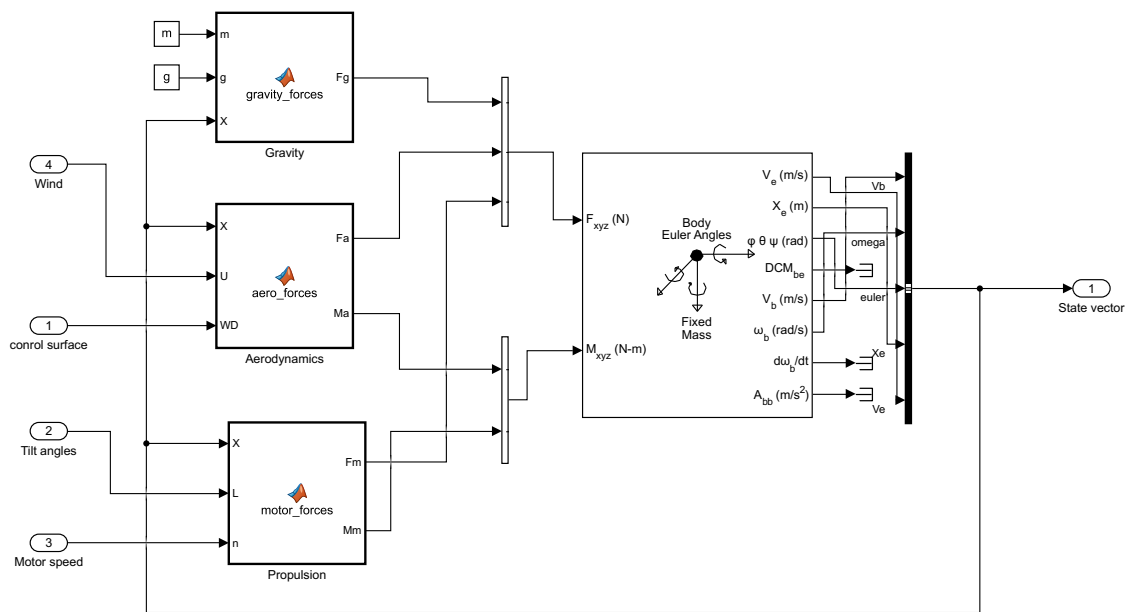


Figure 5.10: Aircraft dynamics block

Chapter 6

Flight control and Simulations

6.1 Fixed-wing flight mode

The dynamics of a fixed wing aircraft are highly coupled. In a broader sense, the 6DoF of the aircraft can be decoupled into two. One involves longitudinal axis and the second involves lateral and directional axes. Four control variables are present to control the aircraft – Ailerons, Elevator, Rudder and Throttle.

Motor thrust for both motors is controlled using same throttle control. Hence no differential thrust is used. Also, the aileron servos have common input signal and differential aileron control is not available.

6.1.1 Actuators for control

Elevator deflection and Motor thrust affect the control in the longitudinal axis of the aircraft. Ailerons and Rudder affect the control in lateral-directional axes. Although the Degrees of Freedom of the aircraft are highly coupled, for the sake of simple control the actuator and affected axis of motion must be highly linearised.

The inner loops of the controller affect the angular motions of the aircraft – roll (p), pitch (q) and yaw (r). They are each controlled by Aileron, Elevator and Rudder control respectively.

Lateral control

Aircraft roll is achieved by differential deflection of Ailerons on the wing. Since the aileron

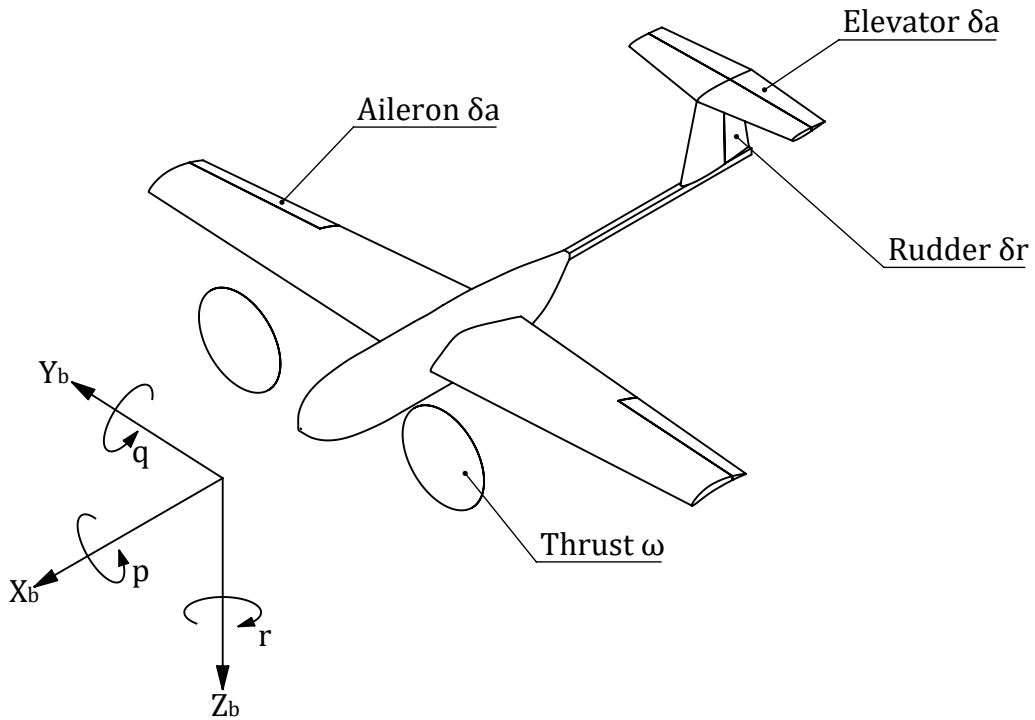


Figure 6.1: Actuators for control in forward flight

servos are controlled using a common control signal, both ailerons can be deflected by same angles in different directions. Aileron deflection is taken as positive when the right aileron moves down and left aileron moves up. This positive aileron deflection δ_a causes a positive rolling moment.

$$\delta_a = \delta_{a,trim} + \delta_\phi$$

Longitudinal control

Pitching up and down is achieved by application of Elevator deflection. Elevator deflection is taken as positive when elevator moves down. This positive elevator deflection δ_e causes a negative pitching moment.

$$\delta_e = \delta_{e,trim} + \delta_\theta$$

Directional control

Yaw authority is obtained by the use of Rudder. Rudder deflection is taken as positive when the rudder moves to the left. This positive rudder deflection δ_r causes a negative yawing moment.

$$\delta_r = \delta_{r,trim} + \delta_\psi$$

6.1.2 Control system

The flight control system used in Ardupilot [1] consists of an outer loop for Navigation and guidance. The inner loops are used for controlling the attitude of the aircraft. The control system for roll, pitch and yaw control is modelled in Simulink for flight simulations.

Roll attitude Controller

The control system used for roll attitude control is a PID cascaded system. A Proportional controller is used for roll angle control which gives reference roll rate required. A Proportional-Integral controller is used for roll rate control. A feed forward is provided to compensate for roll damping. Because the effectiveness of ailerons is proportional to the square of the velocity a velocity scaling is provided.

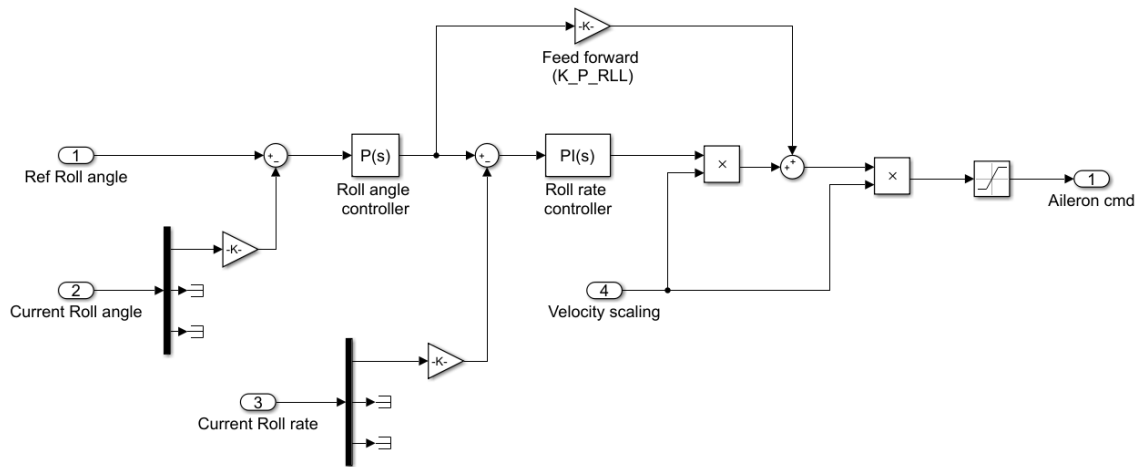


Figure 6.2: Roll attitude controller

Pitch attitude controller

The same controller is used for pitch controller but a roll compensation is provided for pitch control.

Yaw attitude controller

The yaw attitude controller is not truly a Yaw controller but a Yaw damper. Its is called a yaw controller because it uses rudder action to dampen the yaw tendencies in dutch roll mode. Yaw angle of the aircraft is controlled using guidance loops on the autopilot by application of ailerons.

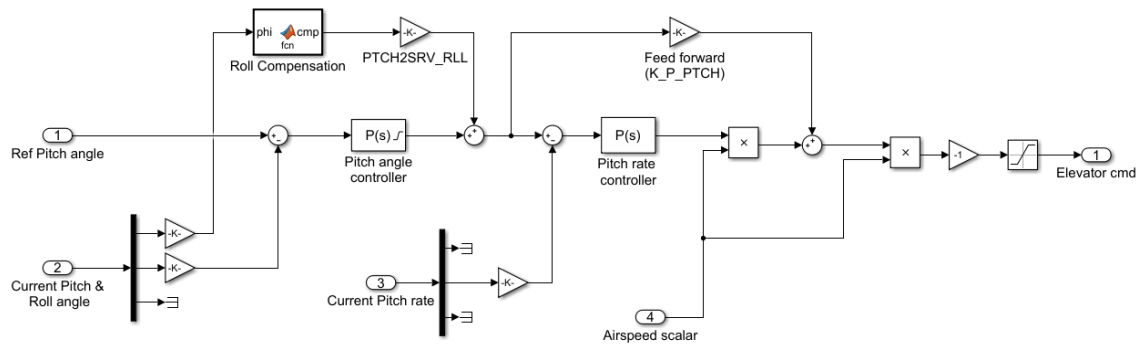


Figure 6.3: Pitch attitude controller

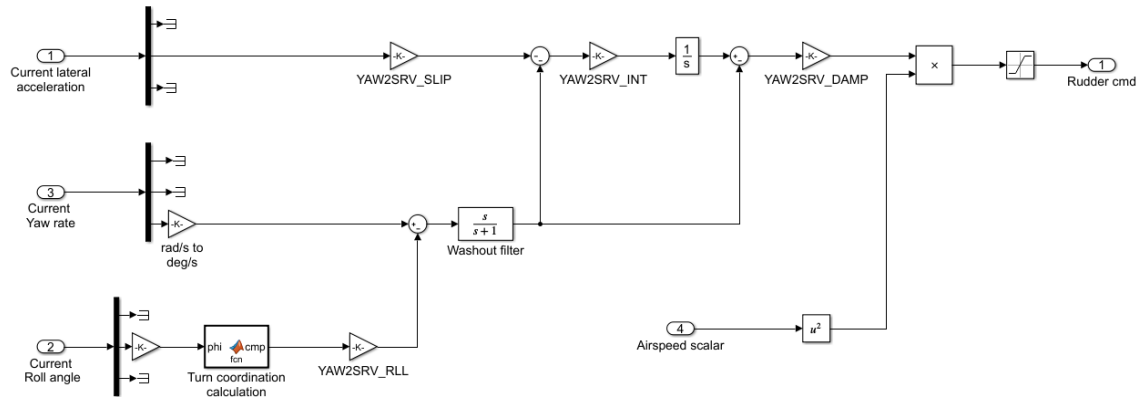


Figure 6.4: Yaw attitude controller

The turn co-ordination calculator provides a reference yaw rate from the bank angle of the aircraft. This and current yaw rate is used to determine the control action required. A washout filter is used to filter out disturbances that may occur as the yaw angle is constantly changing. The controller also tries to reduce sideslip angle by measuring lateral acceleration of the aircraft.

6.1.3 Flight simulations

Since the simulation environment is based on non linear equations of motion, tuning the controller by analytical means is not possible. Ardupilot have described a procedure to manually tune the control while flying the aircraft [1]. The same method is used to tune the controller using flight simulations.

Pitch control

Figure 6.5 shows comparison between manual control and the pitch attitude control of the aircraft. Thrust is not varied when the change is given, only appropriate elevator deflection is given to change the pitch angle from 0° to 5° . It shows that the pitch attitude controller greatly reduces the oscillations in the short period mode.

Roll control

Figure 6.6 shows the simulation of roll when roll angle of 15° is demanded at $30s$. A simulation of manual control using step input of ailerons resulted in uncontrolled roll of the aircraft. The simulation used the above pitch controller to keep the pitch angle at zero. Figure 6.7 shows the path taken by the UAV during this roll.

It can be seen in figure 6.6 that when aileron input is given at time $30s$, there are oscillations in the yaw axis of the aircraft. This is due to coupling of the Lateral and Directional axes of the aircraft.

Yaw control

As explained earlier, the yaw controller does not control the heading of the aircraft but dampens the oscillations of the aircraft in directional axis. This is meant to reduce the dutch roll tendencies of the aircraft. Figure 6.8 shows the effect of yaw damper. The oscillations in directional axis are reduced.

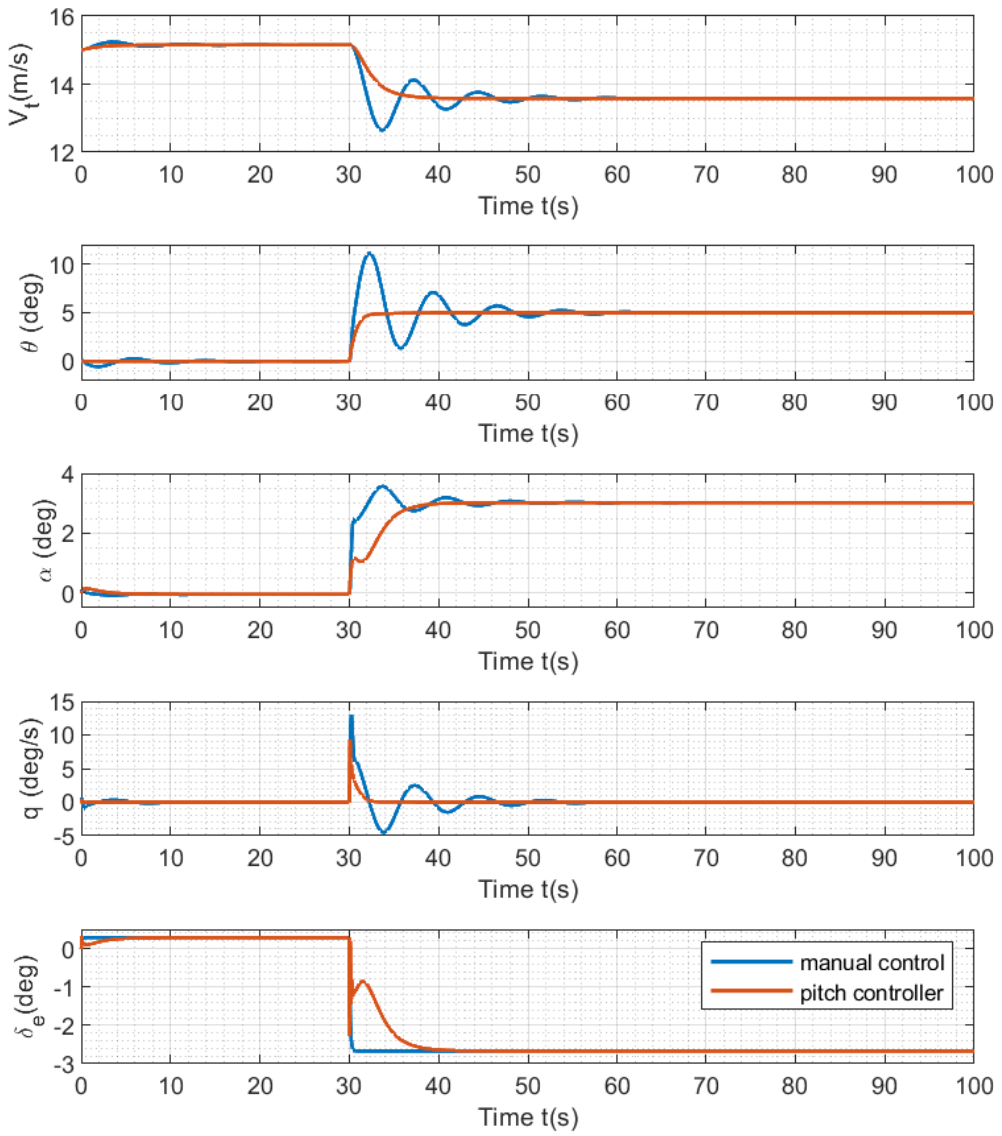


Figure 6.5: Simulation of pitch control

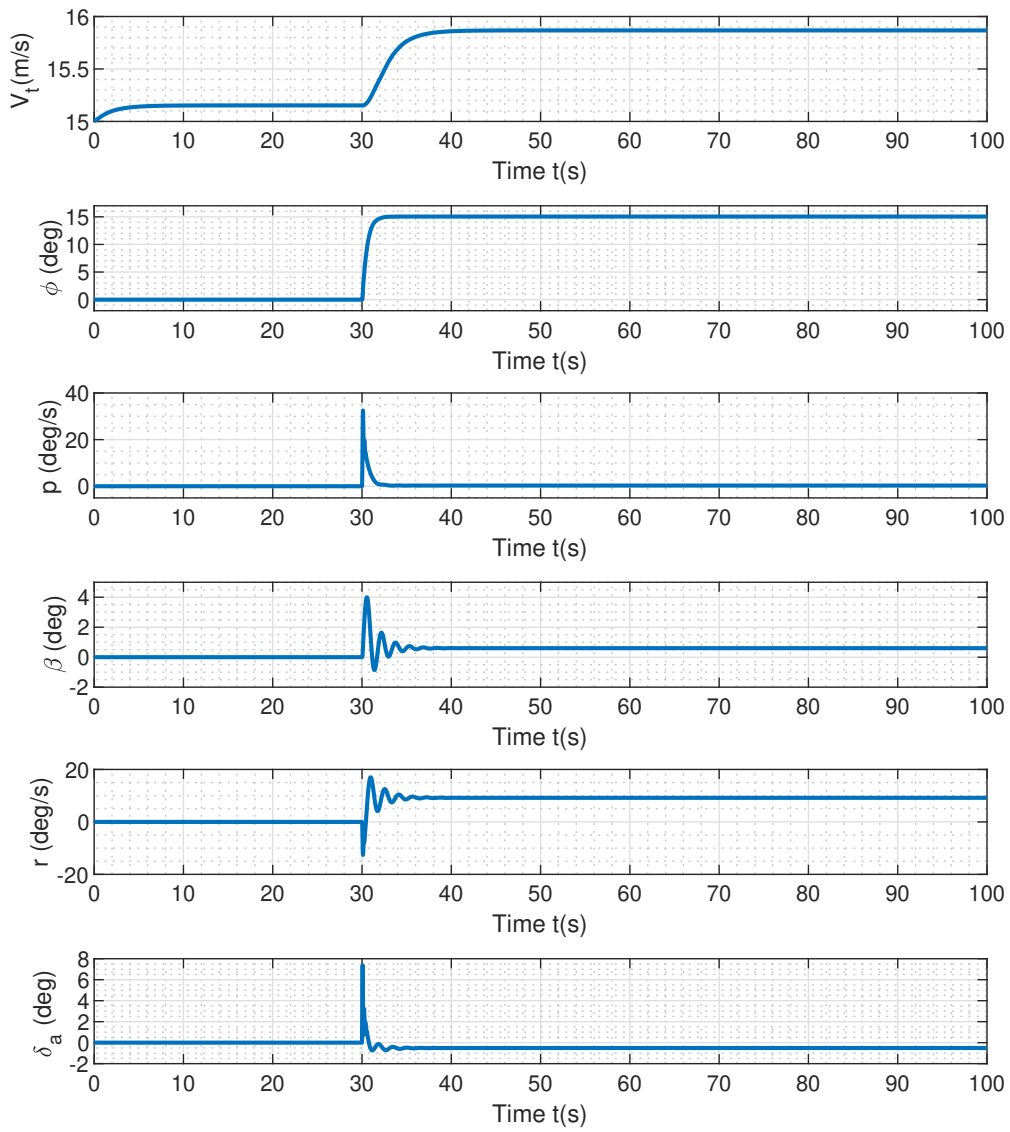


Figure 6.6: Simulation of roll control

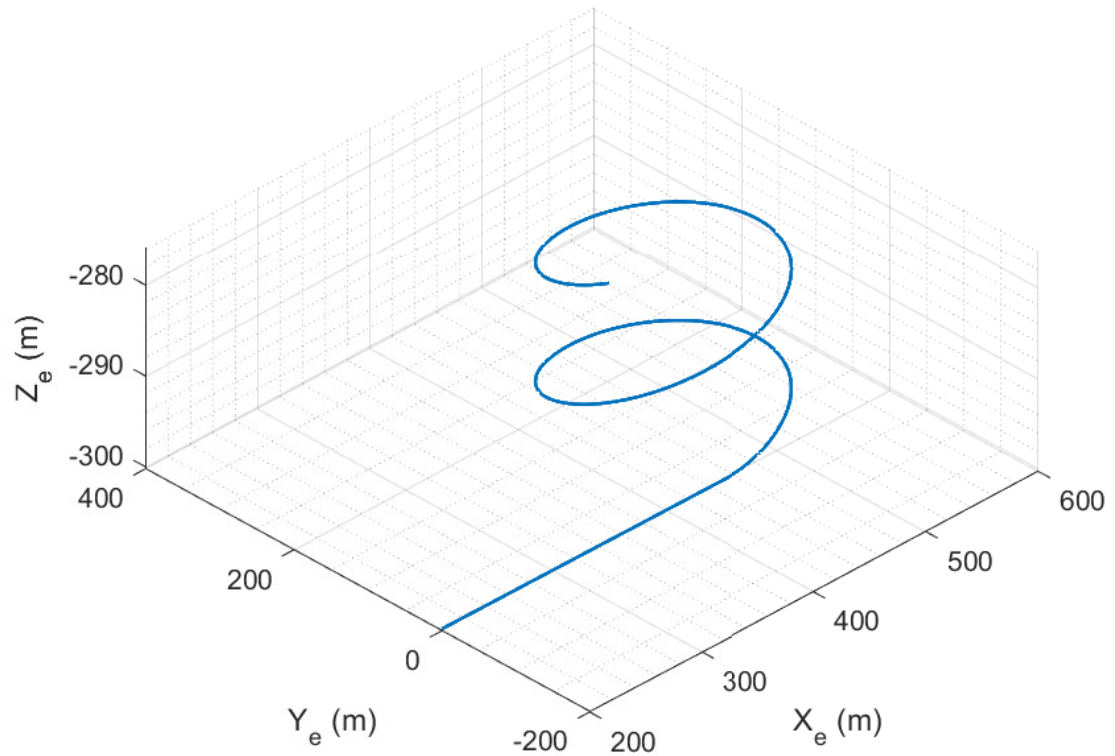


Figure 6.7: Flight path of UAV for roll input

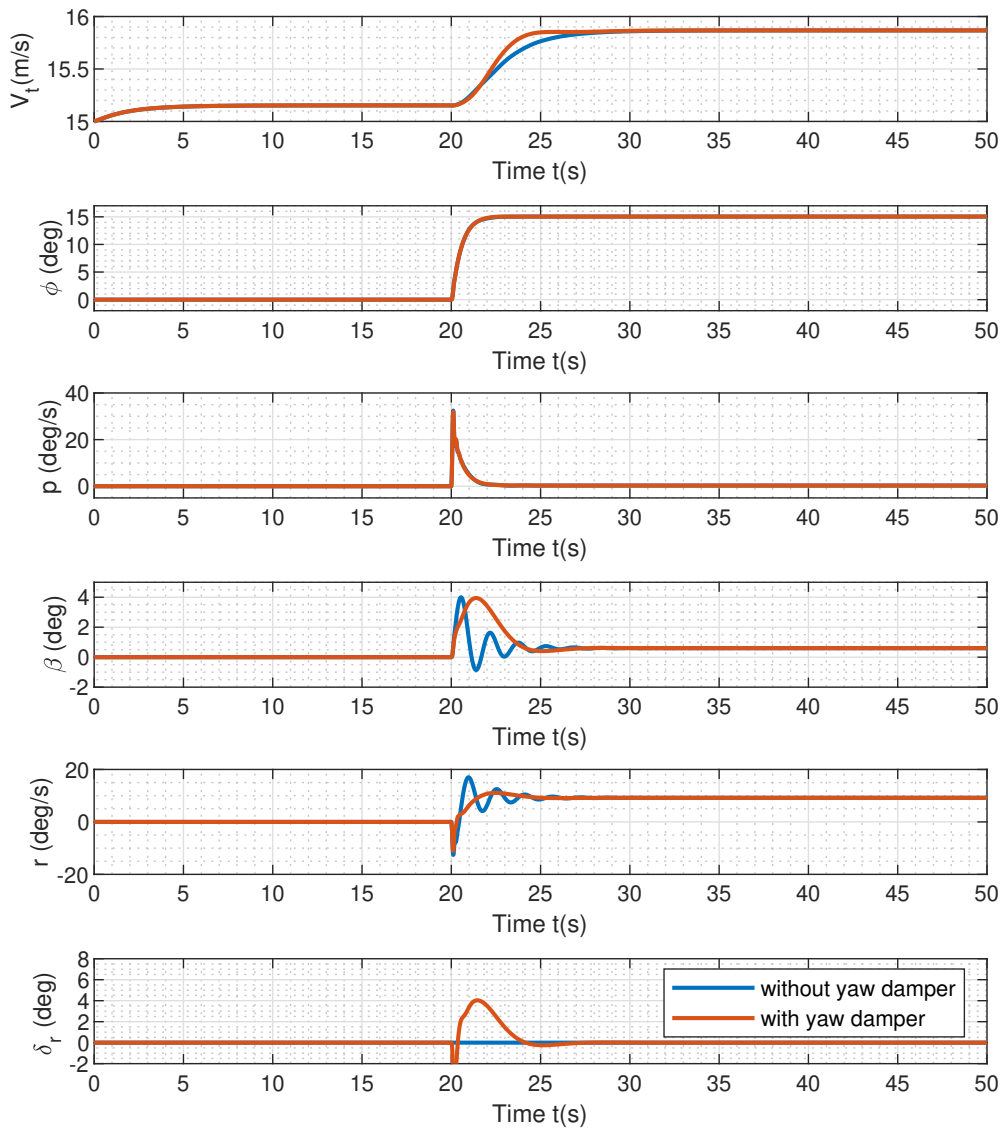


Figure 6.8: Effect of yaw damper

6.2 Hover flight mode

Hover flight mode uses 4 motors for thrust and two servos for tilting front motors. While the configuration is similar to that of a quadcopter, the current configuration has 5 degrees of freedom as compared to a quadcopter which has 4 degrees of freedom.

6.2.1 Actuators for control

The controls for hover mode in linearized form are explained below. There are 6 independent control variables available for controlling the aircraft – four motor speeds and two tilt angles for front two motors.

Z-axis translation control

Translation control along Z-axis or altitude control is achieved by increasing or decreasing the speed of all four motors. For movement along z-axis (decrease in altitude), speed of all motors is decreased. The motor command, $\Delta\omega_z$ represents change in motor speed for movement along z-axis. (Same as a quadcopter)

$$\omega_1 = \omega_{trim} - \Delta\omega_z$$

$$\omega_2 = \omega_{trim} - \Delta\omega_z$$

$$\omega_3 = \omega_{trim} - \Delta\omega_z$$

$$\omega_4 = \omega_{trim} - \Delta\omega_z$$

Z-axis rotation control

Rotation control along z-axis or Yaw control is achieved through differential vectored thrust from two motors at the front. For yaw movement in +ve z-axis, right side motor is tilted backward (λ_1 is decreased) and left motor tilted to forward direction (λ_2 is increased). The tilt command, $\Delta\lambda_\psi$ represents change in tilt angle for Yaw or rotation along ψ .

$$\lambda_1 = \lambda_{trim} - \Delta\lambda_\psi$$

$$\lambda_2 = \lambda_{trim} + \Delta\lambda_\psi$$

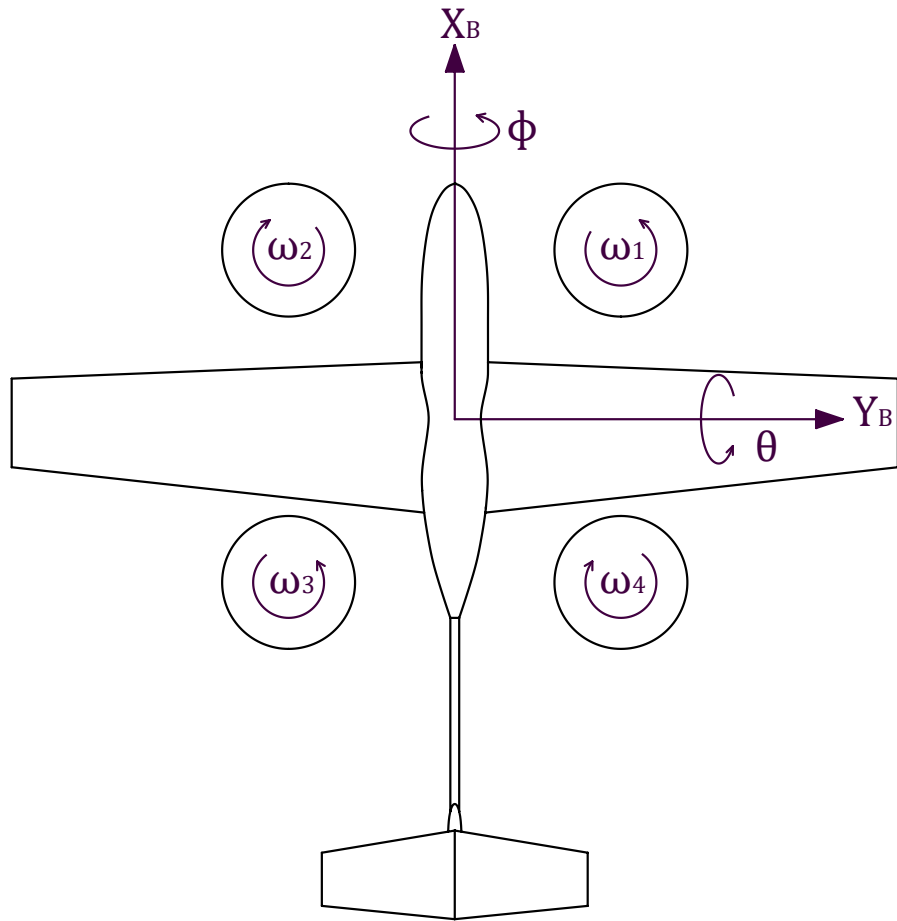


Figure 6.9: Motor placement for hover flight

A quadcopter uses differential speeds of propellers in CCW and CW directions for yaw control. This control authority is very less due to very low magnitudes of propeller torque. Due to large lifting surfaces, yaw damping and drag offered is very high compared to that in a quadcopter. Hence vectored thrust provides better control.

X-axis translation control

Translation control along x-axis or forward movement control is achieved through collective vectored thrust from two motors. For forward movement, both the motors at the front

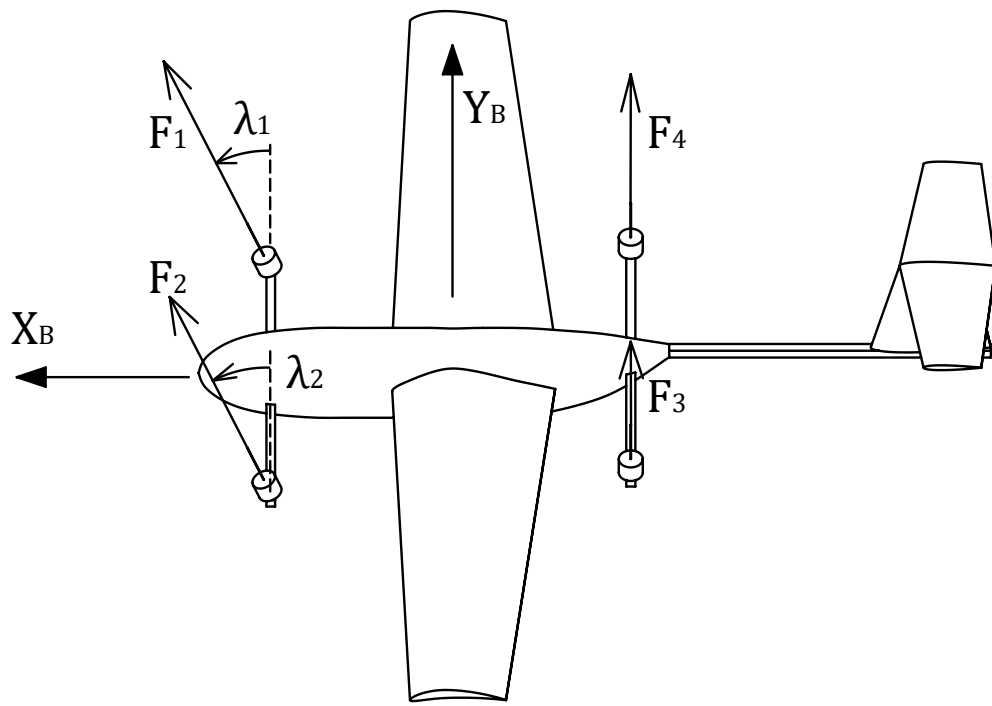


Figure 6.10: Thrust vectoring for hover flight

are tilted forward (both λ_1 and λ_2 are increased). The tilt command, $\Delta\lambda_x$ represents change in tilt angle for translation in x-axis.

$$\lambda_1 = \lambda_{trim} + \Delta\lambda_x$$

$$\lambda_2 = \lambda_{trim} + \Delta\lambda_x$$

In a quadcopter, dynamics in the X-axis translation and Y-axis rotation are coupled. Since the front motors are required to tilt forward for transition into forward flight, this feature can be used for translation along the x-axis. This helps reduce drag that would increase due to tilting of the aircraft.

X-axis rotation control Rotation control along x-axis or roll control is achieved through

differential thrust between the motors on the left and right. For rotation along +ve x-axis, speed of the motors are increased on the left side (ω_2 and ω_3 are increased) and decreased on the right side (ω_1 and ω_4 are decreased). $\Delta\omega_\phi$ represents change in motor speed for roll or rotation along ϕ .

$$\begin{aligned}\omega_1 &= \omega_{trim} - \Delta\omega_\phi \\ \omega_2 &= \omega_{trim} + \Delta\omega_\phi \\ \omega_3 &= \omega_{trim} + \Delta\omega_\phi \\ \omega_4 &= \omega_{trim} - \Delta\omega_\phi\end{aligned}$$

Y-axis translation control

Translation control along y-axis or sideward movement control is achieved by rolling the body in the required direction. For movement to the right, the aircraft is rotated along +ve roll axis and hence rotating the thrust vector sideward.

Since y-axis translation can only be achieved through roll ϕ , an outer control loop is required to command the inner control loop for roll. $\Delta\omega_y$ represents change in speed command for translation along y-axis.

$$\Delta\omega_y = k \Delta\omega_\phi$$

where k is a parameter determined by the outer control loop.

Y-axis rotation control

Rotation control along Y-axis or pitch control is achieved through differential thrust between the motors on the front and back. For rotation along +ve y-axis, speed of the motors are increased in the front (ω_1 and ω_2 are increased) and decreased in the back (ω_3 and ω_4 are decreased). $\Delta\omega_\theta$ represents change in motor speed for pitch or rotation along θ .

$$\begin{aligned}\omega_1 &= \omega_{trim} + \Delta\omega_\theta \\ \omega_2 &= \omega_{trim} + \Delta\omega_\theta \\ \omega_3 &= \omega_{trim} - \Delta\omega_\theta \\ \omega_4 &= \omega_{trim} - \Delta\omega_\theta\end{aligned}$$

During regular operation, pitch axis control is necessary to correct for offsets and disturbances. Pitch of the aircraft is required to be zero at all times. The aircraft when moving forward will have minimum drag while moving with a pitch angle of zero.

In the 6 Degrees of Freedom in the aircraft, Dynamics of rotation in the X-axis and translation in Y-axis are coupled. Hence the aircraft in hover mode is has 5 decoupled axes and a minimum of 5 control parameters for effective control. These control parameters are $\Delta\omega_z$, $\Delta\omega_\phi$, $\Delta\omega_\theta$, $\Delta\lambda_\psi$, $\Delta\lambda_x$.

Motor mixing

The first three commands are used to change speed of motors for control in Z-axis, roll axis and pitch axis.

$$\begin{aligned}\omega_1 &= \omega_{trim} - \Delta\omega_z - \Delta\omega_\phi + \Delta\omega_\theta \\ \omega_2 &= \omega_{trim} - \Delta\omega_z + \Delta\omega_\phi + \Delta\omega_\theta \\ \omega_3 &= \omega_{trim} - \Delta\omega_z + \Delta\omega_\phi - \Delta\omega_\theta \\ \omega_4 &= \omega_{trim} - \Delta\omega_z - \Delta\omega_\phi - \Delta\omega_\theta\end{aligned}$$

The last two commands are used to change tilt angle of front two motors for control in yaw axis and X-axis.

$$\begin{aligned}\lambda_1 &= \lambda_{trim} - \Delta\lambda_\psi + \Delta\lambda_x \\ \lambda_2 &= \lambda_{trim} - \Delta\lambda_\psi + \Delta\lambda_x\end{aligned}$$

6.2.2 Control system

The flight control system used in Ardupilot [1] consists of an outer loop for position control. The inner loops are used for controlling the attitude of the aircraft. Since the simulation environment is based on non linear equations of motion, tuning the controller by analytical means is not possible. Ziegler–Nichols method is used to manually tune the controller using flight simulations.

Position controller The control system used for position and attitude control is a PID cascaded system. A Proportional controller is used for position control which gives refer-

ence velocity required. A Proportional-Integral-Differential controller is used for velocity control.

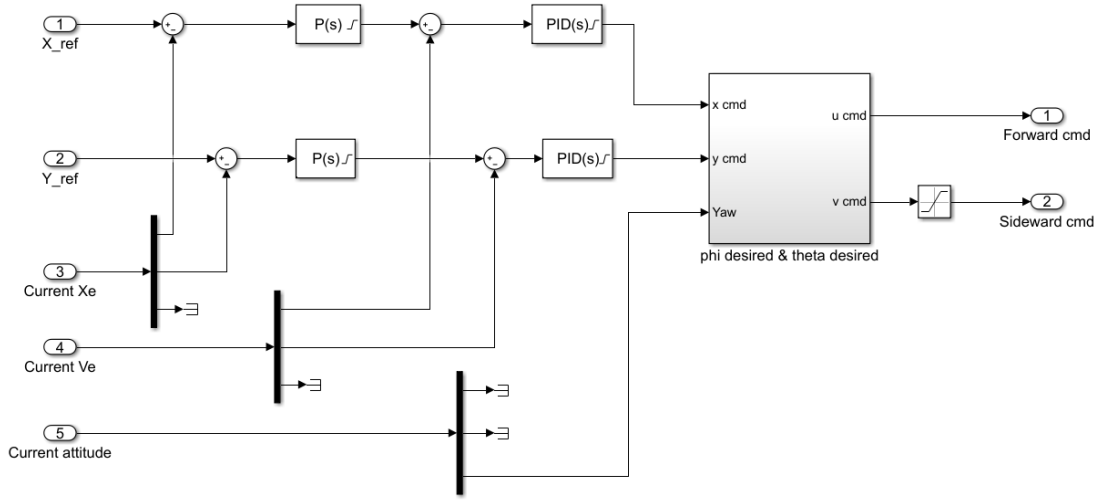


Figure 6.11: Position controller

Attitude controller The control system used for attitude control is a PID cascaded system. A Proportional controller is used for attitude control which gives reference turn rate required. A Proportional-Integral-Differential controller is used for turn rate control.

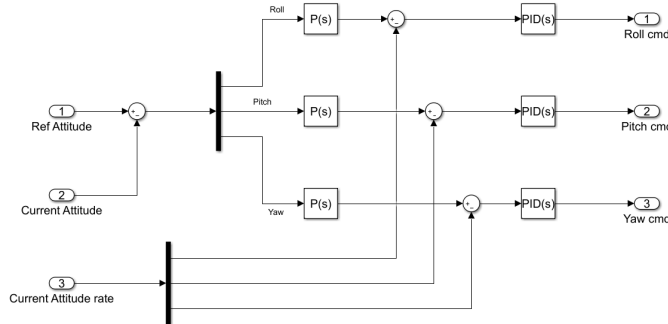


Figure 6.12: Attitude controller

Motor mixing and tilt mixing are done to obtain individual commands for the actuators. The mixing algorithms are described in previous section.

6.2.3 Flight simulations

Altitude control

Altitude control requires all the motors to speed up or down. The response to actuator command is linear and is completely decoupled with other axes of motion. Hence the response

of altitude control is very good. Position control is done with velocity limited. This is the slope of the curve seen 6.13.

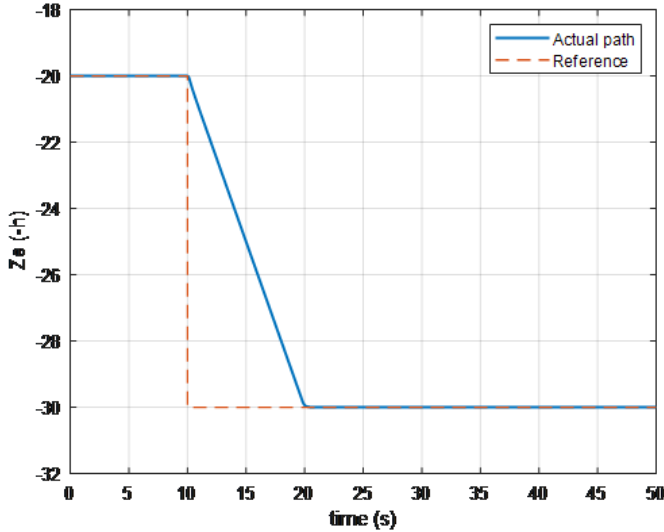


Figure 6.13: Altitude control

x-axis control Position control in X-axis requires collective tilt of both front motors. Although position control in X-axis is decoupled with other axis, tilting of motors in front also affects Pitch axis of the aircraft. This slows the response of the aircraft due to control action in figure 6.14.

y-axis control Position control in Y-axis requires rotation along X-axis or roll axis. Hence for Y-axis control, two PID cascades are used – one inner loop for roll axis control and other outer loop for Y-axis control. Due to coupled nature of this axis, response to control is very slow.

General flight path A helical flight path reference is provided to the control. The reference path and actual flight of the aircraft is given in figure 6.16.

There is a difference in the flight path reference to actual flight path due to both physical limitations that are included in the model and due to controller delay.

When the speed of the reference flight path is reduced, actual flight path is very close to the reference. The latter flight path has same flight time but number circles taken in this

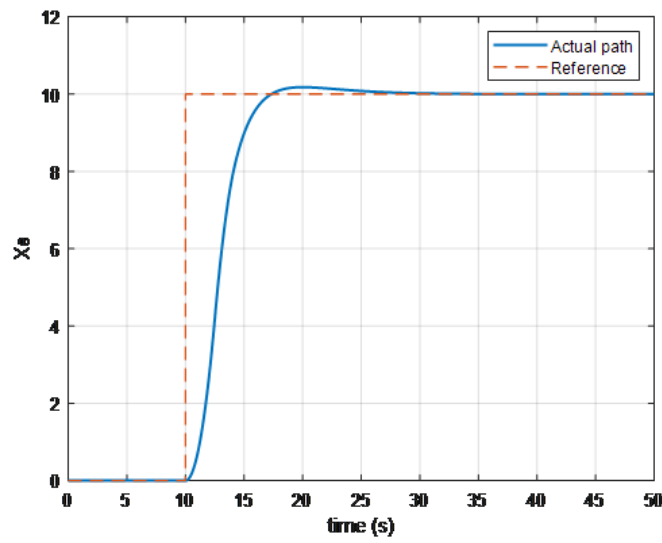


Figure 6.14: x-axis control

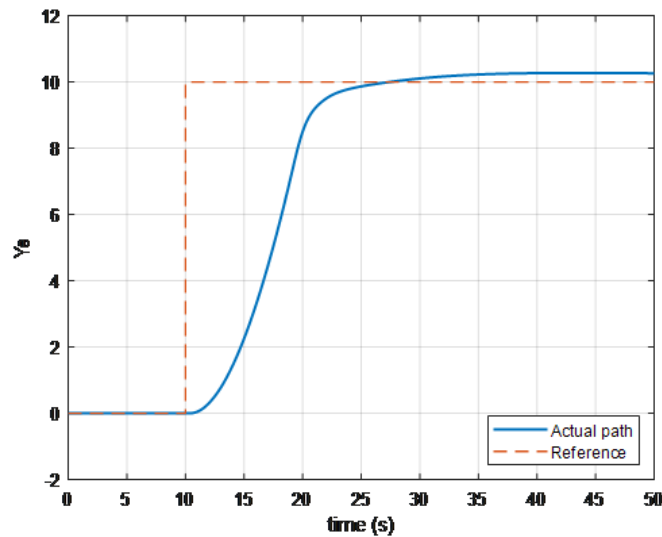


Figure 6.15: y-axis control

time are lesser.

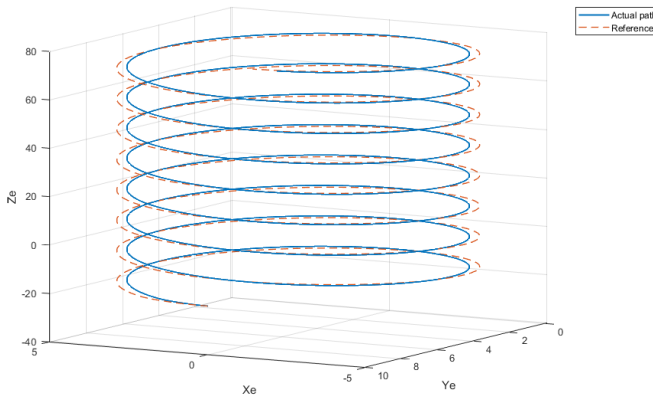


Figure 6.16: General flight path 1

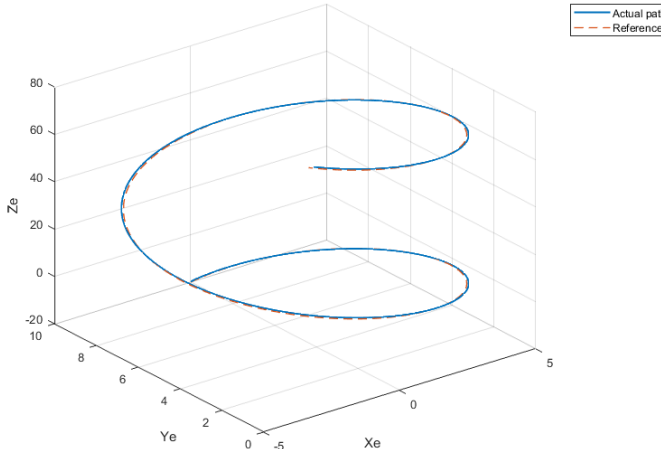


Figure 6.17: General flight path 2

6.3 Flight mode Transition

Controlling and stabilising the UAV during transition is not possible when flight speeds are low. The control surfaces become more effective as the speed increases due to more airflow over them. As the transition nears completion, the motors will be tilted forward and cannot help in stabilising the aircraft. Using multiple actuators for same control without governing law is not possible with linear control systems. Hence during transition, the motors are chosen as means to control the aircraft with some limitations.

The attitude and altitude control loops used in the hover flight are used for transition

with the exception of yaw control. The controller stabilizes the aircraft in roll and pitch axis neglecting the yaw. This allows for free tilting of motors.

6.3.1 Transition from Hover flight to Fixed-wing flight

Flight transition from Hover flight to Fixed-wing flight happens by tilting the front two motors. The front motors tilt forward at a defined tilt rate (tilt-rate) and stop at a specified tilt angle (tilt-lim) till the aircraft reaches a minimum flight velocity (V_{min}). When the flight speed reaches the minimum flight speed, the front motors tilt completely forward and rear motors are switched off.

The recommended values for tilt-rate tilt-lim are 15 deg/s and 45 deg. The minimum velocity to end flight transition is taken as 14 m/s (trim velocity is 15 m/s) shown in figure 6.18. These values have to optimised based on robustness of the controller to external disturbances.

Figure 6.19 shows transition with different tilt angle limits of 30° , 45° and 60° . All three show satisfactory performance but the lesser tilt angle limits show lower thrust requirements during transition. Low thrust requirements mean that there is additional thrust available to correct for disturbances.

Figure 6.20 shows transition with different tilt rates of $10^\circ/s$, $20^\circ/s$ and $30^\circ/s$. Similar to tilt angle limits, the lesser tilt rate flights show lower thrust requirements during transition.

Figure 6.21 shows the transition characteristics of the UAV with tilt angle limit of 45° and tilt rate of $15^\circ/s$. The transition takes 5.4s to complete and has a forward travel of 30.5 m in this time.

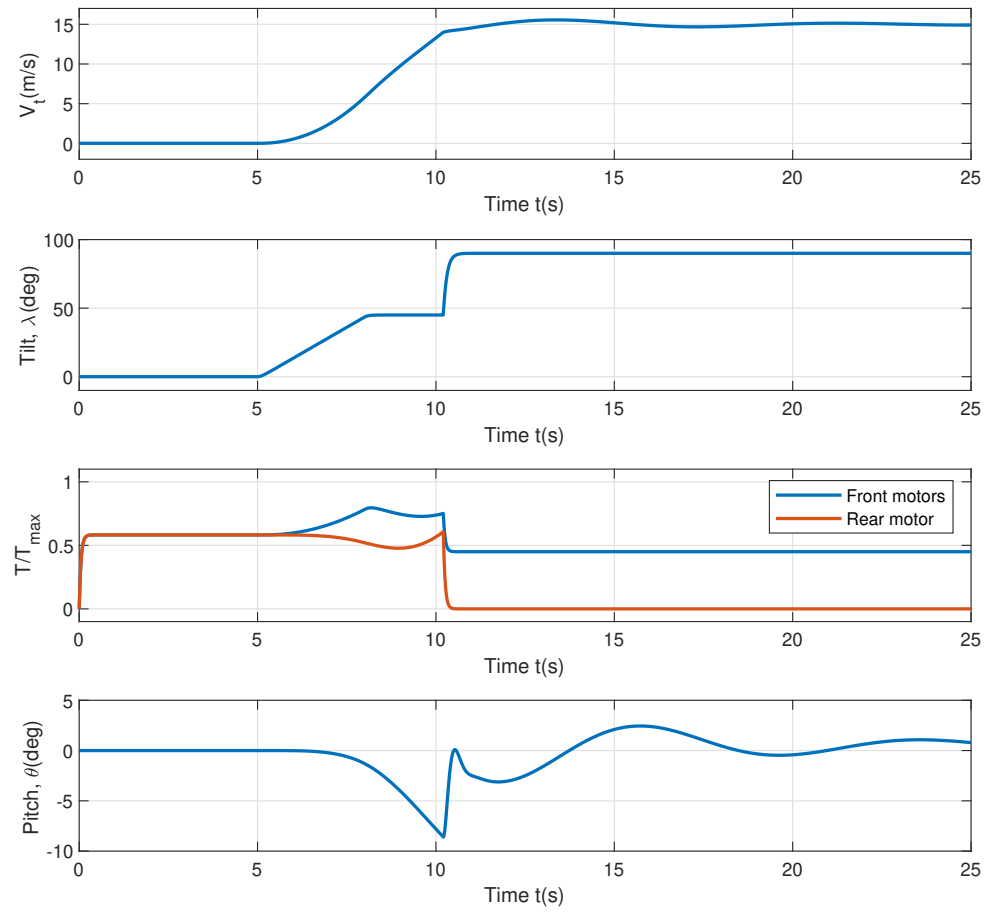


Figure 6.18: Hover to Forward flight transition

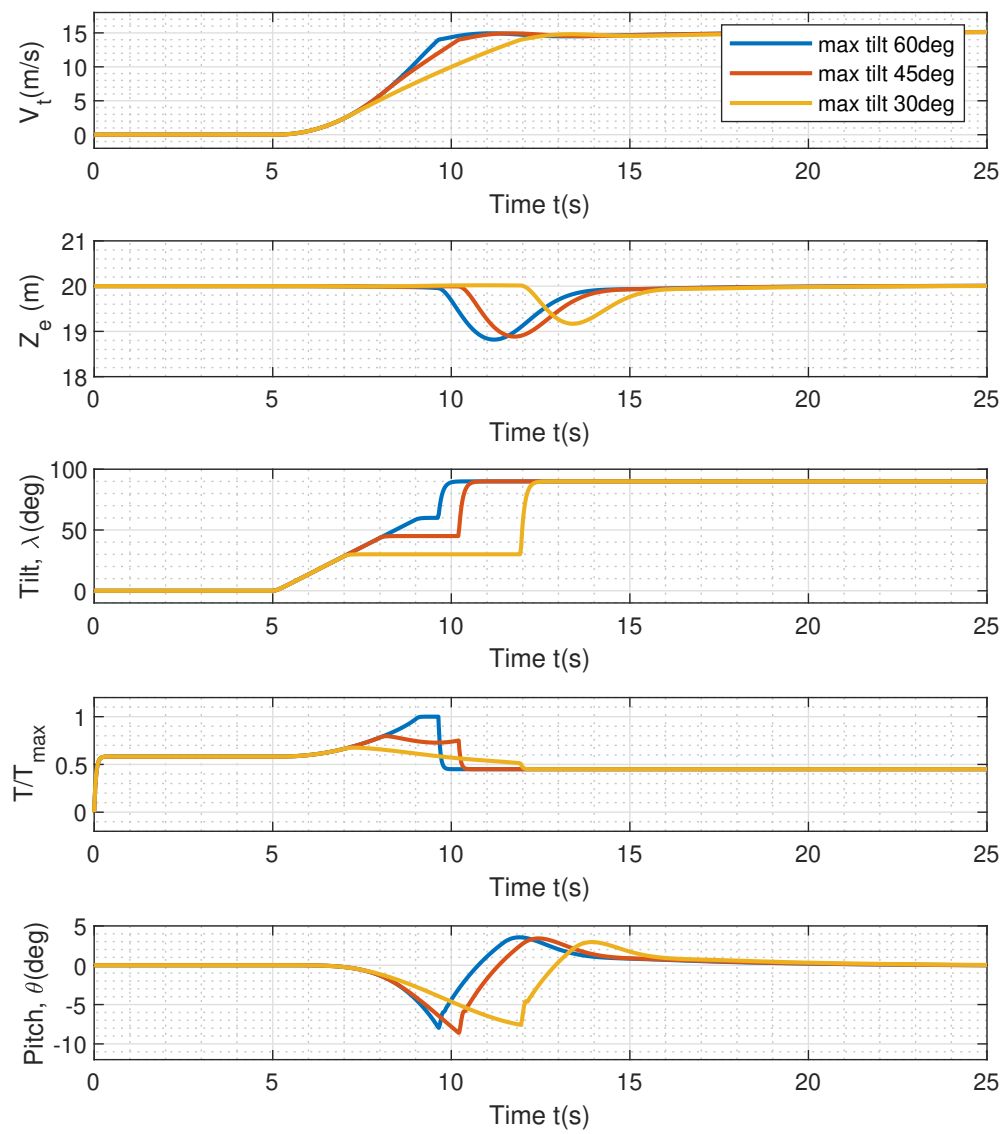


Figure 6.19: Transition with different tilt angle limits

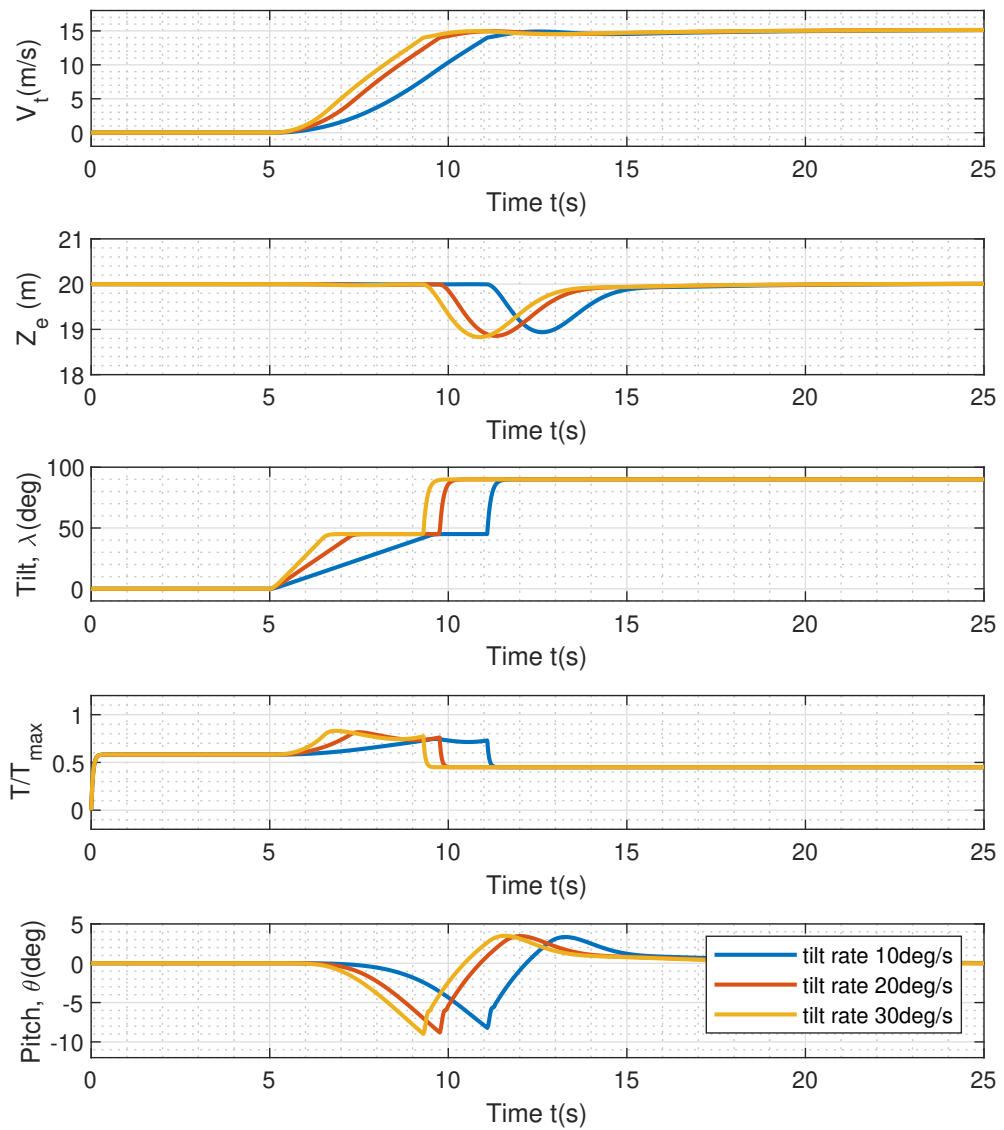


Figure 6.20: Transition with different tilt rates

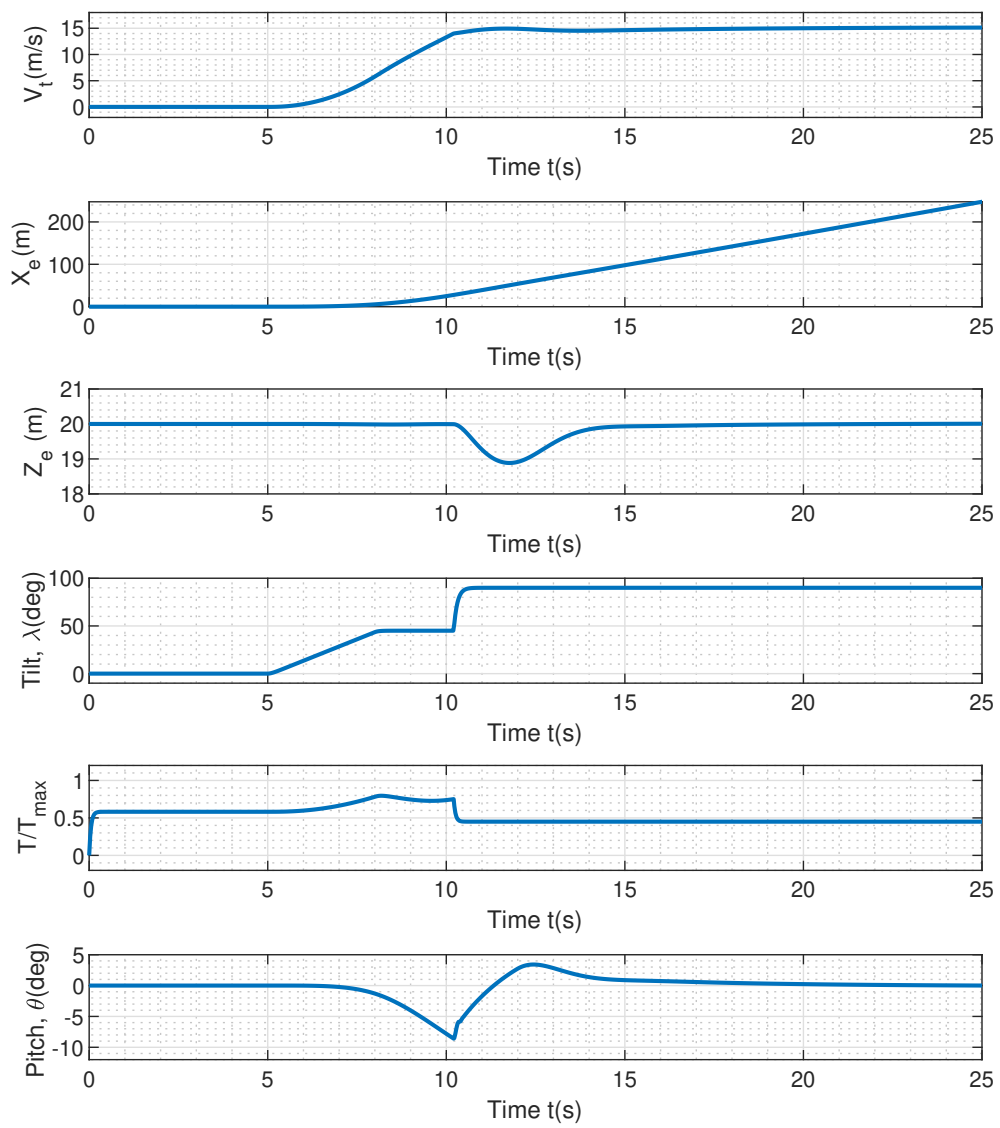


Figure 6.21: Transition characteristics of the UAV

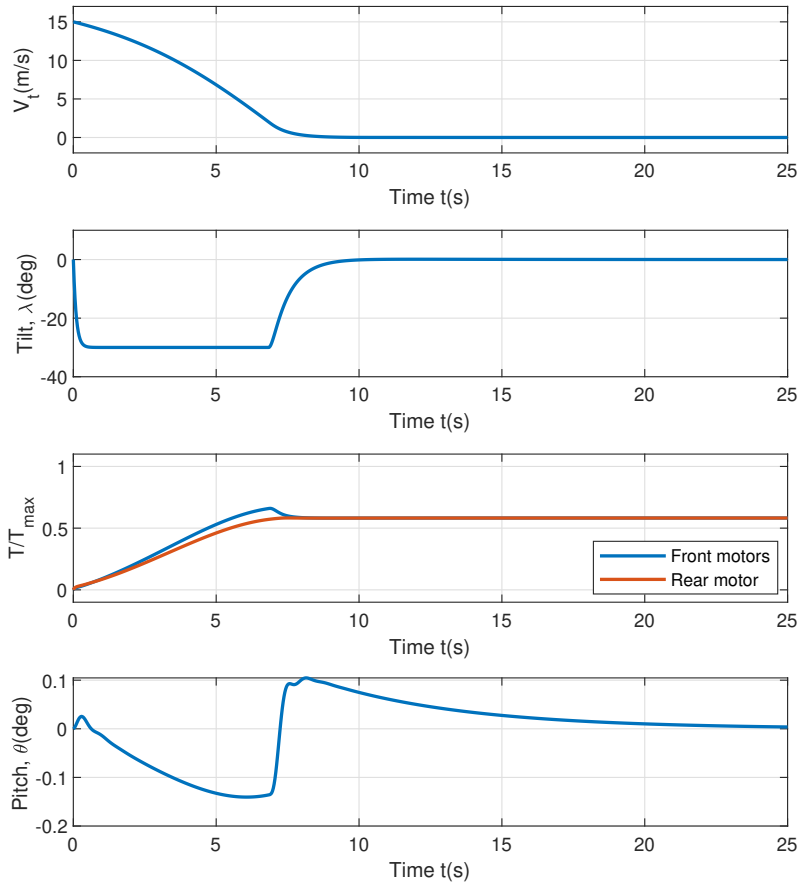


Figure 6.22: Forward flight to hover transition

6.3.2 Transition from Forward flight to Hover flight

Flight transition from Forward flight to Hover flight is achieved by tilting back front motors to vertical position. When flight transition is triggered, the front motors tilt to vertical position as soon as possible. The motors speed up to compensate for loss of lift and maintain attitude using the four motors. To decelerate the aircraft as soon as possible, the front motors tilt back and are controlled using the velocity control loop as shown in figure 6.22.

Chapter 7

Conclusions and Future Work

7.1 Conclusions

This thesis is a starting step in study of hybrid or VTOL UAVs. A tiltrotor UAV has been design that can be used as a proof of concept for tiltrotor VTOL. Future developments in controllers can be implements for experimental tests using this UAV. The UAV is predicted to weight at 6 kg and have an endurance of 30min for forward flight operations. It uses quad motor configuration with front motors tilting and has provision for conventional take-off and landing. The design is found to be feasible for experimental work related to tiltrotors.

A mathematical model of the aircraft has been developed. This model predicts aerodynamics of flight and describes the characteristics of the propulsion system. A simulation environment is developed in MATLAB Simulink to conduct flight simulations. The aircraft model developed along with Ardupilot flight stack has been integrated into the code. Flight simulations show satisfactory operation of the aircraft in all three flight regimes.

7.2 Future Work

The aircraft sizing has been done based on statics and historic aircraft data for the design of UAV. Further optimisations can be performed to the developed model to improve its performance. The airframe structure and tilting mechanisms have been design based on past design experiences. They need to be optimised from structures point of view.

The aerodynamics have been modelling based on VLM analysis. Although results are reasonable, their accuracy can be increased. Better CFD methods, wind tunnel tests and

flight tests have to be made to develop a better model. Aerodynamic models for hover flight and transition have not been modelled. For better results from simulations, these flight regimes have to be studied in detail.

The propulsion model has been simplified and its interactions with aerodynamics has not been accounted for. The effects of propulsion on the aerodynamics have to be modelled especially for flight transition simulations.

Currently for simulations, commercially available Ardupilot flight stack is used for flight control. These controllers simple and robust, but do not suffice the requirements of VTOL UAVs. The complex dynamics involved in the flight modes demand better control algorithms.

References

- [1] “Ardupilot plane documentation,” Available at <https://ardupilot.org/plane/> (Accessed in July 2020).
- [2] “Harrier jump jet,” Available at https://en.wikipedia.org/wiki/Harrier_Jump_Jet (Accessed in July 2020).
- [3] “Yakovlev yak-38,” Available at https://en.wikipedia.org/wiki/Yakovlev_Yak-38 (Accessed in July 2020).
- [4] “Bell boeing v-22 osprey,” Available at https://en.wikipedia.org/wiki/Bell_Boeing_V-22_Osprey (Accessed in July 2020).
- [5] “Bell v-280 valor,” Available at https://en.wikipedia.org/wiki/Bell_V-280_Valor (Accessed in July 2020).
- [6] “Lockheed martin f-35 lightning ii,” Available at https://en.wikipedia.org/wiki/Lockheed_Martin_F-35_Lightning_II (Accessed in July 2020).
- [7] A. S. Saeed, G. Cai, A. B. Younes, S. Islam, J. Dias, and L. Seneviratne, “A review on the platform design, dynamic modeling and control of hybrid uavs,” *International Conference on Unmanned Aircraft Systems (ICUAS)*, 2015.
- [8] “Bell eagle eye,” Available at https://en.wikipedia.org/wiki/Bell_Eagle_Eye (Accessed in July 2020).
- [9] “Iai panther,” Available at https://en.wikipedia.org/wiki/IAI_Panther (Accessed in July 2020).
- [10] A. Lennon, *The basics of R/C Model Aircraft Design.* Air Age Media, 1996.
- [11] D. P. Raymer, *Aircraft Design: A conceptual Approach*, 2nd ed. AIAA education series, 1992.

- [12] M. H. Sadraey, *Aircraft Design: A Systems Engineering Approach*, 1st ed. Wiley, 2013.
- [13] Q. Quan, *Introduction to Multicopter Design and Control*, 1st ed. Springer, 2017.
- [14] Pavan, Aanand, Karthik, and Ravindra, “Development of search and rescue drone,” Project report for Bachelor of Engineering, 2017.
- [15] M. S. Selig, J. J. Guglielmo, A. P. Broeren, and P. Giguere, *Summary of Low-Speed Airfoil Data, Volume I*. SoarTech Publications, 1995.
- [16] M. S. Selig, C. A. Lyon, J. J. Guglielmo, C. P. Ninham, and P. Giguere, *Summary of Low-Speed Airfoil Data, Volume II*. SoarTech Publications, 1996.
- [17] P. Barua, T. Sousa, and D. Scholz, “Empennage statistics and sizing methods for dorsal fins,” Tech. Rep., 2013.
- [18] “Apc propeller performance data,” Available at <https://www.apcprop.com/technical-information/performance-data/> (Accessed in July 2020).
- [19] “Xflr5 documentation,” Available at <http://www.xflr5.tech/xflr5.htm> (Accessed in July 2020).
- [20] R. C. Nelson, *Flight Stability and Automatic Control*, 2nd ed. McGraw Hill Education, Special India Edition, 2010.
- [21] J. W. Vervoost, “A modular simulation environment for the improved dynamic simulation of multirotor unmanned aerial vehicles,” Master’s thesis, 2016.
- [22] F. R. Garza and E. A. Morelli, “A collection of nonlinear aircraft simulations in matlab,” Tech. Rep., 2003.